INFORMATION TO USERS

This manuscript has been reproduced from the microfilm master. UMI films the text directly from the original or copy submitted. Thus, some thesis and dissertation copies are in typewriter face, while others may be from any type of computer printer.

The quality of this reproduction is dependent upon the quality of the copy submitted. Broken or indistinct print, colored or poor quality illustrations and photographs, print bleedthrough, substandard margins, and improper alignment can adversely affect reproduction.

In the unlikely event that the author did not send UMI a complete manuscript and there are missing pages, these will be noted. Also, if unauthorized copyright material had to be removed, a note will indicate the deletion.

Oversize materials (e.g., maps, drawings, charts) are reproduced by sectioning the original, beginning at the upper left-hand corner and continuing from left to right in equal sections with small overlaps. Each original is also photographed in one exposure and is included in reduced form at the back of the book.

Photographs included in the original manuscript have been reproduced xerographically in this copy. Higher quality 6" x 9" black and white photographic prints are available for any photographs or illustrations appearing in this copy for an additional charge. Contact UMI directly to order.

University Microfilms International
A Bell & Howell Information Company
300 North Zeeb Road, Ann Arbor, MI 48106-1346 USA
313/761-4700 800/521-0600

Order Number 9325028

Calcium regulation in neurosecretory cells undergoing regeneration in culture

Graf, Robert Alan, Ph.D.

University of Hawaii, 1993

Copyright ©1993 by Graf, Robert Alan. All rights reserved.

U·M·I
300 N. Zeeb Rd.
Ann Arbor, MI 48106

CALCIUM REGULATION IN NEUROSECRETORY CELLS UNDERGOING REGENERATION IN CULTURE.

A DISSERTATION SUBMITTED TO THE GRADUATE DIVISION OF THE UNIVERSITY OF HAWAII IN PARTIAL FULFILLMENT OF THE REQUIREMENTS FOR THE DEGREE OF

DOCTOR OF PHILOSOPHY

IN ZOOLOGY

MAY 1993

BY

Robert Alan Graf

Dissertation Committee:

Ian Cooke, Chairperson
Richard Allen
Ian Gibbons
S. Randy Haley
Daniel Hartline

© Copyright 1993
by
Robert Alan Graf

To my mother and father, Jo Ann and George Graf, for instilling in me the determination and the patience.

ACKNOWLEDGEMENTS

I would like to express my deepest thanks to those of you who made this experience as rich as it was for me. I thank my advisor, Dr. Ian Cooke, one of the last of the gentlemen biologists, for having a sincere interest in my work and enough confidence in my ability to allow me to influence the laboratory in a new direction. Despite great odds, he consistently worked to provide the conditions and resources necessary for me to learn and study my problem of choice. He exercised great patience during many of the difficult phases, due many times to attempts to use technology before an industry standard had developed. My advisor is also to be thanked for never losing sight of the human being caught-up in the process of researching a topic.

In the Cooke Laboratory, I'd like to thank Ms. Susan Grau for providing me an example of high standards of workmanship and introducing me to cell culture; Dr. Peter Ruben, for encouraging me and introducing me to many of life's splendors both inside the lab and outside, from patch clamping without using the low power objective to appreciating the spectacular cultural diversity that exists in Hawaii. I'd like to thank Dr. Don Meyers, also for providing an example of high standards. I'd like to thank Ms. Bev Quon, Ms. Ann Yamaguchi, Mr. Nathan Enoki, Ms. Mary Raceles, Mr. Rod Martin, Ms. Jackie Tellei, Ms. Bev Yuen, and especially Ms. Jana Watanabe

for helping me with technical aspects of my work. I have learned how incredibly important it is to feel valued, whether at the level of student help or professor.

I'd like to thank Dr. Brad Jones, who always had a patient ear and an important point to add, whether it be about the migratory route of golden plovers or the serial port wiring necessary to configure the filter wheel changer. Also in this category is Mr. Hinano Akaka, who helped me understand many, many things, from the difference between a low and a high in meteorology to the calibration of a Xe arc lamp.

I'd like to thank Mr. Karl Carvalho for making just about anything I needed and showing me just how creative and industrious the mind can be. In the later phases, I'd like to thank Mr. Ted Murphy for all the new solutions that were necessary to move the optical equipment to its new location.

I'd like to thank Dr. John Starkus, the champion of the graduate student cause, for having the foresight to develop a laboratory computer network, something for which he does not receive the credit he deserves. If not for his efforts, I'm not sure what I would have done with the gigabyte of data I generated.

I'd like to thank Dr. Dan Hartline for introducing me to the stomatogastric ganglion, for encouraging me, and for many thought provoking conversations during the years. I'd like Ms. Carol Kosaki, Ms. Angela Lee, and Ms. Catherine Murphy to know that they were much, much more than secretaries, but rather that they provided that something special that makes the place work.

In the area of cultural enrichment, I'd like to thank my sensei: Ms. Noriko Kawaura, Ms. Keiko Yamamoto, and Ms. Miki Ogasawara, who each in their own way showed me a level of devotion to teaching that only a student of Japanese would know. These teachers always had the time and always thought it right to push me just a little bit harder.

Last but not least, I'd like to thank my doctoral committee for their valuable time and their patience.

For the published research paper appearing in *The Proceedings of the National Academy of Sciences*:

I thank T. Weatherby for electron microscopy, B. Quon for bioassays, Prof. S. B. Kater for suggestions and encouragement, and Profs. D. Hartline and J. Corwin for suggestions on the manuscript. We are grateful to Profs. H. Schooneveld and R. Keller for gifts of antisera. Supported by National Institutes of Health grant NS15453 and National Science Foundation grant BNS84-04459 to I.C., National Institutes of Health grants to the University of Hawaii (Research Centers in Minority Institutions and Biomedical Research Support) and by the University of Hawaii Foundation.

For the published research paper appearing in the *Journal of Experimental Biology*: I thank Prof. D. K. Hartline for supplying animals for culture experiments, encouragement and suggestions; Dr. B. R. Jones for suggestions on the manuscript; and Ms. B. A. Tomiyasu for demonstrating the dissection. This research was

supported by National Institutes of Health grant NS15453 and National Science Foundation grant BNS84-04459 to I. C., National Institutes of Health grants to the University of Hawaii (Research Centers in Minority Institutions G12 RR03061, and Biomedical Research Support), and by the University of Hawaii Foundation.

For the published research paper appearing in the *Journal of Neurophysiology*: I gratefully acknowledge Drs. D. K. Hartline, Brad Jones and P. C. Ruben for their critical comments on an earlier version of this manuscript and Dr. S. R. Ikeda for the use of graphing and curve-fitting software. This work was supported by funds from the Ida Russell Cades Fund of the University of Hawaii Foundation, NIH grants R01 NS15453, G 12 RR03061 and an NIH Biomedical Research Support grant, NSF grant BNS89-10432, , and the Whitehall Foundation.

For Chapters 5 and 6 of this dissertation, the research was supported by NSF BNS84-04459 and NIH NS 15453.

ABSTRACT

The ability to regulate intracellular free calcium ion levels ($[Ca^{2+}]_i$) may determine regenerative capability of crustacean peptide-secreting nerve cells. To test this proposal, a culture system was developed since crustacean neurons had not been cultured previously. These neurons consistently exhibited two distinct morphologies, veiling and branching. Because no factors were required, intrinsic outgrowth mechanisms could be studied that may operate to establish a given morphology. Veiling neurons were consistently immunoreactive to crustacean hyperglycemic hormone antisera; whereas, branching neurons were immunopositive to either molt inhibiting hormone or red pigment concentrating hormone antisera.

Electrophysiological observations characterized voltage-dependent outward currents (I_A and I_K) in both morphologies, but inward sodium and calcium currents were prominent only in veiling neurons.

The $[Ca^{2+}]_i$-sensitive dye, fura-2, was used to observe basal $[Ca^{2+}]_i$ as well as responses to stimuli that should activate the voltage-dependent calcium current. Basal levels varied widely, relative to other preparations, but were not significantly different among branching and veiling neurons. In many veiling neurons undergoing active outgrowth, $[Ca^{2+}]_i$ increased as much as 4 times in the veil, then returned to near rest within 20 minutes, whereas in non-growing neurons, $[Ca^{2+}]_i$ increased, but remained high. Branching neurons showed small $[Ca^{2+}]_i$ changes which were not quickly reversed. In general, high basal $[Ca^{2+}]_i$ and poor ability to restore $[Ca^{2+}]_i$ elevations

characterized neurons that had poor initial outgrowth. When cells loaded with $[Ca^{2+}]_i$ dye were touched, a stimulus which initiated outgrowth, $[Ca^{2+}]_i$ levels were transiently augmented, implicating a role for $[Ca^{2+}]_i$ in the outgrowth response.

The same concentration of cadmium-supplemented saline blocked both the Ca^{2+} current and veiling, but not branching outgrowth. Reduced external Na blocked veiling but not branching outgrowth.

In summary, two types of peptidergic neurons regenerate intrinsically different patterns of outgrowth while exhibiting a wide range of basal $[Ca^{2+}]_i$. They differ in electrically-mediated calcium influx, in $[Ca^{2+}]_i$ responses to stimulation, in their ability to restore $[Ca^{2+}]_i$, and finally in the sensitivity of outgrowth (but not its form) to interference with Ca^{2+} transfer mechanisms.

TABLE OF CONTENTS

ACKNOWLEDGEMENTS v

ABSTRACT ix

LIST OF TABLES xv

LIST OF FIGURES xvi

LIST OF ABBREVIATIONS AND/OR SYMBOLS xix

PREFACE xxii

CHAPTER 1

INTRODUCTION 1

Synopsis 1

General Background 5

CHAPTER 2

CRUSTACEAN PEPTIDERGIC NEURONS IN CULTURE SHOW IMMEDIATE OUTGROWTH IN SIMPLE MEDIA. 23

Abstract 23

Introduction 24

Materials and Methods 26

Results 29

Discussion 34

References 36

CHAPTER 3

PRIMARY CULTURE OF CRUSTACEAN STOMATOGASTRIC GANGLION NEURONS IN DEFINED MEDIUM 45

Introduction 45

Methods 46

Results 47

Discussion 49

References 49

CHAPTER 4

IONIC CURRENTS OF MORPHOLOGICALLY DISTINCT PEPTIDERGIC NEURONS IN DEFINED CULTURE. 54

Summary and Conclusions 54

Introduction 56

Methods 59

Results 64

Discussion 80

References 93

CHAPTER 5

CALCIUM REGULATORY RESPONSES OF ADULT NEUROSECRETORY NEURONS REGENERATING DISTINCT MORPHOLOGIES IN DEFINED CULTURE. 121

Introduction 121

Methods 123

Results 131

Discussion 136

References 141

CHAPTER 6

OUTGROWTH PROPERTIES OF X-ORGAN NEURONS UNDER ALTERED MEDIUM CONDITIONS. 161

Introduction 161

Methods 162

Results 164

Discussion 168

Reference 172

CHAPTER 7

SUMMARY AND CONCLUSIONS 188

GLOSSARY 193

REFERENCES 202

LIST OF TABLES

Table		Page
5-1	Basal $[Ca^{2+}]_i$ and $[Ca^{2+}]_i$ responses resulting from high K^+perturbations	148

LIST OF FIGURES

Figure		Page
2-1	Morphology of crustacean peptidergic neurosecretory cells in primary culture	40
2-2	Immunofluorescence of crab peptidergic neurons in primary culture	42
2-3	Current-voltage [I(V)] relationship for Ca current before and after exposure to Cd	44
3-1	Photomicrographs of outgrowth from isolated *Homarus americanus* stomatogastric neurons	51
3-2	Hoffmann modulation contrast images of directed outgrowth from a *Cardisoma carnifex* neuron at different culture ages	53
4-1	Whole-cell voltage-clamp records in physiological-like solutions	102
4-2	Inward current (corrected for leak and capacity current) from a veiled neuron in solutions minimizing Ca and outward current	104
4-3	Identification of I_{Ca} in veiled cells	106
4-4	There is little steady state inactivation of I_{Ca} at a V_h of -40 mV	108
4-5	Prepulse voltage and interpulse interval affect test-pulse current amplitude	110
4-6	Substitution of Sr^{2+} for Ca affects the decay process	112
4-7	Late outward current (I_K): I(V) curve plotted from uncorrected current measured at the end of 80 msec voltage clamp commands from V_h of -50 mV	114
4-8	Outward current reversal potentials	116

4-9 Increased late outward current observed in some neurons following addition of 4-AP 118

4-10 Effect of TEA-Br (50 mM) in a neuron in which the I_K was not enhanced by 4-AP and in which I_A was not apparent even from V_h = -80 mV 120

5-1 Temporal changes in $[Ca^{2+}]_i$ of an X-organ neuron undergoing vigorous veiling outgrowth in response to a short application of 5 times potassium (high K) saline to the bath 146

5-2 Membrane voltage responses from a veiling neuron (soma diameter 35 μm) during exposure to 5X, 10X, and X K^+ saline 150

5-3 Temporal $[Ca^{2+}]_i$ response of a weakly relaxing neuron 152

5-4 High K^+-induced $[Ca^{2+}]_i$ changes of a branching neuron at day 4 in culture 154

5-5 $[Ca^{2+}]_i$ response differences between a branching neuron and a non-growing neuron: branching neuron on the right, soma diameter ~ 20 μm 156

5-6 Differences in the effects of electrical and potassium stimulation on $[Ca^{2+}]_i$ homeostasis in the same veiling neuron 158

5-7 Membrane voltage responses from representative microelectrode experiments from X-organ neurons of branching and veiling morphology type in culture 160

6-1 Typical effects of alterations of culture medium on outgrowth morphology at one day in culture 175

6-2 Fluorescence changes resulting from addition of Cd to a veiling cell at the same concentration used to block veiling outgrowth 177

6-3 Fluorescence changes resulting from addition of Cd to a branching cell at the same concentration used to block veiling outgrowth 179

6-4 Calcium responses to high K^+ from a veiling neuron in reduced sodium saline 181

6-5 Calcium responses to high K^+ from a branching neuron in reduced sodium saline 183

6-6 Initiation of outgrowth resulting from mechanical stimulation with a fire-polished glass probe 185

6-7 Mechanical stimulation of a veiling neuron changed the $[Ca^{2+}]_i$. day 2, fura-2/AM-loaded veiling neuron was mildly touched with the probe 187

LIST OF ABBREVIATIONS AND/OR SYMBOLS

AKH	Adipokinetic hormone.
AM	acetoxymethyl ester form of a chemical.
4-AP	4-amino-pyridine.
ATP	Adenosine triphosphate.
BAPTA	1,2-bis-(2-aminophenyoxy)ethane-N,N,N',N'-tetraacetic acid.
Ba	Barium ion.
BSA	Bovine serum albumin.
Ca	Calcium.
$CaCl_2$	Calcium chloride.
$[Ca^{2+}]_i$	Cytosolic free Ca concentration.
Cd	Cadmium.
CHH	Crustacean hyperglycemic hormone.
DMSO	Dimethylsulfoxide.
E_K	Potassium Reversal Potential.
E_R	Reversal Potential.
EGTA	Ethylene glycol bis(β-aminoethyl ether)-N,N,N',N'-tetracetic acid.
ER	Endoplasmic reticulum.
F_o/F_s	0 $[Ca^{2+}]_i$ fluorescence divided by saturating $[Ca^{2+}]_i$ fluorescence of fura-2.
FITC	Fluorescein isothiocyanate.

fura-2	1-[2-(5-carboxyoxazol-2-yl)-6-aminobenzofuran-5-oxy]-2-(2'-amino-5'-methylphenoxy)-ethane-N,N,N',N'-tetraacetic acid.
GΩ	Gigohm.
HEPES	N-2-hydroxyethylpiperazine-N'-2-ethanesulfonic acid.
I_A	Transient outward current.
I_{Ca}	Voltage-dependent calcium current.
I_K	Voltage-dependent and TEA inhibited delayed rectifying outward current.
I_{Na}	Voltage-dependent TTX blocked sodium current.
[I(V)]	Current-Voltage Relationship.
K_d	Dissociation constant.
KCl	Potassium chloride.
MIH	Molt Inhibiting Hormone.
ml, mm, mg, mM, ms	Milli- liter, meter, gram, molar, second
MΩ	Megohm. Electrical resistance unit
mV	Millivolt.
NaCl	Sodium chloride.
Na_2SO_4	Sodium sulfate.
nm, nM	Nano- meter, molar.
NMG-$MeSO_3$	N-methyl-D-glucamine methane sulphonate.
R	Ratio.

R_{min}	Minimum Ratio
R_{max}	Maximum Ratio
RPCH	Red Pigment Concentrating Hormone.
SIT	Silicon-intensified target.
TEA	Tetraethyl ammonium ion.
TTX	Tetrodotoxin.
µl, µm, µg, µM	Micro- liter, meter, gram, molar
V_c	Command voltage.
V_h	Holding voltage.
XOSG	X-organ - sinus gland.

PREFACE

My topic, the influence of $[Ca^{2+}]_i$ on the regeneration morphology of crustacean peptidergic neurons, addresses the proposal that second messenger systems, such as $[Ca^{2+}]_i$ can integrate and hence regulate the cellular output, or behavior of neuronal process outgrowth during regeneration of adult nerve cells.

Purpose

The purpose of this line of research is to observe, identify, and characterize the means by which neuronal morphology, the specific form of cell motility exhibited in nerve cells, occurs. This cellular process is one of the most sophisticated aspects of cellular function. Neuronal morphology is the result of outgrowth that extends away from the cell body of a neuron to establish connectivity with the developing nervous system as well as provide flexibility of connections (plasticity) in the adult brain. The cellular organelle responsible for the outgrowth, the growth cone, functions in a sensory, integrative, and behavioral capacity. The purpose of this dissertation has been to characterize the specific means by which immunochemically characterized (identified) neurons regulate calcium levels, which in turn can have an influence on cellular behavior--outgrowth in this case.

Choice of Topic

Tools for studying the intricate inner working of living cells have recently been developed. With the advent of biotechnology during the 1980's, the capability to dissect and identify key molecular components of cell function evolved. Recently, an astounding amount of detailed information about many macromolecules has been established which provides a unique opportunity to determine which are involved in the regulation of specific cellular processes. As a consequence of these developments, molecular engineering has evolved that exploits the new knowledge of molecular genetics to synthesize probes specific to ions and biomacromolecules. The case in point for this study is the synthesis of fura-2, a $[Ca^{2+}]_i$-sensitive fluorescent indicator that provides information on $[Ca^{2+}]_i$ gradients and levels. It has been the source of some excitement that cell signaling molecules and messengers have not only been identified but also assigned roles in the integration of cellular functioning. Crustacean preparations provide advantages that permitted experiments from which emerged pioneering concepts that are now established as basic principles of neurobiology. For example, Ca current was first measured in a crustacean muscle preparation. Also, studies using Crustacea provided the first observation of inhibitory synapses and demonstration of synaptic reversal potentials, as well. Although these studies have provided many integrative concepts, the mechanisms by which the processes operate are not known in many cases. Research addressing individual cell functioning has been hampered by the difficulty in controlling for extraneous factors and cell-cell interactions. In order to study these mechanisms in a controlled manner,

it is necessary to devise a way to control for these extra circumstances. Development of a cell culture system to plate out individual neurons at low density in a simple medium afforded the ability to visualize the regenerative outgrowth as well as manipulate the experimental circumstances precisely.

Future research may lend itself to identifying and characterizing many of the specific effector molecules that are influenced by $[Ca^{2+}]_i$ signals during different cellular states and to assigning them to a specific cellular behavior. The number of Ca sensitive molecules known increases almost on a monthly basis. The molecular genetic tools are available to dissect out and study the influence of these molecules, one at a time without potential interference that may result from the introduction of a non-specific pharmacological blocker. Every time a new gene is sequenced, a new opportunity to characterize another facet of cellular functioning arises. The ability to monitor second messengers in living systems affords the opportunity to study the resulting behavior of the system while simultaneously monitoring the second messenger activity and titer. These molecular tools in conjunction with observations on the resulting cellular behavior will now allow us to manipulate precisely specific aspects of the integration signal and assign specific roles to the signal during cell specific and stage specific cellular functioning.

Contribution to the Published Research Papers

In the research paper that appeared in the January 1989 issue of the *Proceedings of the National Academy of Sciences (USA)*, I thought through and

performed experiments supporting the theory of exocytosis' role in neuronal outgrowth. Exocytosis requires an influx of external Ca through ion passing channel proteins (Ca channels) in the plasma membrane. These channels are voltage operated. Theoretically, fast onset, depolarizing electrical activity leads to an influx of Ca^{2+}, and this somehow allows fusion of secretory granule membrane to the plasma membrane. This membrane fusion causes release of neurotransmitter/hormone and the incorporation of the secretory granule membrane into the plasma membrane. In this paper, my contributions provide supporting evidence that secretory vesicle membrane is the resource for initial outgrowth, and that this incorporation is influenced by voltage-dependent exocytotic release without or with delayed membrane re-uptake. Specifically, my contributions include demonstrating block of outgrowth with an inorganic Ca channel blocker at 100 μM. I also performed voltage clamp experiments with a post-doctoral colleague, Dr. D. E. R. Meyers, to demonstrate that the same concentration of Cd needed to block outgrowth also blocked the voltage dependent Ca current in the same cell type. The data for Cd block of outgrowth was mentioned in the published paper, but is actually presented in this dissertation (Chapter 6).

I also demonstrated in this paper that culture of X-organ neurons under completely defined conditions is not specific to one species. Cultures of *Panulirus marginatus*, the Hawaiian spiny lobster, as well as from a tropical land crab, *Cardisoma carnifex*, exhibit the same outgrowth morphologies under the same environmental conditions, including medium, substrate, temperature, and humidity. In addition, I participated in bioassay experiments to show that hormone levels build-up in the cell culture medium

over time post-dissociation relative to controls, providing further evidence that the neurons secrete hormone in culture.

For the research paper that appeared in volume 149 of the *Journal of Experimental Biology*, I performed all of the experiments, processed all of the data, and wrote the manuscript. My advisor provided editorial assistance with the writing.

For the research paper that appeared in the May 1992 issue of the *Journal of Neurophysiology*, I produced all of the experimental preparations, participated jointly with Dr. Donald Meyers in the acquisition of almost all of the reported data, and provided input in the experimental framework. Dr. Meyers analyzed the data and made the Figures. The paper was primarily written by Dr. Meyers. I was involved in rewriting *"Effects of prepulses on I_{Ca}"* section and in editorial rewrites with Dr. Meyers and Dr. Cooke.

CHAPTER 1

INTRODUCTION

Synopsis

This introductory chapter functions to integrate the topics of the published research papers and the final chapter of this dissertation. A background of relevant literature that does not appear in the introductions of the published work is also included.

The complexity of cellular functioning challenges researchers. How can the multitude of physiological processes be coordinated and integrated? Celis perform many functions as a result of their ability to sense and gather information from the surroundings, integrate it, and produce a behavior, or response. Many aspects of sensory and effector systems have been well characterized (see Alberts *et al.*, 1989). The number of molecules that have been isolated and identified is increasing enormously and adding new dimensions to the understanding of functional mechanisms. Only recently, with the advent of fluorescent probes to monitor molecules in living cells, has it been possible to begin to assign roles to second messengers as molecules involved in the integration and coordination of subcellular mechanisms.

Calcium Signaling is Diverse

There now exist many examples in which transient establishment of $[Ca^{2+}]_i$ gradients provide signals that orchestrate functional consequences. Calcium signals have been implicated in the control of neuronal excitability (Marty, 1989), integration of electrical signals (Llinas, 1988), various forms of synaptic plasticity (Malenka *et al.*, 1989), gene expression (Szekely *et al.*, 1990), neuronal differentiation (Holliday *et al.*, 1991; Spitzer, 1991), fertilization (Obata *et al.*, 1989), mitochondrial metabolism (McCormack *et al.*, 1990) , programmed cell death (Chalfie and Wolinsky, 1990), death from pathological conditions (Choi, 1990), cytoskeletal rearrangements (Lankford and Letourneau, 1989) , cell cycle control (Poenie *et al.*, 1985), cell volume regulation (McCarty and O'Neil, 1992), and in nerve regeneration at the cellular level (Kater *et al.*, 1988; Kater and Mills, 1991). How can one molecule selectively direct so many functions? The answer may lie in the nature of the signal. A Ca signal that mediates regulated secretion appears to require at least a very brief (tens of μs; Augustine *et al.*, 1991) signal of magnitude on the order of hundreds of μM (Adler *et al.*, 1991). By contrast, the Ca signal needs to be sustained for hours at the micromolar level to induce pathological states.

Neuronal Preparations for Studying Ca Signaling and Outgrowth

Neurons provide intriguing material for the study of Ca signals. They are unique in that they project processes, sometimes of great length, often maintaining a characteristic, functionally relevant cellular architecture. This specialization has

provided additional insight on Ca signaling. It has been shown that different Ca signals can be occurring simultaneously in different anatomical regions of the neuron, suggesting that spatially segregated signals may mediate different processes. During nerve regeneration, motile organelles, or growth cones, emerge from the cell body and/or residual processes and this outgrowth has been shown to be influenced by cytosolic free calcium levels in most neurons. In fact, Kater and colleagues (Kater *et al.*, 1988; Kater and Mills, 1991) have postulated that an optimal $[Ca^{2+}]_i$ range exists for the outgrowth of neurons: At low $[Ca^{2+}]_i$ levels the cells do not grow and at very high calcium levels, the cells retract or die. Evidence supporting his theory of outgrowth has been reported for cellular preparations from several species [*Helisoma* motorneurons (Cohan and Kater., 1986); fetal mouse dorsal root ganglion neurons (Fields *et al.*, 1990; Fields and Russell, 1992)], but controversy has developed, since some cells, such as cultured rat superior cervical ganglion neurons, will continue to grow processes in cases where the neuron's calcium levels were experimentally increased to very high levels (Garyantes and Regehr, 1992). Others (Ivins *et al.*, 1991) show that calcium levels (in chick dorsal root ganglion neurons) are stable and low during neurite outgrowth, which is in general agreement with Kater's theory. However, when $[Ca^{2+}]_i$ is transiently increased with a depolarizing high potassium stimulus applied externally, no outgrowth rate changes are observed and morphology is unchanged (Ivins *et al.*, 1991). This scientific controversy continues and has provoked interest in examining a wider variety of species for the nature of the calcium signals that are associated with regeneration of neurons.

Dissertation Topic Focus

This dissertation addresses the characterization of cellular mechanisms that regulate intracellular calcium levels in heterogenous populations of peptide-secreting neurons from the X-organ - sinus gland, the major hormone-secreting structure in Crustacea. Since the primary function of these cells is to secrete neuropeptides, which has been shown to be a calcium mediated process, the study of the mechanisms which mediate Ca perturbations is important for its own sake. In order to study the calcium signals in the living tissue it was necessary to examine individual neurons. This then led to the development of a culture system for crustacean neurons. Chapters 2 and 3 of this thesis present published outcomes of this undertaking. Crustacean neurons had not been previously successfully cultured. Upon culturing the cells, it was determined that they will grow processes without the addition of initiating factors, which many other adult neuronal culture systems require for sprouting. This system thus provides unique possibilities for studying cellular signaling mechanisms in the absence of extrinsic determinants such as cell-cell interactions, which might contribute confounding signals in addition to those intrinsic to the regenerating neuron. Further, the neurons, growing as individuals, regenerate to exhibit characteristic morphologies that must be intrinsically determined. This tractable system affords the opportunity to systematically study the nature of the calcium signal under precisely controlled conditions. Because electrical activity is a prominent feature of neuronal function, an

early priority was to characterize the electrophysiological capabilities of the regenerating neurons. These observations are presented in Chapters 2 and 4. One neuronal type (veiling) possessed prominent voltage-dependent calcium current capabilities; another (branching) lacked this capability.

In the final chapters, the nature of the $[Ca^{2+}]_i$ signal is examined: Its magnitude, timing, and location. These are determined by the presence, kinetics, activity, number, and location of various cellular mechanisms that can simultaneously increase and decrease the calcium levels in neurons. In Chapter 5, calcium homeostasis observations are presented. The integrated signal that results can be monitored optically with intracellular calcium indicators, such as fura-2 used for this study. Calcium increases resulting from high potassium depolarization and reduced external sodium are reported. The intrinsic ability of the neurons to decrease calcium levels depends on the presence of mechanisms to buffer, or lower it. In Chapter 6, I return to earlier observations (introduced in Chapter 2) on the effect of voltage-dependent channel blockers on process outgrowth. Additional examples are given in the appendix.

General Background

Much of what we know of neuronal function comes from studies of intact or semi-intact tissue preparations. These preparations give information on the interactions and integration of cellular communication that is controlled and regulated by nervous input, integration, and output, or behavior. Certain nerve and heart cells show activity

that appears to result from intrinsic properties, occurring without external input, although, of course, these properties can be and in fact are modulated by extrinsic inputs. Invertebrate, and in particular crustacean nervous system preparations, have been the material of choice to demonstrate and study many of the concepts that then became basic principles of nervous system function at the cellular level. These include lateral inhibition [from *Limulus*] (see collection in Ratliff and Hartline, 1974), central pattern generation and its modulation (Watanabe *et al.*, 1967; Selverston and Moulins, 1987), facilitation (Fatt and Katz, 1951; Atwood *et al.*, 1983; Atwood *et al.*, 1986; Zucker, 1989), inhibitory synaptic transmission (Furshpan and Potter, 1959), action potential characterization (Hodgkin and Rushton, 1946), transmitter localization (Kravitz *et al.*, 1963), gating properties of channels (Rayner *et al.*, 1993), intrinsic electrical properties (Benson and Cooke, 1984), and densities of channels (Starkus *et al.*, 1981).

The X-organ - sinus gland of crustaceans (Bliss *et al.*, 1954), is a model system for the study of peptidergic neurons. The X-organ - sinus gland has provided fertile material for the study of stimulus-secretion coupling (Cooke *et al.*, 1977; Stuenkel, 1985), rare direct nerve terminal recordings from intact nerve cells (of *Cardisoma*) demonstrating a Ca based overshooting action potential (Cooke, 1985), direct ionic channel recordings from nerve terminals (Lemos *et al.*, 1986; Stuenkel *et al.*, 1990), and biosynthesis, packaging, and transport studies of neuropeptides using pulse-chase radioisotope methods. These studies (Stuenkel, 1983; Stuenkel, 1985; Newcomb *et al.*, 1985) take advantage of the unique morphology of the crustacean X-organ - sinus

gland system. The cell bodies of approximately 200 neurons (X-organ) are located in the eyestalk (Potter, 1956). The somata send axons in parallel that fasciculate forming the sinus gland nerve. Each axon then bifurcates many times to produce a tree-like structure of bulbous terminals that secrete peptides into a blood sinus. This culmination of terminals in association with blood sinuses forms a discrete neurohemal organ, the sinus gland (see Cooke and Sullivan, 1982 for review). The X-organ - sinus gland system produces at least 11 peptides (Newcomb *et al.*, 1985; Newcomb, 1987). Three of these peptides have identified hormonal activities. The amino acid sequence has been determined for crustacean hyperglycemic hormone (CHH) (Kegel *et al.*, 1989) and red pigment concentrating hormone (RPCH) (Ferlund and Josefsson, 1972; Ferlund, 1974a, b). The sequence of a third hormone, molt inhibiting hormone (MIH), has recently been published (Webster, 1991). Extracts of the sinus gland peptides produce a great many physiological responses, but which peptide(s) are responsible remains to be clarified.

All of these studies have provided information fundamental to the understanding of the complexities of nerve cell interactions and function, yet it is difficult to assign which aspect of the principles studied are attributable to the intrinsic properties of neurons in a tissue preparation, considering that many interactions among cells and target tissues are simultaneously occurring. To avoid these complications, neurons can be isolated in culture.

Many neuronal preparations have been developed using tissue culture technology in order to study the intrinsic physiological properties of neurons under

precisely controlled environmental conditions. Pharmacological agents can be introduced easily and effectively; electrical properties can be studied on visualized cells facilitating use of several different technical approaches; powerful molecular biological approaches (transfection of genes) can be effectively introduced, monitored, and manipulated as well. These techniques in conjunction with cell culture have provided the means to tease out and investigate many of the cell signaling pathways involved in key aspects of cell function. (see Darnell *et al.*, 1990), from general metabolic pathways to specialized expression arrays that may occur only during certain phases of a cell's lifetime.

In the case of crustacean neurons, various efforts have been made to culture them for at least the last 15 years. The first real success stemmed from efforts applied to the cell bodies of the X-organ - sinus gland system, the major neurosecretory structure of Crustacea. The culmination of this effort resulted in the publication of the article that comprises Chapter 2 of this dissertation. The neurons of the X-organ system, and crustacean neurons from other groups such as the stomatogastric ganglion (see Chapter 3 of this thesis) possess characteristics enabling them to regenerate neuritic outgrowth (send out processes) in culture medium as simple as saline supplemented with L-glutamine and D-glucose. This observation leads to two important points. First, that this system is particularly well suited for the study of intrinsic physiological mechanisms at the level of the single cell since the cells remain robust for at least a week without the addition of factors of any kind and will produce extensive process outgrowth. Second, that these simple external needs of the system

allow the research to focus attention on the inner workings of the cell. Clearly, such a complex program as neurite outgrowth depends on the coordination of many intracellular events. Moreover, the individual neurons dissociated from the heterogeneous X-organ cell group regenerating under defined conditions produce very distinct neuronal outgrowth patterns after a few days in culture. These patterns are observed unaltered under a variety of culturing conditions.

Significance of Process Outgrowth

The significance of process outgrowth from neurons is that it provides the biological substrate for connectivity of nervous system structure and function that in turn mediates sophisticated behavior during all stages of an animal's lifetime. During early development, an individual neuron's distal projecting processes, or growth cones, extend from initially spherical neuroblast cells to recognize and subsequently connect to appropriate target cells and tissues, thereby laying down the structural circuitry of the nervous system during development. Growth cone and process elongation also occurs during adult regeneration to serve to restore broken connections, and mediate neuronal plasticity, or the adaptive rearrangement of connections during adulthood.

There exists a rich history of studies addressing outgrowth mechanisms. Historically, this research area blossomed with the identification of the growth cone, first defined and described by Ramon y Cajal (1890) as "a living battering ram, soft and flexible, which advances, pushing aside mechanically the obstacles which it finds in its way, until it reaches the area of its peripheral distribution." (Ramon y Cajal,

1937). Cajal never saw a living growth cone and made the above inference based on observations of Golgi staining studies of nerve fibers *in vivo*. From about 1839 - 1910, the question of how nerve processes came about was very controversial. There were three camps. Schwann proposed that the fusion of chains of aligned sheath cells resulted in nerve fibers. The second, Hensen's theory, contended that nerve-target cell pairs result when incomplete cytokinesis and differentiation occur simultaneously forming daughter cell pairs. The third group was the Held camp, which believed that axonal formation occurred from thickening of already present, thin "fibrils" extending from cells in embryonic preparations he studied (Grisolia *et al.* (eds.), 1983). Harrison (1910) obtained evidence using the tissue culture technique, which he invented, to end this controversy. Tissue culture afforded the opportunity to separate out tissue types and make observations of cellular function without interference from other cell types and tissues. He explanted tissue from spinal cord into small drops of clotted lymph. He observed that isolated nerve cells grew via processes which elongated from the soma and was the first person to observe **living** growth cones.

Since then, a huge number of studies (for review, see Beadle *et al.* (eds.), 1988) have appeared using anatomical and physiological approaches to monitor outgrowth. Lines of work continue along many avenues (Letourneau *et al.* (eds.), 1991) . Growth cones are studied *in vivo* in an attempt to assess the mechanisms by which growth cones "choose" their paths and make selective interactions with targets, such as other neurons (Bentley and Keshishian, 1982; Bentley and Caudy, 1983). These studies focus on defining, or identifying, the environmental components

responsible for directing growth cone motility in the developing animal. Other studies have focused on analyzing the molecular constituents of the growth cones themselves. Unfortunately, it is difficult to isolate intrinsic properties of regeneration in the animal. There are few examples demonstrating differences in neuronal regeneration under differing culturing conditions. Frog retinal research provides a promising preparation. In the optic tract, there exist two functional types of axons; namely, the afferent retinal ganglion axons and the tectal efferents. If the nerve is severed, both types of axons experience the same injury under identical environmental conditions. If a response difference is detected, it should reflect intrinsic property differences of the neurons. In fact, what is observed is that the afferent cells regenerate and reinnervate their targets to reform near-perfect retinotectal projections while the efferent neurons do not regenerate much if at all (Fawcett, 1992).

Cell Culture: The Isolation From External Determinants

In order to study the subcellular intrinsic mechanisms that operate to produce and regulate neuronal morphology, it is advantageous to be able to define, or "clamp" extrinsic conditions so that the establishment of a morphological type can be studied in a controlled manner. Although intrinsic regeneration can be demonstrated at the tissue level, it is not a readily tractable system for systematically changing variables and observing the resulting behaviors. An ideal system for studying intrinsic regeneration mechanisms allows visibility of the entire neuron during regeneration, the ability for continuous observation of regeneration for days, and accessibility for experimental

manipulation. The system of choice for regenerative studies is dissociated cell culture since it provides all of these aforementioned conditions.

Many biological preparations have been exploited to study process outgrowth from neurons representing a wide variety of species. In most systems, the initiation of processes requires the addition of growth "factors". For example, neurons isolated from leech (Ready and Nicholls, 1979), sea hares (*Aplysia*) (Dagan and Levitan, 1981) fruit flies (*Drosophila*) (Wu *et al.*, 1983), pond snails (*Helisoma*) (Wong *et al.*, 1981), grasshopper (Seshan and Levi-Montalcini, 1973), mouse (Reichardt and Patterson, 1977), and rat (Patterson and Chun, 1974; 1977) appear to need supplementation to induce outgrowth. In most cases, these factors appear to be necessary to initiate outgrowth from both embryonic and adult starting material and represent extrinsic factors.

Haydon *et al.* (1985) published the first study comparing identified growth cones from molluscan buccal motorneurons B5 and B19 under identical cell culture conditions. The growth cones of B19 consistently have fewer filopodia, or needle-like extensions from the growth cone, longer filopodia, and a greater interfilopodial distance than the growth cones of B5. The behavior, or movement, of these growth cones differs as well. Outgrowth from B19 is halted by exposure to 1-10 μM serotonin, whereas outgrowth from B5 is unaffected. This is an example of a neurotransmitter acting on regeneration of an identified neuron, thereby demonstrating that growth cones are individually sensitive to specific environmental stimuli.

These studies are valuable for looking at environmental mechanisms in tandem, but they can not address what the intrinsic potential of the cell is. In fact since they need factors to initiate outgrowth, it could be argued that they do not have a baseline to start from when addressing intrinsic mechanisms of outgrowth.

Neurons that are capable of initiating outgrowth without these factors are somewhat of a rarity. To date, the only published exceptions to this rule are primary cell cultures from the molluscan peptide-secreting bag cells (Kaczmarek *et al.*, 1979) and crustacean neurons, which are cultured under completely defined medium. The *Aplysia* bag cell culture system uses a defined medium containing essential amino acids and vitamins in sea water. Similarly, crustacean neuronal cultures have been developed in our laboratory that also exhibit outgrowth in defined medium--as simple as saline with glucose--but routinely in a defined medium containing essential amino acids, vitamins, minerals, and glucose.

These crustacean cell cultures were developed from peptide secreting X-organ-sinus gland neurons (Cooke *et al.*, 1989; Chapter 2) from within the eyestalk and from physiologically identifiable stomatogastric ganglion neurons, (Graf and Cooke, 1990; Chapter 3), which are known to mediate rhythmic stomach movements in Crustacea and provide a model system for studying neural networks.

Electrical Activity and Outgrowth in Preparations from Other Species

Recent research on the effect of electrical membrane activity as a factor influencing outgrowth state includes a study in differentiated N1E-115 neuroblastoma

cells (Anglister *et al.*, 1982) and of unidentified vertebrate central nervous system neurons (Connor, 1986), pond snail (*Helisoma trivolvis*) neurons (Cohan and Kater, 1986) and in neuronal vertebrate preparations such as dorsal root ganglion neurons of fetal mice (Fields *et al.*, 1990), chick retinal ganglion neurons, (Ivins *et al.*, 1991) rat superior cervical dorsal root ganglion neurons, (Garyantes and Regher, 1992), and rat sensory neurons (Al-Mohanna *et al.*, 1992).

The neuroblastoma study (Anglister *et al.*, 1982) set the stage for this recent line of research by addressing the role that electrically induced Ca entry may play in regulation of neurite outgrowth. The study reported regional calcium membrane current observations from growth cones and from neurite regions, as demonstrated from simultaneous soma intracellular and neurite/growth cone extracellular microelectrode recordings. This study suggests that membrane channels are less abundant in neurite regions than in growth cone regions. This study also incorporated morphological observations to associate an increase in growth cone area with a high-K challenge. Long high-K stimulation (5X KCl for periods of 10 - 60 minutes) or electrical stimuli (20 - 120 minutes; 0.2 - 0.5 Hz) resulted in a significant increase in growth cone membrane in 60% of the cells, with some observation of neurite elongation as well. The inorganic calcium channel blocker, cadmium, at high concentrations (5 mM) blocked elongation, and Ca ionophores (A23187; 2 μM) increased the growth cone area and resulted in neurite elongation. Electrical stimulation in the presence of pharmacological blockers of Na and delayed rectifier K

current also cause an increase in growth cone area and neurite elongation. These observations pointed toward a role for calcium in regenerative outgrowth.

Subsequent studies to the seminal work by Anglister and colleagues followed on identified adult motorneurons from *Helisoma* dissociated in culture. Use of particular identified neurons acts to substantially lower variability in the experimentally obtained data. The first of this series (Cohan and Kater, 1986) showed that electrical activity caused suppression of neurite elongation and growth cone advance in all identified neurons tested, in a reversible fashion (Cohan and Kater, 1986). These experiments were only convincingly performed on neuron B19, in which an extracellular patch electrode was used to non-invasively stimulate the cell while monitoring growth cone behavior. Neurite outgrowth rates before and after stimulation occur at about 8 μm/hour with a significant suppression or retraction of growth cone advance occurring roughly 15 minutes after the beginning of stimulation (2 hours duration) of action potentials at 4 Hz--similar to the average action potential frequency in B19.

It is noteworthy that a similar effect was observed using patch pipettes where the whole-cell configuration was established, although the growth rate was 12 μm/hour before stimulation and was slowed to 4 μm/hour after stimulation. As was mentioned previously, in the case of the initial neuroblastoma cell study, 60% showed increased growth in response to action potentials induced for periods of 20 to 120 minutes, yet in *Helisoma* it is reported that electrical activity suppresses outgrowth. This disparity may be explained by species differences, neuron vs. cell line differences, or frequency

of stimulation differences. In the case of the neuroblastoma cells, stimulation was done in the presence of TTX to block Na channels and TEA to block the delayed rectifier channels, but in the *Helisoma* study the cells were studied under conditions where all the currents were active. It is difficult to assess which condition would facilitate the influx of more calcium since it depends on so many variables including current density, driving force, and current kinetics, to name a few.

Although this group did not identify or characterize the Ca current, they did provide pharmacological evidence that outgrowth was halted in the presence of Ca channel blockers: Co^{2+}, Cd^{2+} (Cd), and La^{3+} were added to the growth medium 20 hours post-dissociation (Mattson and Kater, 1987). Different concentrations of these Ca channel blockers had differing effects on the outgrowth observed. Low concentrations of La^{3+} (10^{-5} M) caused a decrease in filopodia number and an increase in the rate of neurite elongation. Higher concentrations of La^{3+} (10^{-4} M) also suppressed neurite elongation. Similar results were found for low and high concentrations of the divalent ions Cd^{2+} and Co^{2+}.

Studies on vertebrate neuronal cells corroborate the findings on invertebrate material. Using fetal mouse dorsal root ganglion (DRG) neurons, Fields and colleagues (1990) show that the resultant growth cone response depends on the pattern of electrical stimulation used on the regenerating neuron. Phasic patterned stimuli halted or caused a retraction of neurites--both the lamellipodia and filopodia. In some cases neurite retraction occurred as well. Block of action potentials with TTX

eliminated effects on growth cone behavior of electrical stimulation. Constant stimulation was less effective at halting outgrowth than pulsed stimuli.

Interestingly, the neurons appear to accommodate to the growth halting effects of phasic stimulation by extending neurites if the stimulation is on the order of one day or longer. The authors suggest that the cell accommodates to the challenge by using Ca buffering mechanisms to compensate for the stimulus.

Intracellular Ca Levels and Outgrowth

In order to begin to assess what the net effect of Ca influx into the neuron might be, methods were sought to monitor the resulting neuronal $[Ca^{2+}]_i$. The recently developed intracellular free calcium indicator fura-2 facilitated these studies (Grynkiewicz *et al.*, 1985). Fura-2 is a highly fluorescent Ca indicator with a higher specificity for Ca than other divalent cations. This indicator shifts its excitation wavelength upon binding or unbinding Ca yet it maintains strong fluorescence. The cell fluorescence can be determined with excitation light at two wavelengths and these images can be ratioed to signal Ca independent of the variability caused by gradients in dye concentration, cell thickness, or the content of effective dye, within reasonable limits. The first study to use this indicator to detect levels of $[Ca^{2+}]_i$ within regenerating neurons in culture was performed on unidentified embryonic rat (day 17 or 18) central nervous system diencephalon cells (Connor, 1986). These neurons showed higher $[Ca^{2+}]_i$ in growth cones undergoing regeneration than in other regions of the cell. Newly established growth cones had $[Ca^{2+}]_i$ of 500 nM while growth cones

that were farther away from the soma had $[Ca^{2+}]_i$ of 200 nM or more, while the soma levels were 60-80 nM. Application of saline having five times (5X) normal K for 20 seconds was shown to cause repetitive action potentials at 10 Hz in these cells that were accompanied by increased $[Ca^{2+}]_i$ in soma regions of approximately 250 nM. $[Ca^{2+}]_i$ continued to increase during for the duration of the high K application. It is noteworthy that upon applying a patch pipette to the side of the neuron the Ca increased six-fold without stimulation being applied. In young cultures under 24 hours post-dissociation, growing neurites with high $[Ca^{2+}]_i$ could be halted by changing the growth medium to a HEPES-buffered Kreb's saline, which caused the $[Ca^{2+}]_i$ to decrease to near rest values, but the mechanism by which this Ca decrease occurs is not known. Blockers of voltage activated channels such as TTX and nifedipine had no effect on stopping outgrowth or reducing regionally higher $[Ca^{2+}]_i$. This study found that the inorganic Ca channel blockers Cd and Mn could not be used without generating uninterpretable fura-2 data.

The variation seen in the Connor study may be due to the preparation, which used unidentified cells. This heterogeneous set of cells might be expected to give a wider variation of observations. To get around this problem, identified neurons were used. A study using identified motorneurons B5 and B19 was generated that helped elucidate which of the many mechanisms that regulate calcium in neurons might contribute to outgrowth (Cohan *et al.*, 1987). This study showed that evoked action potentials and neurotransmitter stimuli lead to increased levels of intracellular calcium in the neurons, and that gradients of $[Ca^{2+}]_i$ exist in neurons undergoing active

regeneration. This study differed from the initial neuroblastoma study (Anglister *et al.*, 1982) in that an extracellular patch pipette was used to stimulate the cell, a much less invasive technique. At 3 Hz for 300 s, calcium levels increased from a resting value of about 100 nM to about 600 nM and came back to rest again. This study also showed selective responses to neurotransmitters known to inhibit outgrowth from one cell type (B19), but not the other (B5) (Haydon *et al.*, 1985). Cohan *et al.* (1987) show that outgrowth changes are paralleled by calcium responses from the neurons: B19's calcium increases but B5's does not in response to serotonin application.

This work relating calcium levels to outgrowth led to subsequent studies on a variety of preparations that culminated in a proposal (Mattson and Kater, 1987; Kater and Mills, 1991) that there exists an optimal range of $[Ca^{2+}]_i$ for a given neuron that can determine the outgrowth status for the given growth cone. If the $[Ca^{2+}]_i$ is above or below this optimal range, the growth cone retracts, or neurite extension is halted, respectively. This general theory has provided a useful framework for further studies on factors influencing growth cone behavior and resultant outgrowth pattern.

This theory generated controversy since a handful of researchers have reported observations that do not "fit" it (Silver *et al.*, 1989; Ivins *et al.*, 1991; Garyantes and Regher, 1992). Using N1E-115 neuroblastoma cells, Bolsover and colleagues (Silver *et al.*, 1989) have reported that motile growth cones that were not advancing did have higher $[Ca^{2+}]_i$ in the growth cones than growing cells, but the observation that quiescent (not extended) growth cones and actively growing growth cones had "low and equal" calcium concentrations sparked controversy. Subsequent studies on

cultured neurons continued the controversy. Raper and colleagues (Ivins *et al.*, 1989) show that high K^+ depolarization transiently increased calcium levels several hundred nanomolar but "did not affect the rate of growth cone advance, nor did it have significant effects on growth cone morphology" (Ivins *et al.*, 1989). A similar observation was reported from studies using electrical stimulation from rat superior cervical ganglion neurons in culture (Garyantes and Regher, 1992). The difference is that outgrowth persists using conditions, (action potentials), very similar to those that halt outgrowth from identified neurons of the pond snail *Helisoma trivolvis*. The electrical activity caused $[Ca^{2+}]_i$ increases, just as in *Helisoma*, but growth cones continued to extend under these conditions.

A recent development in this controversy is a report by the Bolsover group on cultured rat sensory neurons (Al-Mohanna *et al.*, 1992) in which they claim that neurite outgrowth occurred over a narrow range of calcium with optimal outgrowth occurring at 35 nM. In contrast to an earlier report (Silver *et al.*, 1989) this laboratory is now claiming that their observations "provide direct evidence for Mattson and Kater's suggestion of an optimal calcium range for growth cone function (Al-Mohanna *et al.*, 1992).

The previous studies used electrical stimulation and high potassium depolarization as stimuli to increase calcium levels. These two stimuli represent depolarizing stimuli but may not represent mechanisms that increase Ca using identical modes of action. In an attempt to increase calcium levels in a receptor-independent fashion, Mills and Kater (1990) used the calcium ionophore A23187 to increase

calcium levels. They show that the calcium economies, or the mechanisms by which identified neurons can regulate intracellular calcium levels, differ with cell identity. These differences were found to correlate with both the neuronal identity of the cell and its outgrowth state. Motoneuron B19 consistently showed a reduced ability to compensate for an experimentally-induced calcium increase. By contrast, neuron B5 had a much larger "clearance capacity", or ability to lower the calcium levels in response to a calcium increase. These clearance mechanisms were found to correlate with the neuron's ability to lower calcium levels in reduced external sodium saline. Growing and non-growing B5s possessed the capability to regulate their calcium levels in reduced sodium saline. After the addition of calcium ionophore to sodium depleted saline to growing and stable-state cultures of B5s, the cells were unable to regulate the calcium and calcium levels rose to and maintained levels of several micromolar. The cells subsequently died. By contrast, in cultures with normal medium and calcium ionophore added, growing and stable-state B5s were consistently able to reduce the calcium load to rest. Only stable outgrowth state B19s were able to reduce their calcium load in normal medium, with growing B19s unable to compensate the calcium load. This study points to different mechanisms existing for regulation of calcium in these neurons, depending on growth state and cell identity.

In summary, although initially electrical activity was shown to be an important mechanism for outgrowth in many systems, it does not appear to be the universal mechanism. $[Ca^{2+}]_i$ does appear to play a role in outgrowth mechanisms, but the route

to the calcium level changes may be of secondary importance, especially if the neuron possesses multiple mechanisms for changing its $[Ca^{2+}]_i$.

CHAPTER 2

CRUSTACEAN PEPTIDERGIC NEURONS IN CULTURE SHOW IMMEDIATE OUTGROWTH IN SIMPLE MEDIA[1]

Abstract

The survival and outgrowth of neurons in culture has usually required conditioning factors. We now report that crustacean neurons, taken from the peptidergic neurosecretory system of the eyestalk of crabs (*Cardisoma carnifex*) and lobsters (*Panulirus marginatus*), show immediate outgrowth, sustained for a week or more, in defined media as simple as physiological saline with glucose and glutamine. The neurons show peptide hormone immunoreactivity that is prominent at growth cones, exhibit differences in form correlated with their immunoreactivity, release peptides to the medium, and have voltage-dependent currents, including a well-sustained Ca-current. Cd blocks secretion, growth, and the Ca current. Peptidergic secretory neurons may be able to utilize existing membrane from their store of granules and already-active synthetic, transport and secretory mechanisms for immediate outgrowth. The mechanisms governing the outgrowth of neuronal processes and the mature form of neurons remain largely unknown. Isolation of neurons in culture potentially provides the possibility of undertaking experimental manipulations

---

[1]**Published previously as Cooke, Graf, Grau, Haylett, Meyers, and Ruben. 1989. *PNAS* 86**: 402-406.

under controlled conditions. However, while outgrowth in low density cultures has now been demonstrated for vertebrate (1-5), annelid (6,7) and molluscan (8-11) preparations, the need for addition of undefined factors has frustrated rigorous studies of the control of outgrowth and form. We report that crustacean neuroendocrine cells show immediate, vigorous outgrowth on a variety of substrates in defined media as simple as physiological saline and glucose. We propose that this capability for immediate outgrowth is made possible by the utilization of already-active synthetic, transport and secretory mechanisms for growth. Different forms of outgrowth are consistently obtained from the heterogeneous group of neurons cultured, and reactivity with antisera raised against peptide hormones suggests correlations with the biosynthetic capabilities of the neurons. These neurons in culture, with their differences in form, thus provide a promising defined starting point for testing hypotheses about mechanisms governing the control of growth and form in regenerating neurons. We are unaware of any previous report of crustacean neurons in culture (12). Abstracts describing some of our work have appeared (13-15).

Introduction

The neurons cultured in these studies form the major neuroendocrine system of crustaceans, the X-organ - sinus gland system of the eyestalk (16, review: 17). For the tropical land crab, *Cardisoma carnifex*, used for most of the work to be discussed,

there have been studies of the morphology of nerve terminals (18), electrophysiological characterization of somata, axons, and terminals (19-22), studies of secretory capabilities (22,23), and characterization of the hormonal peptides present (24), and their biosynthesis (25). These provide a background against which the cultured cells can be evaluated.

The "X-organ" of crabs is a discrete cluster of about 200 iridescent-white neuronal somata (26). These send their axons to terminate as clusters of large (up to 30 μm) dilatations in a neurohemal organ (the "sinus gland"). Two size-classes of neurons are present and are associated with different hormonal peptides on the basis of reactivity to antisera as observed in histological studies: Small neurons (15-25 μm soma diameter) with red-pigment-concentrating hormone (RPCH) (27), and large neurons (30-70 μm) with several peptides and hormonal activities (28), including the most prevalent peptide-hormonal activity, crustacean hyperglycemic hormone (CHH) (29), and molt-inhibiting hormone (MIH) (30). The cells showing outgrowth in culture reflect these size classes and the immunoreactivity shown by the X-organ cells *in situ*. The observations suggest that the form of outgrowth may be correlated with the biochemical competence of the neuron.

Materials and Methods

Animals and Dissection

Cardisoma carnifex were obtained from Christmas Island, Republic of Kiribati; *Panulirus marginatus* were bought in local fish markets. Dissections were performed in a horizontal-flow culture hood (Baker). Eyestalks were removed, rinsed with 70% ethanol, then opened and exposed to 3 changes of sterile crab saline (in mM: NaCl 440, KCl 11.3, $CaCl_2$ 13.3, $MgCl_2$ 26, Na_2SO_4 23, Hepes 10, pH 7.4 with NaOH) with antibiotics (100 units/ml penicillin, 0.1 mg/ml streptomycin, 0.25 µg/ml fungizone). The X-organ with ca. 2 mm of the sinus gland tract was dissected in antibiotic saline, placed in nominally Ca- and Mg-free saline with 0.1% trypsin (Sigma type IV or Gibco) for 90 min (24° C), then rinsed thoroughly with saline. Substitution of collagenase (Sigma type IV), protease (Sigma type IX) or collagenase-dispase (Boehringer-Mannheim) for trypsin gave similar results.

Cell Isolation and Culture Conditions

The routine culture medium consisted of Liebowitz L-15 (Gibco, as powder) reconstituted and mixed with an equal volume of crab saline of 1.75X normal concentration buffered with 20 mM Hepes (pH 7.6 - 7.8); 0.1 mg/ml gentamicin, 120 mM D-glucose, 2 mM glutamine were added immediately before use. Total osmolarity was 1100 mOsm. The dissected X-organs were transferred to a 50 µl drop of medium, the cells were separated by agitation with a stream of medium and

transferred to a culture dish, usually Primaria (Falcon 3801), as for all examples shown. Cultures were held in moist chambers (Billups Rothanberg) in the dark at 22 - 24°C.

Adherence and outgrowth were obtained on the following substrates: a) uncoated plastic dishes including Falcon 3801 and 3001, Permanox (Lux 5223), Corning 25000, and Tekmat plastek; b)Falcon 3001 dishes coated with one of the following attachment factors: 1 mg/ml poly-L-lysine (Sigma) (31), 10 mg/ml laminin (Bethesda Research Labs), 0.1 mg/ml Fibronectin (Cappel-Organon Teknika) (32); c) glass coated with poly-L-lysine. Cells did not show outgrowth on uncoated glass or on plastic coated with 2.5 - 10 µl/dish of Cell-Tak (Biopolymers), or 1 mg/ml gelatin (Gibco). For immunofluorescence, a hole was drilled in a plastic dish and a poly-L-lysine-coated cover glass attached.

Staining With Antisera

Cultures were fixed in 1% paraformaldehyde in crab saline. Cells were permeabilized with 0.1% Triton X-100 (33) and exposed to 3% powdered non-fat milk (Carnation) to prevent non-specific binding, incubated with antiserum for 24 h at 4°C, and reacted with fluorescein- (Sigma) or Texas Red- (Cappel) conjugated goat-anti-rabbit IgG for 30 min. The following antisera, all from rabbit, were used: a) anti-sinus gland homogenate conjugated to bovine serum albumin; b) anti-peptide D (24) conjugated to bovine serum albumin; c) anti-insect adipokinetic hormone, code 433, kindly supplied by H. Schooneveld (34,35); d) anti-crustacean hyperglycemic hormone

(28) and e) anti-molt-inhibiting hormone (28). The latter two were kindly provided by R. Keller. In no case did all cells exposed to antiserum show staining. Preimmune serum and antiserum preabsorbed with sinus gland extract were used as controls and were negative.

Electron Microscopy

Cultures were fixed in 4% phosphate-buffered (pH 7.4) glutaraldehyde and postfixed with 1% OsO_4, dehydrated with ethanol and embedded in LX 112 (Ladd) in the culture dish.

Electrophysiology

Voltage-clamp measurements were made under the whole-cell configuration of the patch-clamp technique, using an Axopatch-1C (Axon Instruments) patch-clamp amplifier with CV3 0.1 headstage (50 megohm feedback resistor). The culture medium was replaced by crab saline; the pipette contained (in mM): Potassium aspartate 300, mannitol 300, ATP 2, $MgCl_2$ 2, EGTA 2, $CaCl_2$ 0.3, streptomycin 1, Hepes 100 (buffered to pH 7.4 with KOH). For study of Ca current with minimal contamination by outward current solutions were K^+-free and contained (in mM): Extracellular - NaCl 44, $MgCl_2$ 24, $CaCl_2$ 13.3, Hepes 10, D-glucose 10, TTX 0.0002 (pH 7.5, adjusted with NaOH); intracellular - N-methyl-glucamine methane sulphonate 300; Mg-ATP 5, Cs4-bis (o-aminophenoxy)ethane-N,N,N',N'-tetraacetic acid () 5, Hepes 50, streptomycin 2, tetraethyl ammonium Cl 10. Tonicity was maintained at

1100 mOsm by addition of sucrose. Patch pipettes were pulled from WPI capillary tubing (TW150F-4), fire polished and coated with bees-wax. Pipette-to-bath resistances were ca. 6 megohms. Seal resistances were >1 gigaohm.

Results

Conditions and Time-Course of Neuronal Outgrowth in Culture

As rapidly as the culture can be put under the microscope following completion of dissociation procedures, cells that have adhered are found to have produced a corona of fine processes around the soma. Outgrowth from the axonal stump, if present and adhering, is seen at the same time. Within 16 hours, the form to be taken by each neuron is well defined. Growth continues for about 7 days in our routine defined medium, after which processes show varying degrees of retraction. Cells survive for at least three weeks. Assuming that the land crab X-organ has 200 neurons, about 40% survive and exhibit outgrowth. We conclude that neither outgrowth or form are dependent on enzymatic treatment of the neurons because we have obtained outgrowth of the same types following dissociations performed without enzyme treatment, as well as following treatment with a number of different enzymatic preparations (see Materials and Methods). However, the survival rate, particularly of larger neurons, is improved by enzymatic treatment that causes the cells to dissociate more easily, a result that we attribute to reduction of the trauma experienced by the neurons. Application of the same culturing procedures to the X-organ of spiny

lobsters, a phylogenetically well separated group, has given cultures showing comparable neuronal survival and forms of outgrowth. Thus we believe that our observations have general applicability and are not the reflection of some unique quality of the land crab principally used for this work.

No outgrowth is observed unless the cell adheres to the substrate. We now routinely use Primaria dishes, but have obtained adhesion and outgrowth of the same types on every type of untreated plastic tested, as well as on polylysine-treated glass (see Materials and Methods).

A number of lines of evidence lead to the conclusion that the neurons do not require any conditioning factors for their outgrowth. The sparsity of cells relative to the volume of medium makes self-conditioning unlikely. Cells exhibit outgrowth at normal rates and of normal form under the following circumstances: When the culture dish is flushed with fresh medium within an hour of plating the cells and changed daily thereafter; when individual neurons are grown in isolation; and when cells are plated in crab saline and glucose without any other additions. In saline, growth slows after two days and ceases soon after. If glucose and glutamine are included growth is sustained for up to a week. This indicates that the standard medium includes no unidentified critical component(s), and that the antibiotic routinely included is not influencing neuronal development.

Forms of Neuronal Outgrowth

The majority of larger (>25 μm) cells show a remarkable outpouring of membrane to form a broad lamellipodium or veil (Fig. 1a,b; Fig. 2a,b,e; Fig. 3 inset). The veil often covers an area larger than the soma within the first day and reaches two or three times the soma membrane area by the second day. Numerous filopodia extend from the margin of the veil. These later become thickened, with minute growth cones at their tips. Filamentous processes like those from the soma also grow from the neurite at areas of adhesion to the substrate. Growth ceases in 7 to 10 days, and retraction of the veil is seen after 14 days.

Cells of <30 μm consistently show a different, branching form of outgrowth (Fig. 1c,d). No processes are extended from the soma; they remain monopolar, with the major outgrowth occurring from the remaining axon at compact growth cones. Neurites reach lengths of ca. 150 μm within 7 days, after which growth slows or stops. A few of the larger cells plated from an X-organ also show outgrowth of a branching form (Fig. 1c). Unlike the smaller cells, processes are also frequently extended from the soma and proximal neurite.

Cells plated without an axonal stump, or whose axonal stump does not adhere, fail to develop a predominant neurite and instead augment the initial halo of fine processes (Fig. 1e).

Reactivity of Cultured Neurons to Antisera

The selectiveness of reactivity to different antisera confirms that neurons of the several biosynthetic types present in the XOSG system survive in culture and retain their distinct capabilities. Cultures having neurons with outgrowth of the various forms described above were exposed to the five antisera reactive to peptides of the X-organ - sinus gland system that were available to us. In each case, some, but not all cells showed reactivity. Certain correlations of cell size and form of outgrowth with antiserum reactivity have been consistently observed. Thus, for example, antiserum to insect adipokinetic hormone N-terminus, known to react with red pigment concentrating hormone (RPCH) (27,34,35), shows reactivity with a few of the small cells of branching morphology in a given culture (Fig. 2c), but never with large cells. Antiserum raised against crustacean hyperglycemic hormone (28) shows reactivity with cells having large veils (Fig. 2e), as does antiserum raised against Peptide D (24) (Fig. 2b), while antiserum raised against molt-inhibiting hormone (28) is reactive with large cells of branching morphology (Fig. 2d). The antiserum raised against crude sinus gland extract reacts with some of the large cells, but not with small cells in a given culture (Fig. 2a). Immunoreactivity is particularly intense in lamellipodia and filopodia.

Electron Microscopy

Electron micrographs of large cells confirm an abundance of microtubules and accumulations of secretory granules in branching processes (Fig. 1f). Granules are

aligned with bundles of microtubules, suggestive of ongoing rapid transport. Somata (not shown) show extensive arrays of rough endoplasmic reticulum (ER) indicating that intense synthetic activity is ongoing, as is also seen in sections of large X-organ somata in situ (unpublished observations). Small cells in situ have fewer granules in their somata and proximal neurite and less extensive ER, which we suggest may have bearing on their different form of outgrowth.

Secretion

If outgrowth involves incorporation of granule membrane by exocytosis, we would expect the release of neuropeptides into the medium by growing neurons. Media samples gave positive RPCH bioassays (36), even when media had been changed at 2-day intervals. Secretory responsiveness of the cells was indicated by increased amounts of neuropeptides present in samples taken after 40 min exposure to elevated [K] (100 mM) compared to amounts present after 2 days in normal medium.

Electrophysiology

Exocytotic secretion requires increased internal Ca concentration that, in neurons, involves the participation of voltage-dependent Ca channels (37). Recent studies (38,39) demonstrate elevated levels of Ca in growth cones relative to other parts of the neuron. Our proposal links these observations. Voltage-clamping of cultured veiling cells using tight-seal patch electrodes reveals, in addition to

tetraethylammonium- and 4-aminopyridine-sensitive outward currents (not shown), inward current that is attributable to Ca: It is unaffected by tetrodotoxin and blocked by the addition of Cd (Fig. 3), its amplitude is markedly decreased in saline containing 1/10th normal Ca. It is unchanged by changes of membrane holding potential between -40 and -60 mV, observable for steps to >-30 mV and maximal at +10 mV. Minimum time to peak is ca. 5 ms. Inward current initially decays rapidly, (τ < 20 ms) then more slowly (τ > 50 ms); at the end of a 160 ms pulse to +10 mV, >50% remains. Both inward and outward currents have been recorded from cells that have been in culture from 2 hours to 10 days.

Arrest of Outgrowth By Addition of a Calcium-Current Blocker

Consistent with an important role of Ca currents in growth (and a link with exocytosis), we observed that addition of 0.2 mM Cd to the culture medium halts outgrowth (see 39). Cd also inhibits secretion from the isolated XOSG system (22).

Discussion

Our results support the proposal (an expansion of a more general one by Bray [40]) that membrane may be added at growth cones by exocytosis of granules synthesized and transported by the mechanisms normally involved in secretion; the re-uptake of membrane is omitted, however. The presence in the newly plated cells of

abundant membrane, in the form of the neurosecretory granules, capable of being added to the surface of the cell, together with transporters (microtubules) for moving them to axon terminations, as well as activated synthetic processes for maintaining the granule population may account for the capability of these cells for immediate outgrowth. The predetermined form of the outgrowth and its independence of external conditioning factors is emphasized by the unaltered initial outgrowth observed in plain crab saline. We have even observed formation of a typical veil at one end of isolated axons. It should be noted, however, that the form and extent of outgrowth in these cultures do show changes in response to manipulations of the culturing conditions such as the addition of crab or bovine serum, incubation with whole sinus gland, or brief exposure to saline containing elevated K^+.

We suggest that differences in outgrowth form may reflect differences in abundance and distribution of granules and microtubules in concert with signals derived from surface membrane contact with the substrate. The role of internal Ca concentration in controlling the assembly and distribution of microtubules as well as the movement of granules by them (41) suggest the possibility that the density and activity of Ca channels in or near the growth cones play crucial roles in governing the form of outgrowth. We are thus interested to find that cells of branching morphology have much smaller Ca currents than those reported above for large veiling cells, although these observations must be regarded as preliminary. The small cells, which consistently show a branching morphology, have less abundant endoplasmic reticulum and granules in the soma. Additional work correlating fine structure,

electrophysiological characteristics, biochemical competence and the form of outgrowth should provide further insight.

To our knowledge, the only other neurons reported to show immediate outgrowth without conditioning factors are also peptidergic neurosecretory cells, the *Aplysia* bag cells (8,42). However, in contrast to our results, outgrowth from these cells has not been reported without the addition of amino acids and vitamins to the medium. The consistency of the time-course, forms and extent of outgrowth of the crustacean peptidergic neurons in our defined culture conditions provides a starting point for experimental manipulations to explore the control of neuronal growth and form.

References

1. Bray, D. (1973) *J. Cell Biol.* **56**, 702-712.

2. Fischbach, G. D. & Dichter, M. A. (1974) *Dev. Biol.* **37**, 100-116.

3. Furshpan, E. J., MacLeish, P. R., O'Lague, P. H. & Potter, D. D. (1976) *Proc. Natl. Acad. Sci.* U.S.A. **73**, 4225-4229.

4. Reichart, G. F. & Patterson, P. H. (1977) *Nature* **270**, 147-151.

5. Bottensten, J. E. & Sato, G. (eds.) (1985) *Cell Culture in the Neurosciences* (Plenum, New York, N.Y.)

6. Ready, D. F. & Nicolls, J. (1979) *Nature* **281**, 67-69.

7. Arechiga, H., Chiquet, M., Kuffler, D. P. & Nicolls, J. G. (1986) *J. Exp. Biol.* **126**, 15-31.

8. Kaczmarek, L. K., Finbow, M., Revel, J. P. & Strumwasser, F. (1979) *J. Neurobiol.* **10**, 535-550.

9. Wong, R. G., Hadley, R. D., Kater, S. B. & Hauser, G. C. (1981) *J. Neurosci.* **1**, 1008-1021.

10. Dagan, D. & Levitan, I. B. (1981) *J. Neurosci.* **1**, 736-740.

11. Schacher, S. & Proshansky, E. (1983) *J. Neurosci.* **3**, 2403-2413.

12. Thomas, E. W., Jordan, F. L., & Townsel, J. G. (1987) *Comp. Biochem. Physiol.* **87A**, 215-222.

13. Graf, R. A., Grau, S., Haylett, B., & Cooke, I. M. (1988) *Soc. Neurosci. Abstr.* **14**, 869, (abstract).

14. Meyers, D., Graf, R., Ruben, P., & Cooke, I. M. (1988) *Soc. Neurosci. Abstr.* **14**, 1128, (abstract).

15. Cooke, I., Graf, R., Grau, S. & Meyers, D. (1988) *J. Gen. Physiol.* **92**, 3a, (abstract).

16. Bliss, D. E., Durand, J. P. & Welsh, J. H. (1954) *Z. Zellforsch. Mikrosk. Anat.* **39**, 520-536.

17. Cooke, I. M., & Sullivan, R. E. (1982) in *The Biology of Crustacea*, ed. Bliss, D. E. (Academic Press, New York, NY), Vol. 3, pp. 205-290.

18. Weatherby, T. (1981) *Cell Tissue Res.* **220**, 293-312.

19. Cooke, I. M. (1985) *J. Exp. Biol.* **118**, 1-35.

20. Lemos, J. R., Nordmann, J. J., Cooke, I. M., & Stuenkel, E. L. (1986) *Nature* **319**, 410-412.

21. Nagano, M. & Cooke, I. M. (1987) *J. Neurosci.* **7**, 634-648.

22. Stuenkel, E. L. (1985) *J. Physiol.* **359**, 153-187.

23. Stuenkel, E. L. & Cooke, I. M. in *Current Topics in Neuroendocrinology*, eds. Ganten, D. & Pfaff, D. (Springer-Verlag, New York, NY) Vol. 9, 123-150.

24. Newcomb, R. W. (1987) J. *Neurochem.* **49**, 574-583.

25. Stuenkel, E. L. (1986) *Peptides* **7**, 397-406.

26. Potter, D. (1956) Observations on the Neurosecretory System of Portunid Crabs. Ph.D. Thesis, Harvard University, Cambridge, MA, 298 pp.

27. Mangerich, S., Keller, R., & Dircksen, H. (1986) *Cell Tissue Res.* **245**, 377-386.

28. Dircksen, H., Webster, S. G., & Keller, R. (1988) *Cell Tissue Res.* **251**, 3-12.

29. Keller, R., Jaros, P. O. & Kegel, G. (1985) *Amer. Zool.* **25**, 207-221.

30. Chang, E. S., Bruce, M. J. & Newcomb, R. W. (1987) *Gen. Comp. Endocrinol.* **65**, 56-64.

31. Letourneau, P. C. (1975) *Dev. Biol.* **44**, 77-91.

32. Hammerback, J. A., Palm, S. L., Furcht, L. T., & Letourneau, P. C. (1985) *J. Neurosci. Res.* **13**, 213-220.

33. Theodosis, D. T., Legendre, P., Vincent, J. D. & Cooke, I. (1983) *Science* **221**, 1052-1054.

34. Bellon-Humbert, C., van herp, F., & Schooneveld, H. (1986) *Biol. Bull.* **171**, 647-659.

35. Schooneveld, H., van Herp, F. & van Minnen, J. (1987) *Brain Res.* **406**, 224-232.

36. Cooke, I. M., Haylett, B. A., & Weatherby, T. M. (1977) *J. Exp. Biol.* **70**, 125-149.

37. Rubin, R. P. (1982) in *Calcium and Cellular Secretion* (Plenum, New York, NY).

38. Mattson, M. P. & Kater, S. B. (1987) *J. Neurosci.* **7**, 4034-4043.

39. Cohan, C. S., Connor, J. A., & Kater, S. B. (1987) *J. Neurosci.* **7**, 3588-3599.

40. Bray, D. (1973) *Nature* **244**, 93-96.

41. Ochs, S., Gaziri, J. C. J., & Jersild, Jr., R. A., in *Axoplasmic Transport*, ed. Iqbal, Z. (CRC, Boca Raton, FL), pp. 57-68.

42. Forscher, P., Kaczmarek, L. K., Buchanan, J., & Smith, S. J. (1987) *J. Neurosci.* **7**, 3600-3611.

Figure 2-1. Morphology of crustacean peptidergic neurosecretory cells in primary culture. Photomicrographs of neurons isolated from the X-organ of *Cardisoma carnifex* (except **b**, *Panulirus marginatus*) in defined medium (phase-contrast images of living neurons except **f**). **a** and **b**: Cells exhibiting extensive veils, 7 and 2 days in culture. **c**: Cell showing branching outgrowth, 4 days (Hoffman modulation contrast). **d**: Small cell of the type associated with red-pigment-concentrating hormone reactivity, 2 days. **e**: Morphology typical of cells plated without a neurite, 14 days. **f**: Electron micrographs of a horizontal section through a filopodial process of a veiling cell, 14 days. Note density of secretory-type granules and (**inset**) apparent alignment with microtubules.

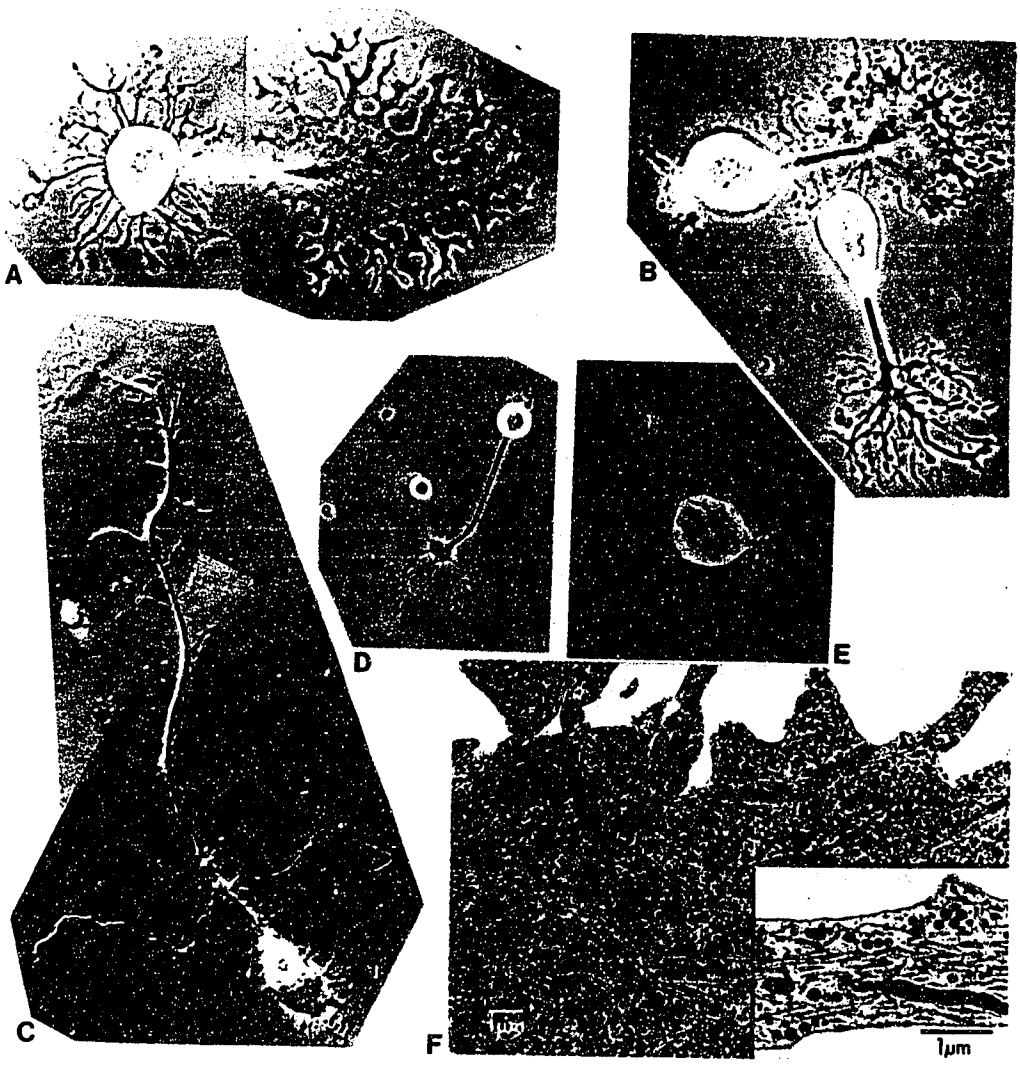
A
B
C
D
E
F
1μm

Figure 2-2. Immunofluorescence of crab peptidergic neurons in primary culture. The fluorescent second antibody was Texas Red, except **e**, FITC; the primary antisera, and days in culture of the cells were as follows: **a**: anti-sinus gland homogenate conjugated to bovine serum albumin (BSA) 1:500, 10 days; **b**: anti-Peptide D-BSA 1:1000, 8 days; **c**: anti-AKH N-terminus 1:2000 (reactive with red-pigment-concentrating hormone), 8 days; **d**: anti-molt-inhibiting hormone 1:1000, 7 days; **e**: anti-crustacean hyperglycemic hormone 1:5000, 7 days. Note brilliant staining of veils (**a, b, e**), granular appearance of staining in **c** (processes extending to the left and right edge of the photo were dimly stained but did not reproduce).

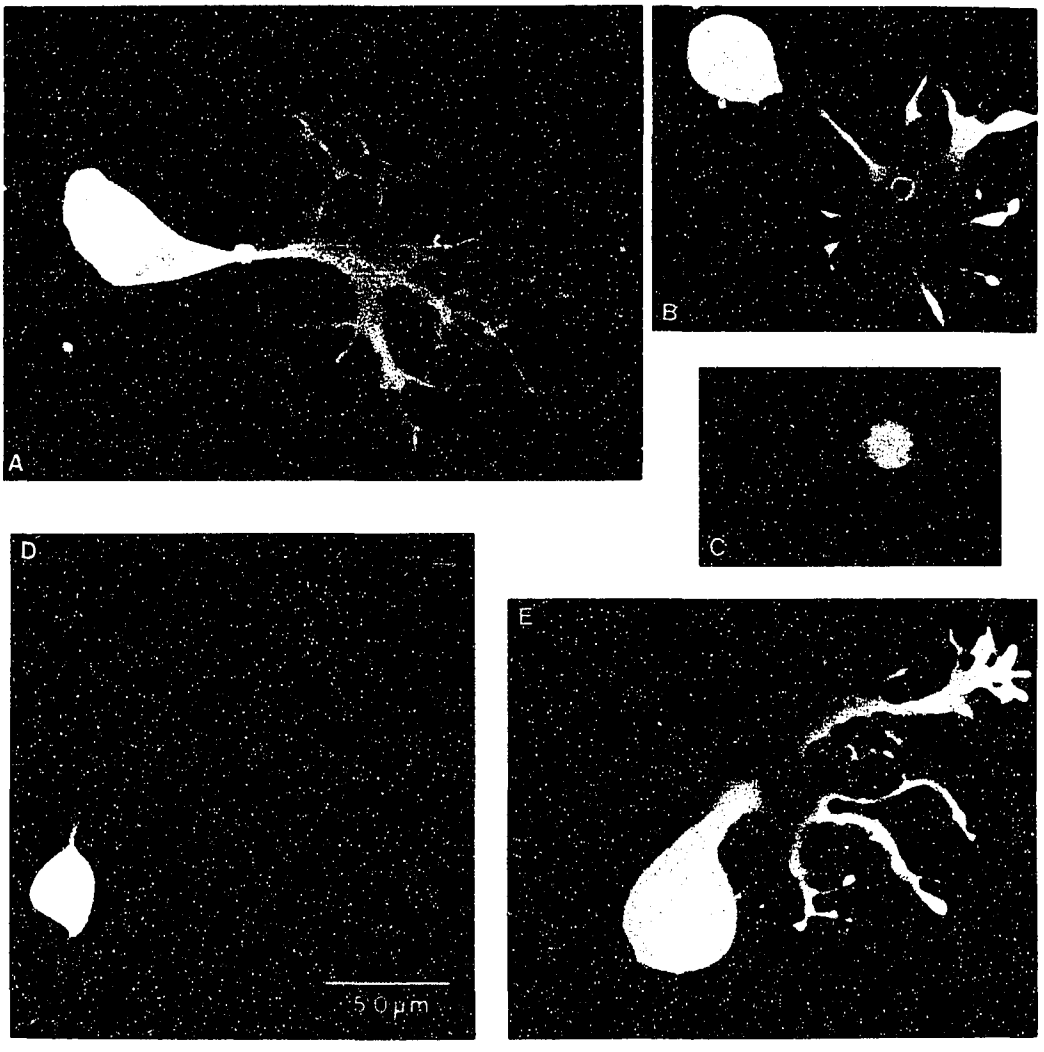
A
B
C
D
50 µm
E

Figure 2-3. Current-voltage [I(V)] relationship for Ca current measured at the end of 160 ms voltage steps before (control O) and after exposure to Cd (O). Whole-cell configuration of patch clamp, with monovalent ion-deficient solutions, membrane potential held at -40 mV and stepped from -80 to +50 mV in l0 mV increments (17). The magnitude of current and form of this I(V) curve are typical of those obtained from >10 cells having large veils. **Inset (top)**: Photomicrograph (Hoffman modulation contrast) of the neuron taken immediately before the recordings were made. The neuron was plated 12 h prior to making the recordings. Note large veil. **Inset (below)**: Examples of recordings: Superimposed current traces in response to step to +10 before and after exposure to Cd (0.2 mM), from data used to construct the graph.

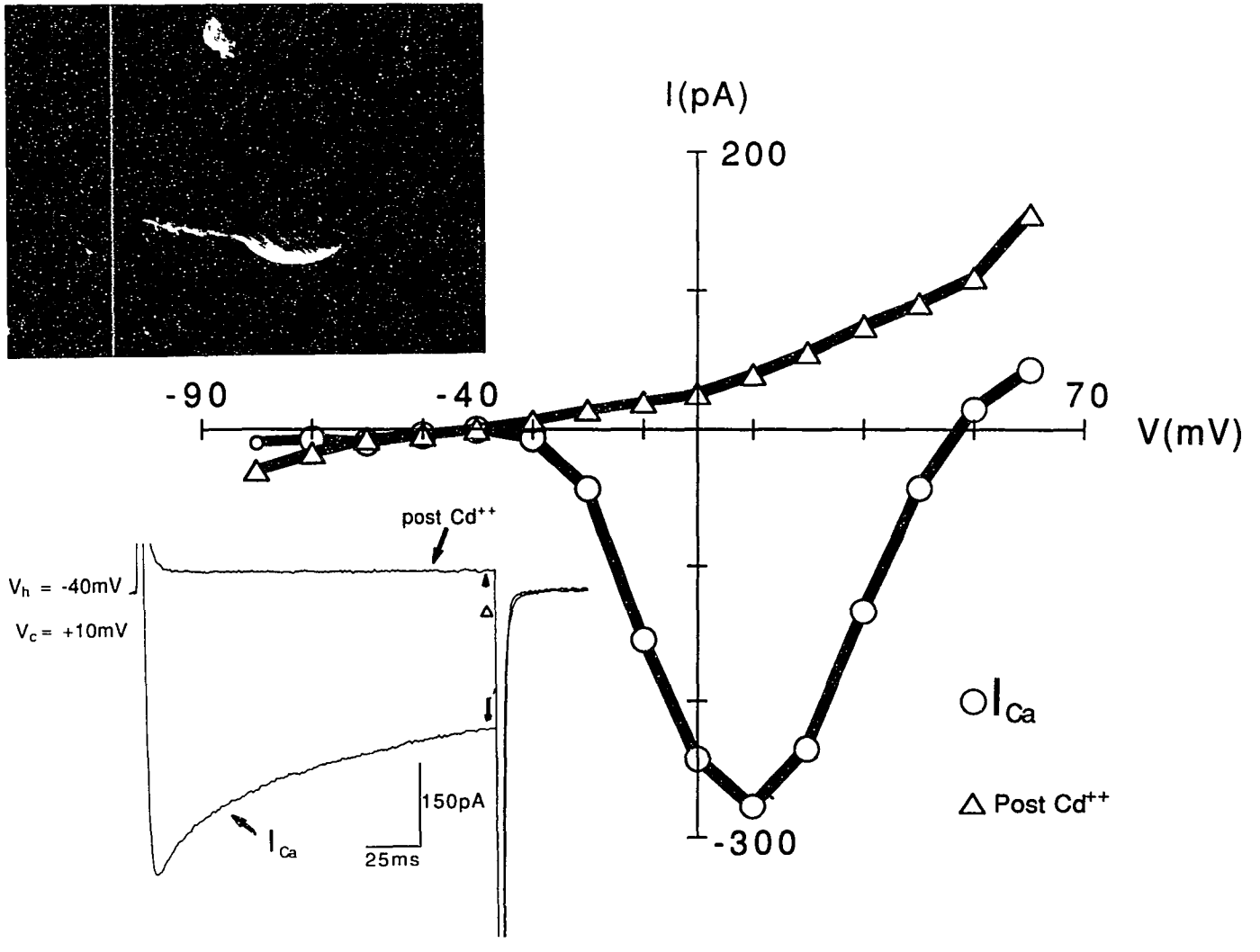
I(pA)
200
-90
-40
70
V(mV)
-300
post Cd++
Vh = -40mV
Vc = +10mV
150pA
25ms
ICa
ICa
Post Cd++

CHAPTER 3

PRIMARY CULTURE OF CRUSTACEAN STOMATOGASTRIC GANGLION NEURONS IN DEFINED MEDIUM[1]

Introduction

The crustacean stomatogastric ganglion, consisting of about 30 reidentifiable neurones, produces several distinct patterned outputs governing rhythmic movements of the stomach. This preparation has become a model system for addressing cellular properties and synaptic interactions underlying pattern generation in neural networks (see Selverston & Moulins, 1987). Studies of the system have been limited by the need to use acutely isolated intact or semi-intact ganglion preparations. Also, while interesting membrane responses and synaptic interactions occur in neuropil, recording from sites other than the somata has been difficult using an intact preparation.

Primary culture of dissociated neurones from the ganglion may yield new insights on regional membrane properties and long-term (days) responses to neuromodulators of individual neurones that have regenerated neuritic processes.

This paper presents our culture methods and some observations of outgrowth from neurones that have been dissociated from the stomatogastric ganglia of two evolutionarily diverse species, the Maine lobster, *Homarus americanus*, (Fig. 1) and a tropical semi-terrestrial crab, *Cardisoma carnifex* (Fig. 2). The only other study on stomatogastric neurones in culture of which we are aware used a freshwater crayfish,

---

[1]**Graf and Cooke 1991.** *J. exp. Biol.* **49**: 521-525.

(*Pacifastacus lenusculus*), in which neurones were plated in media supplemented with serum (Krenz & Fischer, 1988).

Methods

The culturing procedure is based on that developed for crustacean X-organ neurones (Graf *et al.*, 1988; Cooke *et al.*, 1989) with a number of modifications that optimize conditions for culturing the larger and more delicate stomatogastric neurones. Ganglia were removed from adult animals with 0.5 cm lengths of connective, and submerged for 5 minutes in an antibiotic crab or lobster saline containing 100 units ml^{-1} penicillin-G, 75 units ml^{-1} streptomycin, (both from frozen powder); and 0.25 µmol ml^{-1} fungizone (all from Gibco), pH 7.6. The dissection and plating were performed in a laminar horizontal flow hood (Baker) using a Wild M5 dissecting microscope equipped with fiber optic illumination. Dissected ganglia were transferred to 35 mm culture dishes containing an enzymatic saline: 2 mg ml^{-1} collagenase/dispase (Boehringer Mannheim) and 0.4 mg ml^{-1} elastase I (Sigma) in crab or lobster saline (pH 7.6) sterilized by filtration (0.22 µm pore size). The covered dishes were agitated (22 cycles min^{-1}) on a shaker for one hour at room temperature. Somata with neurites were further separated from their surrounding ganglionic tissues by freeing the loosened connective tissue using a fine jet of enzymatic saline blown from a capillary tube drawn down to an inner tip diameter of 10 - 20 µm. The dangling somata, held to the ganglion by their neurites, were rinsed of enzyme with two changes of filtered antibiotic saline. Unidentified somata were then individually aspirated using ethanol-

sterilized capillary tubes, pulled and fire polished to yield a smooth tip with an inside diameter of roughly 100 μm. The neurones were plated onto 35 mm culture dishes (for substrate, see below) containing 2 ml of defined medium; the fluid depth was approximately 2 mm. The defined medium was prepared by mixing sterile Leibowitz-15 (L-15, Gibco) with an equal volume of buffered double strength crab or saline (pH 7.9, 20 mmol l^{-1} HEPES) containing nutrient and antibiotic constituents. At final volume, these were: 120 mmol l^{-1} D-glucose, 2 mmol l^{-1} L-glutamine (from frozen stock), and 0.1 mg ml^{-1} gentamicin. Without adjustments, the final medium pH was usually near the optimal value, 7.7. Medium was usually made just prior to use. The substrates used included uncoated Primaria dishes (Falcon 3801) and Falcon 3001 dishes coated with sterile 0.1 mg ml^{-1} poly-L-lysine (Sigma). After neurone dispersal, the dishes were covered and not moved for at least 2 hr to aid neuronal adhesion to the substrate. They were then transferred to a sterile, humidified portable incubator chamber (Billups Rothanberg), and placed in the dark at room temperature (20 - 21° C).

Results

Outgrowth generally occurred from sites where membrane was in direct contact with the substrate. If only the soma contacted the substrate, with primary neurite suspended in the medium or severed during dissociation, it sometimes adhered via sparse, thin, membranous protrusions that cling to the dish after one day in culture (not shown). Extensive outgrowth occurred if the severed end of the primary neurite

adhered to the substrate. Two forms of outgrowth predominated: A large, thin, veiling (lamellipodial) type (Fig. 1, d), and a directed branching type (Fig. 1, a; Fig. 2). These forms were not mutually exclusive (Fig. 1, b and c) and when both types were present, the neurone's growth was in transition, usually from veiling to branching. Maximum veil size was typically reached by day 2 and was maintained for a week in static culture. The breadth reached by the veil roughly equaled the soma diameter. The margins of veils were skirted with growth cones that appeared phase dark under phase contrast optics (not shown).

Neurones displaying the more directed (linear) growth morphology (Fig. 2) developed neuritic extensions that represented the stabilization of processes following outgrowth from one or a few motile growth cones. The neuritic processes arose from the periphery of a veil within a day of plating (compare day 1 and day 2 of Fig. 2). Well stabilized regions of the major neurites often appeared to have filamentous structures in parallel array (Fig. 2, day 2).

The neurones having well-directed outgrowth continued to show process elongation in static culture up to day 7, at which time the cultures were used for other purposes. Typical neurite extension rates may be seen by comparing the leading growth margins of the *Cardisoma* neurone shown in Fig. 2. From day 1 to day 2 the primary neurite elongated 165 µm, and from day 2 to day 3 the new growth traversed 143 µm. These growth rates varied from cell to cell with a range of 80 - 170 µm per day.

Discussion

Previous *in situ* EM indicates that stomatogastric somata and primary neurites are entirely covered by an unbroken glial sheath (King, 1976) which may explain why it was necessary to change the enzymatic regime from that used for the X-organ neurones. These appear to separate more easily from surrounding glia or other material.

Successful outgrowth appears to depend largely on whether conditions are provided that favor neuronal adherence and direct contact with the substrate.

Since these neurones grow vigorously in a simple medium that is completely defined, exploration of conditions and factors that modify cell outgrowth and electrical responses should be facilitated.

References

Cooke, I., Graf, R., Grau, S., Haylett, B., Meyers D., and Ruben, P. (1989). Crustacean peptidergic neurons in culture show immediate outgrowth in simple medium. *Proc. Natl. Acad. Sci. USA* **86**, 402-406.

Graf, R. A., Grau, S., Haylett, B., & Cooke, I. M. (1988). Crustacean peptidergic neurons in primary culture show immediate outgrowth in defined media. *Neurosci. Abstr.* **14**, 869.

King, D. (1976). Organization of crustacean neuropil. II. Distribution of synaptic contacts on identified motor neurons in lobster stomatogastric ganglion. *J. Neurocytol.* **5**, 239-266.

Krenz, W. D. & Fischer P. (1988). Ionic conductances in crustacean stomatogastric neurons in primary culture. *Neurosci. Abstr.* **14**, 295.

Selverston, A. I. & Moulins, M. (1987). *The Crustacean Stomatogastric System.* New York: Springer-Verlag.

Figure 3-1. Photomicrographs of outgrowth from isolated *Homarus americanus* stomatogastric neurones. A: low power phase contrast image of soma with residual axon and lateral processes, 2 days in culture. Arrow marks end of residual axon. B: higher power image of the growth cone from A taken at the same time as A. C: Same growth cone on day 3. Note directed growth extending from the veil. D: Composite photographs pieced together from 2 focal planes (soma and growth cone) to give an example of neuronal surface membrane contour. Note large veil, day 2 in culture. B - D: Hoffman modulation contrast microscopy. All cells in defined medium. Calibration bars = 50 μm.

Figure 3-2 Hoffmann modulation contrast images of directed outgrowth from a *Cardisoma carnifex* stomatogastric neurone at different culture ages (as indicated) in static defined medium. At day 1, filapodia are seen at peripheral margin of small veil. By day 2, there has been extensive directed outgrowth from day 1 filapodia. Further extension of several processes occurred by day 3. Note fibrillar appearance of the stabilized major neurite.

2
Day 1
Day 2
Day 3

CHAPTER 4

IONIC CURRENTS OF MORPHOLOGICALLY DISTINCT PEPTIDERGIC NEURONS IN DEFINED CULTURE[1]

Summary and Conclusions

1) The X-organ - sinus gland is a major peptidergic neurosecretory system in Crustacea, analogous to the vertebrate hypothalamo-neurohypophyseal system. Neuronal somata isolated from the crab (*Cardisoma carnifex*) X-organ and maintained in primary culture in unconditioned, fully-defined medium show immediate regenerative outgrowth. Outgrowth occurring as broad lamellipodia ("veiled") distinguishes neurons consistently showing crustacean hyperglycemic hormone immunoreactivity. Neurons that are immunoreactive against molt inhibiting hormone and red pigment concentrating hormone antisera give rise to branched neurites ("branched").

2) The whole-cell variation of the patch-clamp technique was used to study the electrophysiology of these two cell types 24 to 48 hr after plating. Under current-clamp, only veiled neurons fired overshooting action potentials either spontaneously or in response to depolarization.

---

[1]Meyers, D. E. R., Graf, R. A., and Cooke, I. M. (1992) *J. Neurophysiol.* 67: 1301-1315.

3) Under voltage-clamp, net current was predominantly outward. Using solutions which suppressed outward current, only veiled neurons showed significant inward current. These included a tetrodotoxin (TTX)-sensitive Na current and a slow (time to peak 6-10 msec at 0 mV) Cd-sensitive Ca current (I_{Ca}) that was activated at potentials >-30 mV, was maximal at 0 to +20 mV and did not reverse at potentials up to +60 mV.

4) In TTX, the form of the Ca current I(V) curve was unchanged by changes of holding potential between -40 and -80 mV, and 75 to 100% of I_{Ca} was available from -40 mV.

5) I_{Ca} inactivated slowly and incompletely. Analysis with two-pulse regimes suggested that both inactivation and facilitation mechanisms were present.

6) Outward current was examined in the presence and absence of 0.5 mM Cd^{2+} (1 μM TTX was always present in the external medium). Cd^{2+} ions slightly *reduced* the peak outward current, usually by <10% (V_C = -10 to +20 mV; V_h = -80 mV). All additional observations were in the presence of TTX and Cd_{2+}.

7) Both cell types expressed a 4-aminopyridine (4-AP)-sensitive transient current, analogous to I_A and a slower-rising (minimum time to peak, 20 msec), sustained current that was partially sensitive to tetraethylammonium (TEA) analogous to I_K.

8) The mean V_h at which I_A was half inactivated was -46 mV and the mean time constant for removal of inactivation was 46 msec. The time-constant for inactivation of I_A approached a minimum of 4 msec during depolarizations to >0 mV.

9) In about 60% of cells tested, 4-AP blockade of I_A resulted in an *increase* in I_K of 30 - 80%.

10) Reversal potentials of tail currents in normal K^+ (11 mM) were on average 15 mV depolarized to the Nernst potential for K (E_K). Changes of Na^+ and Cl^- gradients produced no evidence for participation of other ions. In high external K^+ (110 mM) the reversal potential was within 5 mV of the calculated E_K. We consider that the outward current is carried predominantly by K ions.

11) We conclude that the electrophysiological properties of crustacean X-organ somata in primary culture are very similar to those of some X-organ neurons *in situ*. Na and Ca current is robust in veiled neurons but appears to be lacking in branched neurons after one day in culture. Whether these neurons develop inward currents at later times remains to be determined.

Introduction

Studies utilizing conventional intracellular recording from peptidergic secretory neurons of various animal groups have established that they exhibit a number of electrical characteristics more prominently than other neurons. These include long duration impulses that often show broadening during repetitive activity, patterned or burst firing associated with secretory activity, the participation of Ca current in impulse generation at the soma and terminals, and often well developed Ca-dependent K current that controls firing frequency (review: Cooke and Stuenkel, 1985; Andrew

and Dudek, 1985; Bourque and Renaud, 1985a,b; Bourque, Randle and Renaud, 1980; Nagano and Cooke, 1987; Bourque, 1990).

Extensive voltage-clamp studies are available on molluscan peptidergic neurons, the most completely characterized neuron being the endogenous hyperbolic burster, *Aplysia* R15 and its homologues (for review see Adams and Benson, 1985). Unfortunately, the secretory function of these neurons has not been well defined. There are also several voltage-clamp studies of the ionic currents in *Aplysia* bag cells maintained in primary culture (Kaczmarek and Strumwasser, 1984; Conn, Strong and Kaczmarek, 1989). Bag cell somata exhibit substantial Ca current, as well as a conventional Na current and outward currents that include a transient potassium current (I_A) and a more slowly activating and inactivating current analogous to the delayed rectifier, I_K. Voltage-clamping of cultured rat oxytocin- or vasopressin-immunoreactive neurons has recently been reported (Cobbet and Mason, 1987; Cobbet, Legendre and Mason, 1989).

Our study examines neurons of the X-organ - sinus gland (the major neurosecretory system of crustaceans) of the tropical land crab, *Cardisoma carnifex* (review: Cooke and Sullivan, 1982). Our laboratory has provided information on the physiology of this system in the crab (review: Stuenkel and Cooke, 1988). Other electrophysiological studies of X-organ cells have utilized various species of crayfish (Iwasaki and Satow, 1971; Glantz, Kirk and Aréchiga, 1983; Onetti, García, Valdiosera and Aréchiga, 1990; see Discussion). Recordings from the crab X-organ reveal a variety of electrical responses and activity, as might be expected since the X-organ

neurosecretory cell group is a heterogeneous population of neurons producing several neuropeptides (Newcomb, 1987) and showing distinct differences in immunoreactivity (Mangerich, Keller and Dircksen, 1986; Dircksen, Webster and Keller, 1988), histochemical profile (Potter, 1956; Rhem, 1959) and ultrastructure (Bunt and Ashby, 1967; Weatherby, 1981).

Dissociated X-organ neurons from *Cardisoma*, cultured in simple medium, show immediate outgrowth of processes. Neurons having a characteristic soma size, morphology and outgrowth pattern consistently show immunoreactivity to particular antisera made against certain neuropeptides (Cooke, Graf, Grau, Haylett, Meyers and Ruben, 1989). The cultured neurons thus provide material suitable for examining the electrical properties of cells in relation to their differing biosynthetic capabilities.

This study presents observations primarily from cultured neurons that exhibit an unambiguous morphology: ovoid somata (minor diam. ~ 35 μm or larger), with outgrowth consisting of a broad lamellipodium or veil extended from the cut end of the original major neurite. Neurons of this form characteristically show immunoreactivity to antisera made against crustacean hyperglycemic hormone (CHH; Dirksen, Webster and Keller, 1988). The results show the presence of a TTX-sensitive Na current and a robust Ca current with competing inactivation and facilitation processes. In contrast, voltage-clamped somata of neurons with small or large spherical somata that give rise to branched neurites show very little inward current. These neurons show immunoreactivity indicative of molt inhibiting hormone (MIH) or red pigment concentrating hormone (RPCH). Both cell types express similar 4-AP and

TEA-sensitive potassium currents. Some of these observations have been reported previously (Meyers, Graf, Ruben and Cooke, 1988; Graf, Grau, Haylett and Cooke, 1988; Cooke, Graf, Grau and Meyers, 1988; Graf and Meyers, 1990; Meyers and Graf, 1990).

Methods

X-Organ Cell Culture

Cells were isolated from the X-organ tissue of *Cardisoma carnifex* (males, ~200 grams). They were cultured in defined medium according to previously described methods (Cooke *et al.*, 1989). Briefly, eyestalks were removed and rinsed with 70% ethanol, then exposed to antibiotic-containing saline (crab saline, plus streptomycin at 0.1 mg/ml, penicillin at 100 units/ml and fungizone at 0.25 μg/ml.) The X-organ plus ~0.5 mm of nerve were dissected from the surrounding nervous tissue and transferred to a 35 mm culture dish containing nominally Ca/Mg-free crab saline with 0.1% trypsin (Sigma, type IV). Dishes were covered and gently rocked for 1.5 hr in the dark. Enzymatic activity was arrested by diluting the enzyme with a large volume of nominally Ca/Mg-free saline. Cells were then dissociated from the X-organ by gently triturating the tissue in a 50 μl drop of culture medium on 35 mm Primaria dishes (Falcon 3801). The culture media consisted of equal parts of double strength crab saline and Leibowitz L-15 (Gibco) containing 120 mM glucose, 2 mM L-glutamine, and 0.1 mg/ml gentamicin; pH was 7.7. After allowing at least 2 hr for the cells to adhere to the substrate, the dishes were carefully flooded with approximately 2 ml of

culture medium. The cultures were held in humidified incubators in the dark at 24 - 27° C.

Electrophysiological Recording Techniques

Tight-seal whole-cell recordings were made from the somata of X-organ neurons that had regenerated in tissue culture for 24 to 48 hr. Unless noted otherwise, recordings were made at room temperature (24 - 26° C). Cells were visualized at 400X on the stage of an inverted microscope (Nikon Diaphot) equipped with Hoffman modulation optics (Modulation Optics). Patch pipettes were pulled from 1.5 mm O.D. thin-walled capillary tubing (World Precision Instruments, TW150F-4) on a vertical pipette puller (David Kopf Instruments, model 700 C) and fire polished with a microforge (Narishige, model MF-83). Pipettes were coated with Sylgard (Dow Corning, 184 elastomer kit) to reduce capacitance. Pipette-to-bath resistances ranged from 1 to 10 megohms (MΩ) with a variety of intracellular and extracellular solutions. The standard intracellular and extracellular recording solutions for the various experiments were as follows: Current clamp and net current under voltage clamp (intracellular; extracellular, in mM): K-Gluconate 300, NaOH 10, Mg-ATP 5, EGTA 5, HEPES 50, pH adjusted with KOH; NaCl 440, KCl 11, $MgCl_2$ 24, $CaCl_2$ 13.3, Na_2SO_4 26, HEPES 10, D-Glucose (omitted for crab saline) 10, pH adjusted with NaOH; *Sodium current*, CsCl 300, NaOH 10, Mg-ATP 5, EGTA 5, HEPES 50, pH adjusted with CsOH; NaCl 220, Choline-Cl 220; $MgCl_2$ 24, $CaCl_2$ 13.3, HEPES 10, TEA-Cl 20, 4-AP 3, D-Glucose 120, $CdCl_2$ 0.5, pH adjusted with NaOH.

Calcium current

N-methyl-D-glucamine methane sulphonate (NMG-$MeSO_3$) 300, NaCl 10, Mg-ATP 5, Cs-BAPTA (1,2-bis(*o*-aminophenoxy) ethane-N,N,N1,N1- tetraacetic acid (Tsien, 1980) 5, HEPES 50, TEA-Br 10, pH adjusted with CsOH; NaCl 440 (sometimes partially or completely replaced with NMG-$MeSO_3$), $MgCl_2$ 24, $CaCl_2$ 13.3, HEPES 10, TEA-Cl 20, 4-AP 3, D-Glucose 120, TTX 0.5-1.0 μm, pH adjusted with NaOH or CsOH; *Potassium current*, KCl or K-Gluconate 300, NaCl 10, HEPES 50, Mg-ATP 5, BAPTA 5, pH adjusted with KOH; NaCl 440, KCl 11, $MgCl_2$ 24, $CaCl_2$ 13.3, HEPES 10, D-Glucose 120, TTX 0.5 - 1 μM, $CdCl_2$ 0.5, pH adjusted with NaOH. The pH of all solutions was 7.4 and tonicity was adjusted with sucrose to 1095 to 1100 mOsm for intracellular solutions and 1100 mOsm for extracellular solutions.

Whole-cell current-clamp recordings were made with an Axoclamp 2A amplifier (Axon Instruments) equipped with an HS-2 headstage (X=0.01). Seal formation was performed in "bridge" mode. Voltage-clamp recordings were made with an Axopatch-1C patch-clamp amplifier (Axon Instruments) with either a CV-3 (0.1/100) or CV-4 (1/100) headstage. The electrode transient was nulled during seal formation. With pipette solutions containing CsCl or NMG-$MeSO_3$, the pipette-membrane seal was always greater than 1 gigaohm (GΩ) and usually on the order of 10 GΩ. Seal resistances obtained with K-containing pipettes tended to be lower but were always greater than 0.5 GΩ. After establishing electrical continuity with the cell interior, the series resistance and whole-cell capacity compensation (CV-4

only) was adjusted to give maximum frequency response while insuring that the decay of the remaining uncompensated transient maintained a smooth time course. Correction for leak and capacity current was performed by subtracting an appropriately scaled average of eight responses to hyperpolarizing commands (20 or 30 mV negative to the holding potential). In most experiments, currents were low-pass filtered (-3 db at 1 KHz) using an 8-pole Bessel filter. The filtered data were digitized (10 to 400 μsec/data point) and stored on the fixed disk of an 80286-based personal computer using the data acquisition and analysis program pCLAMP (V 5.5, Axon Instruments). In order to maintain an acceptable sample rate for long-duration test pulses in two-pulse experiments, prepulse data were not acquired. With the exception of curve fitting, all off-line analysis was performed on the same computer using pCLAMP.

Capacitance measurements were made from currents evoked by 20 mV hyperpolarizing voltage commands presented once every 7 sec. Averages of six sweeps were made and the integration was performed between the onset of the command and the time at which steady state was reached. Electrode capacitance compensation was employed and the rise time of the whole-cell transient was less than 600 μs. Estimates of cell surface area were also made from photomicrographs taken just prior to recording. The soma was assumed to be spherical and the "veil" was considered to be a cylinder of negligible height leading to a total surface area of:

$$Area_{total} = 2\ \pi\ (2r_{soma}^{2} + r_{veil}^{2}).$$

An average radius (r) was calculated for somata without circular profiles, and the area

of irregularly shaped veils was approximated by the sum of the areas of rectangles and circles. Estimates of cell surface area based on capacitance assumed 1 $\mu F/cm^2$.

Curve fitting was performed on a MacIntosh II computer using the program Nonlin II which performs a least-squares nonlinear regression based on the Marquardt-Levenberg algorithm (see McIntosh and McIntosh, 1980, for further details).

Pharmacology

Tetrodotoxin (Sigma), cadmium chloride (Mallinckrodt), TEA-Cl (or Br, 30 - 300 mM) and 4-AP (1-3 mM), were used in various phases of this study. Except where noted, exposure to these compounds was achieved by exchanging the external medium with five to seven bath volumes of the desired solution. Solutions containing TTX and TEA were made up from concentrated aqueous stocks and the remaining solutions were made up from the crystalline compound. All solutions were prepared on the day of the experiment. The pH of 4-AP-containing solutions was always adjusted after addition of 4-AP as the alkalinity of the solution is increased by as much as one-half log unit.

I_{Ca} "rundown"

Observations on Ca currents are unavoidably complicated by the presence of rundown (Forscher and Oxford, 1985; Byerly and Yazejian, 1986). We attempted to stabilize the loss of Ca current by adding Mg-ATP and a high-affinity Ca buffer,

BAPTA, to the pipette solution. Nevertheless, the degree to which the Ca current declined varied greatly from cell to cell. In some experiments, the decline in I_{Ca} was evident from the outset and these data were discarded. In other experiments, rundown was not significant for between 15 to 45 minutes. Rather than attempting to perform several voltage-clamp protocols in each experiment and attempting to correct for rundown, we present data that is drawn from the first and/or second voltage-clamp protocol applied to the cell after a four to five minute period of dialysis, with no correction for rundown. The consistency of our observations suggests that this strategy is sound. Experiments requiring exchange of the extracellular solution, as for example to exchange divalent cations, resulted in a 5 min delay between consecutive voltage-clamp protocols. Estimating the effects of rundown following such manipulations is difficult as it is affected not only by the concentration but also by the identity of the external divalent ions. In addition, changes in external divalent ions affect the apparent voltage dependence of channel gating. We have not attempted to correct for rundown in this type of experiment.

Results

A total of 269 whole-cell patch clamp recordings were made from the somata of peptidergic neurons dissociated from the crab X-organ and placed in primary culture in defined medium. The neurons were plated at such low density as to be effectively

isolated. They were examined after periods ranging from 24 - 48 hr after plating and had well-defined neuritic outgrowth. Recordings were made from neurons that could be unambiguously identified as being of the veiled or branched type (Cooke *et al.*, 1989).

Current Clamp Recordings

A total of eighteen (nine veiled cells and nine branched cells) recordings were made under whole-cell current clamp conditions from neurons that had been in culture for 24 to 48 hr. Resting potentials were low in both cell types, ranging from -20 to -40 mV. In two veiled and six of the small branched cells, there were slow, irregular membrane potential fluctuations of up to 10 mV. An additional four veiled cells discharged overshooting action potentials. In two of these cells we observed interruption of the regular discharge (0.5 - 2 Hz) by bursts of action potentials having a relatively high frequency (5 - 10 Hz). These varied from a few extra impulses interrupting the regular discharge to a 2 - 3 sec burst of dozens of impulses. The firing rate for the first few seconds following a sustained burst was considerably slower than the rate preceding the burst. In all cases, regular discharge and bursting activity could be terminated by hyperpolarizing the membrane 5 to 10 mV below the interspike membrane potential. Depolarization by a similar amount increased the firing rate. Cells in which no spontaneous activity was observed and in which regenerative activity could not be initiated with depolarizing current usually had membrane

potentials at the negative end of the observed range. These cells also failed to give any indication of active responses upon release from hyperpolarization.

Measurements of input resistance, R_N, were difficult to obtain due to membrane potential fluctuations. Thus, R_N could only be measured during hyperpolarization which stabilized the membrane potential. In this situation, R_N ranged from 0.8 to 11 GΩ (two veiled and four branched cells). There was no obvious correlation between morphology and R_N.

Membrane Area

In six veiled neurons we made estimates of cell capacitance 131 pF, sd = 66 pF). In five of these cases the estimates made from electrical recordings (see methods) were substantially greater (1.5 - 3.6 fold) than estimates made from surface area calculations based on photomicrographs (membrane capacitance of 1 $\mu F/cm^2$ assumed). Some of this difference may be attributed to ignoring small processes in surface area calculations, but it may also indicate that the membrane of these cells is infolded.

Net Current Under Voltage-Clamp

Recordings were made from four veiled and five small branched neurons bathed in culture medium or crab saline. All four of the veiled cells expressed a fast inward current that was followed by a slow outward current which showed little decay during 90 msec voltage-clamp commands (Fig. 1A). In contrast, inward current was

detected in only one small branched neuron in response to the same series of voltage commands. Outward current was readily apparent in all the small branched neurons studied (Fig. 1B).

Inward Current

I_{Na}

Attempts were made to isolate I_{Na} in 36 veiled neurons. Recordings were made with pipettes containing CsCl, and both intracellular and extracellular solutions were devoid of K^+. The extracellular medium contained Cd^{2+} to block voltage-dependent Ca current (see below) and TEA-Br (or Cl) and 4-AP to block any residual current that might flow through K channels. Inward current (100 pA to >1 nA) was readily observed in 34 of 36 neurons under these conditions. Six neurons were held sufficiently long to test the effect of adding TTX (0.5 - 1.0 μM) to the external medium (Fig. 2, inset). In each case, the inward current was rapidly abolished.

A typical current-voltage [I(V)] relation for the peak inward current (after leak and capacity subtraction) is illustrated in Figure 2. In this and most of these experiments, $[Na^+]_o$ was reduced to 1/2 or 1/4 of the normal concentration (440 mM; NaCl replaced with choline-chloride or NMG-$MeSO_3$) to reduce the magnitude of the current and thus improve membrane potential control. In the experiment illustrated, which was performed at 10°C with 110 mM NaCl in the external medium and 10 mM NaCl in the pipette solution, the current peaked at +20 mV and the extrapolated reversal potential was +58 mV. The Nernst potential for Na under these conditions is

+62 mV (T = 10° C). Thus, on the basis of reversal potential and blockade with TTX, we consider this current to be a voltage-dependent Na current (I_{Na}).

The large cell capacitance and rapid kinetics of I_{Na} made it difficult to perform a more detailed analysis using the whole-cell patch-clamp technique. For example, we found that the increase in activation rate that occurred during large positive commands and following hyperpolarizing conditioning potentials precluded accurate resolution of peak I_{Na}.

I_{Ca}

Inward currents were recorded under conditions as mentioned above designed to suppress K currents and in the presence of 0.5 - 1 μM TTX to block I_{Na}. Under these conditions, depolarizing voltage steps evoked inward current that developed slowly compared to I_{Na} (time to peak, 6 - 10 msec at 0 mV) and decayed slowly and incompletely during commands lasting over 700 msec. Figure 3 shows I(V) curves made under several conditions designed to test whether the TTX-resistant inward current can be attributed to Ca^{2+}. Figure 3A plots values of peak current (after capacity and leak subtraction) for a series of commands (V_c) from a holding potential (V_h) of -40 mV and the current at the end of the 720 msec pulse in normal extracellular Ca ($[Ca^{2+}]_o$ = 13.3 mM). The activation threshold for the current was approximately -30 to -20 mV, was maximal during commands to between 0 and +20 mV (usually +10 mV) and failed to reverse during depolarizing commands as positive as +60 mV. Both the peak current and the current remaining at the end of the voltage command displayed essentially the same voltage dependence although it was not

uncommon for the maximum peak current to occur 10 mV hyperpolarized to the maximum current at 720 msec. Values of peak I_{Ca} ranged from 0.2 to 2.5 nA. The current density in the six neurons for which estimates of surface area were made (based on cell capacitance), ranged from 3.4 to 12.7 $\mu A/cm^2$.

The I(V) plots (made from raw data) shown in Fig. 3B illustrate the effect of altering $[Ca^{2+}]_o$ (n = 4). The recording was commenced in medium containing 1.3 mM Ca^{2+}. Raising $[Ca^{2+}]_o$ to 13.3 mM resulted in an increase in the inward current at all step potentials. Figure 3B also shows the effects on the same neuron of the complete replacement of Ca^{2+} with Sr^{2+}. The amplitude of the inward current measured at the end of a 160 msec command in Sr-substituted saline showed no consistent difference compared to that in Ca saline (n = 3). As the exchange time for the extracellular solution was approximately 5 min, we could not control for rundown effects. Here, as also observed in a number of other studies (see Discussion), maximal I_{Sr} occurred during voltage commands that were 10 to 20 mV hyperpolarized to the command generating maximal I_{Ca} in the same neuron.

The inward current was abolished following the addition of Cd^{2+} (0.5 mM) to the bathing medium (Fig. 3C and D). Thus, on the basis of voltage dependence, blockade with Cd^{2+}, the ability of Sr^{2+} to substitute for Ca^{2+}, the increase in current amplitude following a ten fold increase in $[Ca^{2+}]_o$ and the apparently very positive reversal potential we consider this to be a Ca current (I_{Ca}).

Effects of Holding Potential on I_{Ca}

In other neurons, the presence of different types of Ca channels can be revealed during depolarizations from different levels of V_h. Thus, in order to further characterize the I_{Ca} of veiled neurons, the effects of changed V_h on inward current were examined. In three of four cells, comparison of leak-subtracted I(V) curves made from hold potentials of -40 and -80 mV suggested that close to 100% of I_{Ca} was available at -40 mV (Fig. 4). In the remaining cell, I_{Ca} generated from -80 mV was 25% greater than that generated from -40 mV.

As I(V) curves required 2 - 3 min to complete, we considered it possible that the relatively small effect of holding potential might have been due to "rundown" of the Ca current. We addressed this possibility by adopting a conditioning protocol in which only two depolarizing voltage commands (to -20 and +20 mV) separated by 10 sec were made sequentially from the two holding potentials thereby keeping the time in which rundown might occur to a minimum. This protocol was applied to five neurons, four of which were held at -40 and -80 mV with the remaining cell being held at -40 and -60 mV. In all five neurons of this series, the peaks of the leak- and capacity-subtracted records differed by no more than 10% (Fig. 4 inset), suggesting that our original observations did not result from "rundown". There was no evidence in any experiment for the activation of a transient component of Ca current during commands from relatively negative holding potentials as described in certain mammalian and invertebrate neurons (Carbone and Lux, 1984; Bossu, Feltz and Thomann, 1985; Nowycky, Fox and Tsien, 1985, Angstadt and Calabrese, 1991).

Effect of Prepulses on I_{Ca}

In studies of Ca currents in other invertebrate neurons, inactivation has been attributed to both voltage-dependent and current-dependent processes, with the latter apparently reflecting the accumulation of intracellular Ca^{2+} (Brown, Morimoto, Tsuda and Wilson, 1981; Chad, Eckert and Euald, 1984). Examination of the effects of a prepulse in relation to the inward current it has produced provides a test of the possible effects of intracellular accumulation of the permeating ion on the availability of channels for opening. The protocol utilized in these experiments consisted of a 200 msec prepulse (V_c = -30 to +60 mV, no prepulse = control) that was followed after a 200 msec period at V_h, by a 720 msec test pulse to the V_c generating maximal I_{Ca} (example of test-pulse I_{Ca}, Fig. 5A). Pulse pairs were presented every 10 sec. Under these conditions, the peak current in response to the test pulse of all cells studied (n = 10) displayed a U-shaped relation to the prepulse command voltage (Fig. 5B). This was so whether Ca^{2+} or Sr^{2+} carried the charge. The maximum depression for the eight cells bathed in Ca-containing medium ranged from 20 to 45% of control (-410 pA to -1.9 nA) while the corresponding values for the cells bathed in Sr^{2+} were 12% and 23% (maximum I_{Sr} = -840 pA and -1.4 nA respectively). In seven of these experiments (including the two experiments performed in Sr^{2+}), maximal depression of the test inward current followed the prepulse that was expected to have generated maximal inward current as determined from the I(V) relation (Fig. 5B). In the remaining three cells maximal depression of the test I_{Ca} occurred within 10 mV of the voltage at which maximal I_{Ca} was recorded. The U-shaped depression curve was

nearly symmetrical about the point of maximal depression (Fig. 5B). Thus, substantial relief from depression was observed when prepulse command voltages exceeded that eliciting maximal depression. Of particular interest, in five of the ten cells examined, the test-pulse current was facilitated (i.e. > control) following prepulses to +60 mV. The facilitation was 13% greater than controls in two cells and up to 10% in the other three cells (including one cell bathed in Sr^{2+}). Among the remaining five cells not showing facilitation, responses following very depolarized prepulses returned to better than 83% of control.

Effect of Interpulse Interval

Because the observations just described indicate that there is an effect of a preceding depolarizing command and inward current on the responsiveness of the conductance mediating I_{Ca}, we have used paired pulses separated by increasing intervals to examine the time course of recovery from the effects of the preceding pulse. In these experiments, the prepulse and test-pulse voltage commands were identical (usually 0 or +10 mV). The interval between the pulses was varied from 15 msec to 10 sec. The length of the prepulse and test pulse was again 200 and 720 msec respectively. As expected from the experiments described above, in all four cells examined, the peak test pulse current was depressed with short intervals, the depression being relieved as the interval was increased (Fig. 5C). Unlike the situation where only the prepulse voltage was varied and very depolarized prepulses were tested, the test current following prepulses giving maximal I_{Ca} never recovered to

control levels even for intervals of 10 sec. Maximal recovery for the four cells tested ranged from 85 to 90% of control values and by about 1 sec, recovery was better than 90% of its maximum. No further recovery and sometimes a decline in current was seen after 2 sec. Semilogarithmic plots of interval against test-pulse current showed that recovery followed an approximately exponential time course with a τ that ranged from 150 to 200 msec for the four cells studied (Fig. 5D).

Effects on Decay of Sr^{2+} Substitution

As noted above, the Ca channels in cultured X-organ somata can also be permeated by Sr ions. (In three experiments we attempted Ba substitution but in each case, the inward current was lost within 30 sec of commencing the bath exchange and we therefore made no further attempt to replace Ca^{2+} with Ba^{2+}). Substitution of Sr^{2+} for Ca^{2+} clearly affected the decay process. Comparing the maximal I_{Sr} and I_{Ca} (which occurred at different voltages) demonstrated that, irrespective of the peak-current amplitude, I_{Sr} was always greater than I_{Ca} at the end of the command (Fig. 6A). That this could not be accounted for by differences in the peak amplitudes or in the commands eliciting peak currents, was shown by responses in which the voltage commands used elicited responses of similar amplitude in the Sr- and Ca-salines. In these examples as well, the magnitude of I_{Sr} decay was less than that of I_{Ca} (Fig. 6B). At very positive command potentials, where inactivation became much more rapid, the difference in decay was less dramatic and the time course of decay for both currents was similar (Fig. 6C). Thus, it appears that the differences in the magnitude of inward

current decay seen following the substitution of Sr^{2+} for Ca^{2+} is dependent on command potential, being most pronounced during relatively small depolarizations. Substitution of Sr^{2+} for Ca^{2+} never eliminated the decay process entirely.

Outward Current

In the presence of TTX (1 μM) alone or TTX and Cd^{2+}, voltage-dependent outward current (0.5 - 10 nA) was present in all but one of 119 X-organ neurons in which whole-cell patch clamp was established. These included 87 veiled neurons and 32 branched neurons. As veiled cells can generate considerable Ca current (see above), experiments involving the identification of K currents, reversal potentials and pharmacology were performed with 0.5 mM Cd^{2+} in the bathing solution (this was also the case for branched neurons, although we did not resolve Ca current in somatic recordings). With TTX in the bathing medium, application of Cd^{2+} (0.5 mM) *reduced* outward currents, usually by less than 10% in a non-voltage-, non-time-dependent manner. This was so for both veiled and branched neurons. We did not observe major differences in the characteristics of the outward currents that were correlated with neuronal morphology.

Outward Current Analogous to I_K

Figure 7A shows a typical I(V) curve for the outward current measured at the end of an 80 msec voltage-clamp command. From a holding potential (V_h) of -50 mV, the activation threshold was approximately -30 mV and the current grew substantially

with increments in command potential (V_c). In this particular cell (branched cell, 20 μm diameter) the current rise time was relatively slow (~ 20 msec to peak at +20 mV, see inset Fig. 7A) and the decay was modest, such that greater than 80% of the current remained at the end of the command. This current is qualitatively similar to the classical delayed rectifier identified in many preparations (Rudy, 1988). It will be referred to as I_K because of its similarity to the molluscan K current (Thompson, 1977). This identification is further supported by its selective inhibition by TEA as described below.

Outward Current Analogous to I_A

In the majority of cells, the outward current rose and decayed considerably faster than in the above example, especially during voltage steps from relatively negative holding potentials (Fig. 7B, upper panel). Commands to +20 mV from sequentially more negative levels of V_h resulted in a substantial increase in the peak outward current (Fig. 7B, lower panel), suggesting that the availability of this component for activation by a depolarizing step was dependent on V_h. By contrast, the current measured at the end of the 80 msec command was little affected by the V_h (Fig. 7C). The I(V) relations for activation and removal of inactivation are shown in Fig. 7C.

This type of behavior makes this current analogous to I_A of molluscs (Connor and Stevens, 1971a). It was observed in 23 of 25 neurons (seventeen veiled and eight branched cells) in which it was specifically sought. For the cell shown in Figure 7B and C, the V_h giving half-maximal current was approximately -45 mV. The average value for the nine neurons in which inactivation was unequivocally removed at V_h = -80 mV was -46 mV (sd = 4 mV). Although this value is more depolarized than that reported for I_A of many neurons (see Discussion), the identification of the early peak outward current as I_A is supported by its selective block by 4-AP as described below.

In six cells, we tested the effect of the duration of a conditioning step on the removal of inactivation. Conditioning steps of from 15 msec to 2 sec and were applied from a V_h of -40 mV. In all six cells, at least 85% of the inactivation was removed with a conditioning pulse of 200 msec. In four of the six neurons, there was

a slight decrease in the peak current with longer conditioning pulses. The time constant for the removal of inactivation ranged from 29 to 85 msec.

The time constant (τ) of inactivation of I_A appeared to be voltage-dependent with τ reaching a minimum value of 4 msec for depolarizations >0 mV. Characterization of I_A inactivation required pharmacological manipulation and is therefore described after the presentation of the pharmacological data.

Estimation of Reversal Potential (E_R)

In an attempt to determine which ions were responsible for the outward currents, we examined the reversal potential of tail currents. We usually maximized the tail current amplitude by using short-duration test commands (8 to 10 msec at +20 mV). It should be noted, however, that the reversal potentials of tail currents examined following longer clamp commands (18 and 80 msec) were essentially identical suggesting that E_R was the same for I_A and I_K. In normal extracellular K^+ (11 mM), the mean tail current E_R was -69 mV (sd = 9 mV, n = 24; Fig 8A). Raising extracellular K^+ produced a significant depolarizing shift of E_R. In three experiments, raising extracellular K^+ to 110 mM shifted E_R to -20 to -28 mV (Fig. 8B, calculated E_K = -25 mV).

As the calculated E_R for potassium (E_K) is -83 mV ($[K^+]_i$ = 300 mM, $[K^+]_o$ = 11 mM, T = 25°C), we considered it possible that the E_R measured in normal K might result from the presence of ion currents other than voltage-dependent K currents. Manipulations of the Cl^- gradient in which the calculated E_{Cl} was -64 mV or more

positive, had little effect on E_R. Surprisingly, E_R was shifted in the *depolarizing* direction by approximately 20 mV (mean E_R = -50 mV, sd = 3, n = 7) when external Cl^- was held normal (525 mM) and internal Cl^- was lowered to 10 mM (calculated E_{Cl} = -100 mV). Thus, the presence of a Cl current cannot explain the observations. Further experiments in which the Na ion gradient was manipulated showed no observable effect on the reversal potential.

Although our results show that E_R in normal K^+ is depolarized with respect to the calculated E_K, we have been unable to demonstrate that this is due to the activation (or inactivation) of a conventional ion current involving a Na or Cl permeability change. On the other hand, in raised external K^+, there was a large shift in E_R to a value that was very close to E_K, suggesting that the outward currents were carried predominantly by K ions.

Pharmacology of K Currents

Our experiments with K-channel blockers revealed an unexpected phenomenon which is illustrated in Figure 9. In seven of eleven experiments (six veiled and five branched) in which 4-AP was added to the bathing medium, we observed not only blockade of I_A but paradoxically, an increase in the late outward current (Fig. 9A). The amplitude of the enhanced currents ranged from about 0.5 to 4 nA (30 to 85% greater than control, four veiled and three branched cells) and remained sensitive to TEA (> 30 mM; Fig. 9A). The late current in the remaining four neurons was within 10% of control values following the addition of 4-AP (Fig. 9B). Interestingly, in three

of four veiled neurons that were exposed to 4-AP after the addition of 50 mM TEA-Br (Fig. 9C), these increases were not observed. Thus, in these three cells, TEA decreased the late outward current and there was no change in the late current associated with the addition of 4-AP.

Figure 10A shows the current-voltage relation for the late current before and after the addition of TEA-Br (50 mM). This particular cell was one of the four described above, which showed no increase in late current following addition of 4-AP. The late current was reduced at all test potentials but in no case was it completely blocked.

The effect of 4-AP (1-3 mM) was tested on eighteen neurons (twelve veiled and six branched neurons). In the experiment illustrated in Figure 10B, the transient component of the outward current could not be detected following the addition of 3 mM 4-AP (see inset Fig. 10B) confirming the identification of this component as I_A. Comparison of peak currents measured before and after the addition of 4-AP (the latter measured at the same points in time as the corresponding peaks in control records) showed that the sensitivity to V_h was virtually eliminated. Indeed, in all eighteen cells tested (thirteen veiled and five branched cells), 4-AP produced a substantial or complete blockade of the peak current.

Inactivation of I_A

The increase in late outward current produced by 4-AP complicates the use of this agent to isolate I_A by subtraction of 4-AP-insensitive current from total outward

current. Thus, we could only examine cells which showed no increase in the late current following the addition of 4-AP. In three of these cells, the decay phase of I_A was suitable for curve fitting. The smallest current that could be fit, which was generated by a step to -20 mV (V_h = -40 mV), decayed with a time constant in the order of 20 msec while at +20 mV the time constants ranged between 4 and 8 msec.

Discussion

This paper presents whole-cell patch clamp recordings from peptidergic secretory neurons that have been in defined culture for 1 to 2 days. We have focused on CHH-secreting cells whose outgrowth is characterized by large lamellipodia (veiled cells), because they exhibit a full repertoire of electrical responses: They are the only type in which we observed overshooting action potentials, and they consistently show voltage-dependent inward currents and outward currents under patch-clamp. Branched cells (reactive to anti-MIH or anti-RPCH sera) were seen to have slow membrane potential fluctuations of up to 10 mV, but never spontaneous or inducible action potentials. Under patch-clamp, outward currents predominate in these cells. As the input resistance of both types of cells was usually in the GΩ range and the extent of outgrowth limited, we think it unlikely that we failed to record or elicit active responses due to spatial decrement from distal regions of active membrane. A more likely explanation for the lack of regenerative responses is that the somata of branched cells do not normally exhibit inward currents, as is often the case for arthropod neurons. Thus, it may be that these neurons have yet to develop the neuritic membrane that gives rise to regenerative activity.

Previous recordings from somata of the intact crab X-organ have shown that many failed to exhibit active electrical responses, while in about half of those showing responses, the decremented impulses indicated that they were initiated some distance from, and did not invade, the soma (Stuenkel, 1985; Nagano and Cooke, 1987). The recordings show a variety of spontaneous activity including irregular firing, pacemaker-like firing and rhythmical bursting in a number of patterns. The morphology and hormone content of the neurons from which these types of activity were recorded is unknown. Overshooting action potentials were found to involve both Na- and Ca-mediated current.

Other studies from crayfish X-organ somata have provided evidence for both Na- and Ca-dependence of impulses (Iwasaki and Satow, 1971; Iwasaki, Satow and Kuroda, 1973; Glantz, Kirk and Aréchiga, 1983). Whole-cell voltage clamp of superficial or acutely isolated X-organ cells has shown the presence of Na and Ca currents, a non-specific cation current, and currents corresponding to I_A and I_K (Onetti *et al.*, 1990). Na current was absent following axotomy, and is thus attributed to axonal membrane. The crab studies with conventional intracellular electrodes do not permit such intimate resolution of the regional distribution of these currents.

Na and Ca Current

The inward current in veiled cells was readily separated into Na- and Ca-based components. The kinetics of the Na current were rapid and the initial inward current was poorly resolved. Our identification of this current is based on 1) rapid,

voltage-dependent activation and rapid decay, 2) an extrapolated reversal potential near that expected for Na^+ and 3) abolition of the current in the presence of submicromolar concentrations of TTX. Thus, with respect to these basic properties, I_{Na} in our preparation is similar to that described in many other preparations (Hille, 1984).

Because of the vital role of Ca^{2+} in both regeneration and peptide secretion, we have given most attention to the characterization of I_{Ca}. Studied under conditions minimizing the possibility of non-linear outward current and Na-mediated inward current, the veiled neurons exhibited substantial (up to 2.5 nA) inward current. This was identified as I_{Ca} on the basis of the apparently very high reversal potential, sensitivity of current amplitude to $[Ca^{2+}]_o$, the presence of inward current in salines having Sr substituted for Ca and blockade following the addition of Cd^{2+}. With optimal experimental conditions we routinely found I_{Ca} to be inward at +60 mV suggesting that outward currents were largely absent or eliminated. The presence of non-specific outward current, previously identified in molluscan neurons (Kostyuk and Krishtal, 1977; Byerly and Hagiwara, 1982), cannot be excluded. The observation that the membrane area under clamp, as calculated from capacitance (assuming 1 $\mu F/cm^2$) is consistently greater than surface area estimates made from photomicrographs, together with the absence of step changes in the current recordings or discontinuities in the I(V) curves over a wide range of membrane potential suggests that the spatial control of membrane potential was adequate.

The response of I_{Ca} under different steady-state conditions suggests that the Ca channels underlying I_{Ca} represent a population having quite uniform properties. In this

respect, I_{Ca} of these peptidergic neurons is quite similar to that of lobster cardiac ganglion motorneurons (Tazaki and Cooke, 1986; 1990), crayfish giant motorneurons (Bruner, Czternasty, Shimahara and Stinnakre, 1986; Czternasty, Kado and Bruner, 1989) and molluscan neurons (Thompson and Coombs, 1988). Evidence was obtained in crayfish X-organ neurons that hyperpolarization and depolarization from an optimal V_h actually reduces I_{Ca} (Iwasaki *et al.*, 1973). This effect of hyperpolarized V_h on I_{Ca} has also been reported for *Aplysia* R15 (Adams and Gage, 1979) and for the lobster cardiac motorneurons. None of these studies, including ours, have found any evidence for a component of transient Ca current activated from hyperpolarized V_h as has been described in some other neuronal preparations. Thus, with the exception of certain leech interneurons (Angstadt and Calabrese, 1991), many invertebrate neurons clearly differ from isolated neurohypophyseal nerve terminals (Lemos and Nowycky, 1989) and cultured vertebrate neurons in which two (Carbone and Lux, 1984; Bossu *et al.*, 1985; Ikeda, Schofield and Weight, 1986; Meyers and Barker, 1989) or possibly three (Nowycky *et al.*, 1985; Fox *et al.*, 1987a, b) populations of Ca channels have been distinguished.

It is clear that inactivation of I_{Ca} is complex. Brown *et al.* (1981) have proposed a dual voltage/Ca^{2+} mechanism for the decay of I_{Ca} in *Helix* neurons. Thompson and Coombs (1988) have suggested that inactivation in *Aplysia* neurons cannot be related in any simple way to the absolute concentration of internal Ca^{2+}. They demonstrated, using a combination of two-electrode voltage clamp and loose patch recording, that the decay of I_{Ca} in patches of membrane with equivalent current

densities can be substantially different. They concluded, however, that the differences in the rates of Ca-dependent inactivation were probably related to compartmentalization of cytoplasmic factors controlling $[Ca^{2+}]_i$, rather than to the expression of different populations of channels or multiple decay mechanisms.

The results of our double-pulse experiments indicate that both Ca- and possibly voltage-dependent mechanisms of inactivation may be present. In support of a mechanism involving increased $[Ca^{2+}]_i$, similar to that described for molluscan neurons (Tillotson, 1979; Eckert and Tillotson, 1981; Eckert and Ewald, 1983; Chad *et al.*, 1984; Thompson and Coombs, 1988), we have found that: 1) the effect of prepulses in depressing current generated by an optimal test command is related to the prepulse current and 2) that substitution of Ca with Sr reduced the extent of decay, although in no case did it eliminate inactivation entirely. In addition, the disparity in the extent of decay of I_{Ca} and I_{Sr} seen with relatively modest depolarizations was substantially reduced during large commands, suggesting that inactivation was now dominated by voltage-dependent processes. It should be remembered, that comparison of these currents is complicated by the fact that Ca^{2+} is highly buffered by the BAPTA included in the pipette solution. The extent to which this affects the inactivation of I_{Ca} is unknown.

The observation that test pulse current responses, after showing depression, then return close to (>90% recovery) or even exceed control amplitudes following large depolarizing prepulses that admit considerable Ca^{2+} (e.g. +40 to +60 mV, Fig. 5B) suggests that a facilitation mechanism may be present. Prepulse facilitation of

Ba^{2+} and/or Ca^{2+} currents has also been observed in vertebrate sympathetic neurons (Jones and Marks, 1989; Elmslie, Zhou and Jones, 1990; Ikeda, 1991) and in adrenal chromaffin cells, in which inactivation following single depolarizing commands is weak or absent (Fenwick, Marty and Neher, 1982; Hoshi, Rothlein and Smith, 1984; Artelejo, Dahmer, Perlman and Fox, 1991). Both Elmslie *et al.* (1990) and Ikeda (1991) have argued that the facilitation in sympathetic neurons results from a voltage-induced change of state of a single type of Ca channel, which contrasts with the case for chromaffin cells where it appears that facilitation is due to the recruitment of a separate population of Ca channels (Artelejo *et al.*, 1991). As prepulse facilitation is more readily observed when Ba^{2+} carries the charge, it seems reasonable to conclude that under physiological conditions, net Ca^{2+} influx is determined by competition between inactivation and facilitation processes. Results from theoretical treatments of Ca-dependent inactivation support this idea, as these models predict test-current recovery on the order of only 50 to 85% following prepulses to +60 mV with interpulse intervals of 10 to 100 msec (Standen and Stanfield, 1982; Sherman, Keizer and Rinzel, 1990). It should be noted, however, that Jones and Marks (1989) successfully modeled the full recovery of test current recorded in Ba^{2+} from bull-frog sympathetic neurons with a purely voltage-dependent mechanism. Although, it is unclear whether this model can account for the extent or rates of decay seen for current recorded in Ca^{2+}, it suggests that fully voltage-dependent mechanisms are worthy of further investigation.

K Current

While Na and Ca current appears to be expressed only in veiled neurons, the outward currents, I_K and I_A are expressed in both veiled and branched cell types. The similarity of the outward current profile of the X-organ neurons stands in contrast to that of cultured leech neurons, in which inward currents were similar and outward currents differed with neuronal type (Stewart, Nicholls and Adams, 1989).

Effect of Cd^{2+}

Application of the inorganic Ca channel blocker Cd^{2+}, resulted in a decrease of the depolarization-evoked outward current over the entire duration of a 135 msec command and was apparently independent of voltage and time. Clearly, if the effect of Cd^{2+} was solely to block voltage-dependent Ca channels, an increase in outward current would have been expected in veiled neurons and no change in current would have been expected in branched neurons. As the effect was observed at a Cd^{2+} concentration of 0.5 mM, it seems unlikely that the reduction is related to changes in membrane surface charge (Hille, 1984). It is possible that the reduction of outward current resulted from the loss of Ca-activated K current. Although this explanation is plausible for veiled neurons, it seems an unlikely explanation for the observations in branched neurons where I_{Ca} has not been observed. Another explanation, which cannot be discounted at this point, is that Cd^{2+} has a direct effect on some potassium channels (Schwindt and Crill, 1981; MacDermott and Weight, 1982; Salkoff, 1983). At this point, we do not have sufficient data to resolve this question. Isolated-patch recordings may well be more useful than the whole-cell approach.

I_A and I_K

The presence of a transient outward K current, originally described by Hagiwara, Kusano and Saito (1961) in the mollusc *Onchidium*, has been noted in a plethora of vertebrate and invertebrate, neuronal and non-neuronal preparations (for review see: Rudy, 1988). This current, which is usually referred to as I_A (Connor and Stevens, 1971a), is characterized by rapid activation and decay, blockade with 4-AP and inactivation at relatively depolarized potentials. Activation of I_A in cultured X-organ neurons is certainly rapid and the decay rates that we have been able to measure are also rapid and are comparable to those seen in lobster cardiac ganglion (Tazaki and Cooke, 1986) and cultured hippocampal neurons (Segal and Barker, 1984; Segal, Rogawski and Barker, 1984). Blockade of I_A with 4-AP at concentrations of 3 mM or less is also typical of a number of neuronal preparations (Thompson, 1977; Gustaffson, Galvan, Grafe and Wigstrom, 1982; Segal *et al.*, 1984; Strong, 1984).

With respect to steady-state inactivation, however, we have found that the point at which I_A is half inactivated is about 15 to 25 mV more depolarized than that reported for most other neuronal preparations (-60 to -70 mV). Unlike crayfish X-organ neurons, we have found no evidence for two populations of A currents with different half-inactivation points (Onetti *et al.*, 1990). Relatively depolarized half-inactivation points have been reported for transient K currents in *Drosophila* muscle (Wu and Haugland, 1985), *Limulus* ventral photoreceptors (Lisman, Fain and Swan, 1978; Leonard and Lisman, 1981), goldfish retinal horizontal cells (Tachibana, 1983) and coelenterate egg cells (Hagiwara, Yoshida and Yoshii, 1981). In contrast to

cultured X-organ neurons, inactivation rates in these cells tend to be slow, on the order of hundreds of msec.

As I_A is usually considered to play a primary role in controlling the frequency of repetitive firing (Connor and Stevens, 1971b), it would seem necessary for the steady state inactivation properties to be related to both the resting potential and the inactivation properties of conductances that generate the upstroke of the action potential. As veiled neurons have relatively depolarized resting potentials (-20 to -40 mV) and as 75 to 100% of the Ca conductance is available for activation at -40 mV, it therefore seems reasonable to argue that, at least for these cells, the steady-state inactivation properties of I_A are suited to performing the postulated role in controlling firing frequency. The role of I_A in branched neurons remains unclear.

The slow development and relative insensitivity to V_h of the current remaining following blockade of I_A, together with its sensitivity to TEA (30-50 mM) suggests that it is similar to the delayed rectifier, I_K. High concentrations of TEA (300 mM) did not produce complete blockade, suggesting that I_K in these neurons may have a TEA-insensitive component or that the probability of channel blockade is <100% even with 300 mM TEA. It seems unlikely that the TEA-insensitive current is a Ca-dependent K current, as Cd^{2+} was present in all of these experiments. The sensitivity of I_K to TEA is similar to that observed in crab and lobster cardiac ganglion cells (Tazaki and Cooke, 1986) and crayfish X-organ neurons (Onetti *et al.*, 1990).

The K^+ Reversal Potential

The reversal potentials measured in normal K^+ were on average 14 mV depolarized to the calculated E_K. Error in measuring E_R can arise from at least three sources. Firstly, there is the possibility of contamination from another ionic current with a different reversal potential. The experiments in which we manipulated the Cl and/or Na concentrations externally and the Cl concentration internally failed to provide evidence for the presence of contaminating Cl or Na currents (Ca current was blocked with Cd^{2+}).

The presence of a non-specific cation conductance would also result in an unusually depolarized reversal potential. Recently, Onetti *et al.* (1990) have described a putative non-specific cation current in crayfish X-organ neurons. This current is not well defined but appears to be carried predominantly by Na ions and inactivated when $[Ca^{2+}]$ is low (10^{-9} M) suggesting that Ca influx is necessary for activation. Non-specific cation currents in molluscan neurons are suppressed by agents which block voltage-dependent Ca^{2+} entry (Eckert and Lux, 1976; Lewis, 1984; Adams and Levitan, 1985; Kramer and Zucker, 1985; Swandulla and Lux, 1985) and are reduced by lowering the external Na^+ concentration (Adams and Levitan, 1985) or by injecting EGTA (Lewis, 1984). As in our experiments Cd^{2+} was present in the external medium and the pipette solution contained a substantial concentration (5 mM) of a high affinity Ca^{2+} chelator (BAPTA, Tsien, 1980), it seems unlikely that similar cation currents would be present. In addition, a 10-fold change in external Na^+ had no effect on the reversal potential. We cannot, however, exclude the possibility that cultured X-organ

neurons possess a cation current with low permeability to Na^+ that is insensitive to Cd^{2+}. As E_R was within 3 mV of the calculated E_K when external K^+ was raised to 110 mM, it is possible that the depolarized E_K seen in normal K^+ may be related to the asymmetry of the normal K^+ gradient. Experiments in which the Cl gradient was manipulated suggest that the ratio of internal K^+ to Cl^- may also affect E_K.

A second possible source of error, which may also have bearing on our pharmacological data (see below), may arise from inadequate control of membrane voltage (space-clamp artifact). Thus, in an unfavorable situation, for instance when the axial resistance of the neurite(s) is large, it is possible that distal regions of membrane are charged relatively slowly and partially such that significant activation of conductances in these regions does not occur. During the subsequent tail-current clamp command, this membrane (i.e. the membrane capacitance) will discharge, primarily through the axial resistance (membrane resistance is comparatively high), and will be measured as an inward current in well-clamped regions, thereby moving the reversal potential in the depolarization direction. This condition should be revealed, however, in responses to hyperpolarizing commands from V_h, as the return to steady state should be considerably slower than the normal capacity transient. Although we have not studied this systematically, it appears that steady state is achieved rapidly even in large neurons (< 6 msec in uncompensated recordings). Even so, we cannot entirely rule out the possibility that our tail currents are contaminated by the discharge of distal membrane capacitance.

A third possibility is that K ions become concentrated in confined extracellular spaces (e.g. under the veil and soma) thereby reducing the K^+ gradient and shifting E_K in the depolarizing direction. The increase in $[K^+]_o$ might come from both leakage and voltage-activated K current. As only a two fold increase in $[K^+]_o$ results in a calculated E_K of -67 mV (T = 25°C) this hypothesis must be considered worthy of further investigation. Information concerning the distribution of K channels would seem to be essential.

Novel Pharmacology

Another interesting finding in the present work was the augmentation of I_K during blockade of I_A in about 60% of cells. We consider it unlikely that this observation can be attributed to an electrode series-resistance artifact as the augmentation occurred for large and small currents, in veiled and branched cells and in situations where electrode resistances were a MΩ or less. Similar phenomena have been observed in voltage clamped stomatogastric neurons (Jones and Hartline, 1989; Graubard and Hartline, 1991) and epithelial cells of sea anemone tentacles (Hessinger and Brehm, 1990).

One possible explanation for our observations is that additional conductance is recruited following exposure to 4-AP. For instance, a high density of A channels in the neurite(s) would severely limit the effectiveness of the clamp in more distal regions of membrane (e.g., the veil). Following blockade, it might be possible to activate and clamp the conductance of the more distal membrane. If this were so it suggests that

the distribution of K^+ channels in both veiled and branched cells is similar even though their morphology and distribution of depolarizing conductances are substantially different. Recordings from somata following removal of the neurites should help in resolving this issue.

In conclusion, these experiments demonstrate that two readily identifiable types of peptidergic neurons from the crustacean X-organ express substantially different classes of ion channels. Net Ca^{2+} influx in veiled neurons appears to be controlled by competition between inactivation and facilitation processes. Inward currents are largely absent from the somata of branched cells. It remains to be determined whether, after longer periods in culture, the processes of branched neurons become endowed with inward current channels at a density capable of supporting electrically regenerative responses.

References

Adams, W.B. and Benson, J.A. The generation and modulation of endogenous rhythmicity in the *Aplysia* bursting pacemaker neurone R15. *Prog. Biophys. Molec. Biol.* **46**: 1-49, 1985.

Adams, D.J. and Gage, P.W. Characteristics of sodium and calcium conductance changes produced by membrane depolarization in an *Aplysia* neurone. *J. Physiol. (Lond).* **289**: 143-16, 1979.

Adams, D.J. and Levitan, I.B. Voltage and ion dependencies of the slow currents which mediate bursting in *Aplysia* neurone R15. *J. Physiol. (Lond).* **360**: 69-93, 1985.

Andrew, R.D. and Dudek, F.E. Spike broadening in magnocellular neuroendocrine cells of rat hypothalamic slices. *Brain Res.* **334**: 176-179, 1985.

Angstadt, J.D. and Calabrese, R.L. Calcium currents and graded synaptic transmission between heart interneurons in the leech. *J. Neuroscience.* **11**: 746-759, 1991.

Artalejo, C.R., Dahmer, M.K., Perlman, R.L., and Fox, A.P. Two types of Ca^{2+} currents are found in bovine chromaffin cells: facilitation is due to the recruitment of one type. *J. Physiol. (Lond).* **432**: 681-707, 1991.

Bossu, J-L., Feltz, A., and Thomann, J.M. Depolarization elicits two distinct calcium currents in vertebrate sensory neurones. *Pflügers Archiv.* **403**: 360-368, 1985.

Bourque, C.W. Intraterminal recordings from the rat neurohypophysis *in vitro*. *J. Physiol. (Lond).* **421**: 247-262, 1990.

Bourque, C.W. and Renaud, L.P. Calcium-dependent action potentials in rat supraoptic neurosecretory neurones recorded *in vitro*. *J. Physiol. (Lond).* **363**: 419-428, 1985a.

Bourque, C.W., Randle, J.C.R., and Renaud, L.P. Calcium-dependent potassium conductance in rat supraoptic nucleus neurosecretory neurons. *J. Neurophysiol.* **54**: 1375-1382, 1985.

Brown, A.M., Morimoto, K., Tsuda, Y., and Wilson, D.L. Calcium current-dependent and voltage-dependent inactivation of calcium channels in *Helix aspera*. *J. Physiol. (Lond).* **320**: 193-218, 1981.

Bruner, J., Czternasty, G., Shimahara, T., and Stinnakre, J. Arsenazo III transients and Ca current in a normally non-spiking neuronal soma of crayfish. *J. Physiol. (Lond).* **374**: 571-583, 1986.

Bunt, A. and Ashby, E. Ultrastructure of the sinus gland of the crayfish *Procambarus clarkii. Gen. Comp. Physiol.* **9**: 334-342, 1967.

Byerly, L. and Hagiwara, S. Calcium currents in internally perfused nerve cell bodies of *Lymnea stagnalis. J. Physiol. (Lond).* **322**: 503-528, 1982.

Byerly, L. and Yazejian, B. Intracellular factors for the maintenance of calcium currents in perfused neurones from the snail, *Lymnaea stagnalis. J. Physiol. (Lond).* **370**: 631-650, 1986.

Carbone, E. and Lux, H.D. A low voltage-activated calcium conductance in embryonic chick sensory neurons. *Biophys. J.* **46**: 413-418, 1984.

Chad, J., Eckert, R., and Ewald, D. Kinetics of calcium-dependent inactivation of calcium current in voltage-clamped neurons of *Aplysia californica. J. Physiol. (Lond).* **347**: 279-300, 1984.

Cobbett, P., Legendre, P., and Mason, W.T. Characterization of three types of potassium current in cultured neurones of rat supraoptic nucleus area. *J. Physiol. (Lond).* **410**: 443-462, 1989.

Cobbett, P. and Mason, W.T. Whole-cell voltage clamp recordings from cultured neurones of the supraoptic area of neonatal rat hypothalamus. *Brain Res.* **409**: 175-180, 1987.

Conn, P.J., Strong, J.A., and Kaczmarek, L.K. Inhibitors of protein kinase C prevent enhancement of calcium current and action potentials in peptidergic neurons of *Aplysia. J. Neuroscience.* **9**: 480-487, 1989.

Connor, J.A. and Stevens, C.F. Voltage clamp studies of a transient outward membrane current in gastropod neural somata. J. Physiol. (Lond). 213:21-30, 1971a.

Connor, J.A. and Stevens, C.F. Prediction of repetitive firing behavior from voltage clamp data on an isolated neurone soma. *J. Physiol. (Lond).* **213**: 31-53, 1971b.

Cooke, I.M. and Sullivan, R.E. Hormones and neurosecretion. In: *The Biology of Crustacea*, Vol 3 (Atwood, H. and Sandeman, D., eds). New York, Academic, 1982, pp 205.

Cooke, I. and Stuenkel, E. Electrophysiology of invertebrate neurosecretory cells. In: *The electrophysiology of the secretory cell* (Poisner, A.M. and Trifaro, J., eds), pp 115-164. Amsterdam, Elsevier, 1985.

Cooke, I., Graf, R., Grau, S., and Meyers, D. Crustacean peptidergic secretory neurons in culture: outgrowth, secretory competence, and Ca^{++} currents. *J. Gen. Physiol.* **92**:3a, 1988.

Cooke, I., Graf, R., Grau, S., Haylett, B., Meyers, D., and Ruben, P. Crustacean peptidergic neurons in culture show immediate outgrowth in simple media. *Proc. Natl. Acad. Sci. USA.* **86**:402-406, 1989.

Czternasty, G., Kado, R.T., and Bruner, J. Analysis of mechanisms of spiking in normally "non-spiking" motoneurone somata in crayfish. *J. Exp. Biol.* **147**: 91-110, 1989.

Dircksen, H., Webster, S.G., and Keller, R. Immunocytochemical demonstration of the neurosecretory system containing putative moult-inhibiting hormone and hyperglycemic hormone in the eyestalk of brachyuran crustaceans. *Cell Tissue Res.* **251**: 3-12, 1988.

Eckert, R. and Ewald, D. Calcium tail currents in voltage-clamped intact nerve cell bodies of *Aplysia californica. J. Physiol. (Lond).* **345**: 533-548, 1983.

Eckert, R. and Lux, H.D. A voltage-sensitive persistent calcium conductance in neuronal somata of *Helix. J. Physiol. (Lond).* **254**: 129-151, 1976.

Eckert, R. and Tillotson, D.L. Calcium-mediated inactivation of the calcium conductance in caesium-loaded giant neurones of *Aplysia californica. J. Physiol. (Lond).* **314**: 265-280, 1981.

Elmslie, K.S., Zhou, W., and Jones, S.W. LHRH and GTP-γ-S modify calcium current activation in bullfrog sympathetic neurons. *Neuron.* 5:75-80, 1990.

Fenwick, E.M., Marty, A., and Neher, E. Sodium and calcium channels in bovine chromaffin cells. *J. Physiol. (Lond).* **331**: 599-635, 1982.

Forscher, P. and Oxford, G.S. Modulation of calcium channels by norepinephrine in internally dialyzed avian sensory neurons. *J. Gen. Physiol.* **85**: 743-764, 1985.

Fox, A.P., Nowycky, M.C., and Tsien, R.W. Kinetic and pharmacological properties distinguishing three types of calcium currents in chick sensory neurones. *J. Physiol. (Lond).* **394**: 149-172, 1987a.

Fox, A.P., Nowycky, M.C., and Tsien, R.W. Single-channel recordings of three types of calcium channels in chick sensory neurones. *J. Physiol. (Lond).* **394**: 173-200, 1987b.

Graf, R.A., Grau, S., Haylett, B., and Cooke, I.M. Crustacean peptidergic neurons in primary culture show immediate outgrowth in defined media. *Soc. Neurosci. Abstr.* **14**: 869, 1988.

Graf R.A., and Meyers, D.E.R. Pharmacology of I_A and I_K of crustacean peptidergic neurons in culture. *FASEB J.* **4**: 1200, 1990.

Graubard, K. and Hartline, D.K. Voltage clamp analysis of intact stomatogastric neurons. *Brain Res.* **557**: 241-254, 1991

Gustafsson, B., Galvan, M., Grafe, P., and Wigstrom, H. Transient outward current in a mammalian central neurone blocked by 4-aminopyridine. *Nature.* **299**: 252-254, 1982.

Hagiwara, S., Kunsano, K., and Saito, N. Membrane changes of *Onchidium* nerve cell in potassium-rich media. *J. Physiol. (Lond).* **155**: 470-489, 1961.

Hagiwara, S., Yoshida, S., and Yoshii, M. Transient and delayed potassium currents in the egg cell membrane of the coelenterate, *Renilla koellikeri. J. Physiol. (Lond).* **318**: 123-141, 1981.

Hessinger, D.A. and Brehm, P. Voltage-gated ionic currents in epithelial sensory cells from sea anemone tentacles. *Soc. Neurosci. Abstr.* **16**: 509, 1990.

Hille, B. *Ionic Channels of Excitable Membranes.* Sunderland (Massachusetts), Sinauer, 1984, pp. 316-326.

Hoshi, T., Rothlein, J., and Smith, S.J. Facilitation of Ca^{2+}-channel currents in bovine adrenal chromaffin cells. *Proc. Natl. Acad. Sci. USA.* **81**: 5871-5875, 1984.

Ikeda, S.R. Double-pulse calcium channel current facilitation in adult rat sympathetic neurones. *J. Physiol. (Lond).* **439**: 181-214.

Ikeda, S.R., Schofield, G.G., and Weight, F.F. Na^+ and Ca^{2+} currents of acutely isolated adult rat nodose ganglion cells. *J. Neurophysiol.* **55**:527-539, 1986.

Iwasaki, S. and Satow, Y. Sodium- and calcium-dependent spike potentials in the secretory neuron soma of the X-organ of the crayfish. *J. Gen. Physiol.* **57**: 216-238, 1971.

Iwasaki, S., Satow, Y., and Kuroda, T. On the hyperpolarizing inactivation of the Ca^{++}-dependent action potentials. *Proc. Jap. Acad.* **49**: 564-568, 1973.

Jones, B.R. and Hartline, D.K. Anomalous coupling between I_A and I_J in lobster stomatogastric neurons. *Soc. Neurosci. Abstr.* **15**: 76, 1989.

Jones, S.W. and Marks, T.N. Calcium currents in bullfrog sympathetic neurons II. Inactivation. *J. Gen. Physiol.* **94**: 169-182, 1989.

Kaczmarek, L.K. and Strumwasser, F. A voltage clamp analysis of currents underlying cAMP-induced membrane modulation in isolated peptidergic neurons of *Aplysia*. *J. Neurophysiol.* **52**: 340-349, 1984.

Kostyuk, P.G. and Krishtal, O.A. Separation of sodium and calcium currents in the somatic membrane of mollusc neurones. *J. Physiol. (Lond).* **270**: 545-568, 1977.

Kramer, R.H. and Zucker, R.S. Calcium-dependent inward current in *Aplysia* pace-maker neurones. *J. Physiol. (Lond).* **362**: 107-130, 1985.

Lemos, J.R. and Nowycky, M.C. Two types of calcium channels coexist in peptide-releasing vertebrate nerve terminals. *Neuron.* **2**: 1419-1426, 1989.

Leonard, R.J. and Lisman, J.E. Light modulates voltage-dependent potassium channels in *Limulus* ventral photoreceptors. *Science.* **212**: 1273-1275, 1981.

Lewis D.V. Spike aftercurrents in R15 of *Aplysia*: Their relationship to slow inward current and calcium influx. *J. Neurophysiol.* **51**: 387-403, 1984.

Lisman J., Fain G., and Swan M. Voltage-dependent conductance in *Limulus* ventral photoreceptors. *Biol. Bull.* **155**: 453-454, 1978.

MacDermott, A.B. and Weight, F.F. Action potential repolarization may involve a transient Ca^{2+}-sensitive outward current in a vertebrate neuron. *Nature.* **300**: 185-188, 1982.

Mangerich, S., Keller, R., and Dircksen, H. Immunocytochemical identification of structures containing putative red pigment-concentrating hormone in two species of decapod crustaceans. *Cell Tissue Res.* **245**: 377-386, 1986

McIntosh, J.E.A. and McIntosh, R.P. *Mathematical modelling and computers in endocrinology*. Springer-Verlag, New York, 1980.

Meyers, D., Graf, R., Ruben, P., and Cooke, I. Patch-clamp of cultured crustacean peptidergic neurons. *Soc. Neurosci. Abstr.* **14**: 1128, 1988.

Meyers, D.E.R. and Barker, J.L. Whole-cell patch clamp analysis of voltage-dependent calcium conductances in cultured embryonic rat hippocampal neurons. *J. Neurophysiol.* **61**: 467-477, 1989.

Meyers, D.E.R. and Graf, R.A. Inactivation of I_{Ca} in cultured crustacean peptidergic neurons. *FASEB J.* **4(3,II)**: A1201, 1990.

Nagano, M. and Cooke, I.M. Comparison of electrical responses of terminals, axons, and somata of a peptidergic neurosecretory system. *J. Neuroscience.* **7**: 634-648, 1987.

Newcomb, R.W. Amino acid sequences of neuropeptides in the sinus gland of the land crab, Cardisoma carnifex: A novel neuropeptide proteolysis site. *J. Neurochem.* **49**: 574-583, 1987.

Nowycky, M.C., Fox, A.P., and Tsien, R.W. Three types of neuronal calcium channel with different calcium channel sensitivity. *Nature.* **316**: 440-443, 1985.

Onetti, C.G., García, U., Valdiosera, R.F., and Aréchiga, H. Ionic currents in crustacean neurosecretory cells. *J. Neurophysiol.* **64**: 1514-1526, 1990.

Potter, D.D. Observations on the neurosecretory system of portunid crabs. PhD thesis, Harvard University, 1956.

Rehm, M. Observations on the localization and chemical constitution of neurosecretory material in nerve terminals in *Carcinus maenas*. *Acta Histochem.* **7**: 88-106, 1959.

Rudy, B. Diversity and ubiquity of K channels. *Neuroscience.* **25**: 729-749, 1988.

Salkoff, L.B. *Drosophila* mutants reveal two components of fast outward current. *Nature.* **302**: 249-251.

Schwindt, P.C. and Crill, W.E. Differential effects of TEA and cations on outward ionic currents of cat motoneurons. *J. Neurophysiol.* **46**: 1-16, 1981.

Segal, M. and Barker, J.L. Rat hippocampal neurones in culture: Potassium conductances. *J. Neurophysiol.* **51**: 1409-1433, 1984.

Segal M., Rogawski, M.A., and Barker J.L. A transient potassium conductance regulates the excitability of cultured hippocampal and spinal neurons. *J. Neuroscience.* **4**: 604-609, 1984.

Sherman, A., Kreiger, J., and Rinzel, J. Domain model for Ca^{2+} channels at low channel density. *Biophys. J.* **58**: 985-995, 1990.

Standen, N.B. and Stanfield, P.R. A binding-site model for calcium channel inactivation that depends on calcium entry. *Proc. Roy. Soc. Lond. B.* **217**: 101-110, 1982.

Stewart, R.R., Nicholls, J.G., and Adams, W.B. Na^+, K^+ and Ca^{2+} currents in identified leech neurons in culture. *J. Exp. Biol.* **141**: 1-20, 1989.

Strong, J.A. Modulation of potassium current kinetics in bag cell neurons of *Aplysia* by an activator of adenylate cyclase. *J. Neuroscience.* **4**: 2772-2783, 1984.

Stuenkel, E. Simultaneous monitoring of electrical and secretory activity in peptidergic neurosecretory terminals of the crab. *J. Physiol. (Lond).* **359**: 163-187, 1985.

Stuenkel, E. and Cooke, I.M. Electrophysiological characteristics of peptidergic nerve terminals correlated with secretion. In: *Current topics in neuroendocrinology*, Vol 9 (Ganten, D., and Pfaff, D., eds). Berlin, Springer, 1988, pp 123-150.

Swandulla, D. and Lux, H.D. Activation of a non-specific cation conductance by intracellular Ca^{2+} elevation in bursting pacemaker neurons of *Helix pomatia.* *J. Neurophysiol.* **54**: 1430-1443, 1985.

Tachibana, M. Ionic currents of solitary horizontal cells isolated from goldfish retina. *J. Physiol. (Lond).* **345**: 329-351, 1983.

Tazaki, K. and Cooke, I.M. Currents under voltage clamp of burst-forming neurons of the cardiac ganglion of the lobster (*Homarus americanus*). *J. Neurophysiol.* **56**: 1739-1762, 1986.

Tazaki, K. and Cooke I.M. Characterization of Ca current underlying burst formation in lobster cardiac ganglion motoneurons. *J. Neurophysiol.* **63**: 370-384, 1990.

Thompson S.H. Three pharmacologically distinct potassium channels in molluscan neurones. *J. Physiol. (Lond).* **265**: 465-488, 1977.

Thompson, S. and Coombs, J. Spatial distribution of Ca currents in molluscan neuron cell bodies and regional differences in the strength of inactivation. *J. Neuroscience.* **8**: 1929-1939, 1988.

Tillotson, D. Inactivation of calcium conductance dependent on entry of Ca ions in molluscan neurons. *Proc. Natl. Acad. Sci. USA.* **77**: 1497-1500, 1979.

Tsien, R.Y. New calcium indicators and buffers with high selectivity against magnesium and protons: design, synthesis and properties of prototype structures. *Biochemistry* **19**: 2396-2404, 1980.

Weatherby, T.M. An ultrastructural study of the sinus gland of the crab, *Cardisoma carnifex. Cell Tiss. Res.* **220**: 293-312, 1981.

Wu, C.F. and Haugland, F.N. Voltage-clamp analysis of membrane currents in larval muscle fibers of *Drosophila*: Alteration of potassium currents in *Shaker* mutants. *J. Neuroscience.* **5**: 2626-2640, 1985.

Figure 4-1. Whole-cell voltage-clamp records in physiological-like solutions. A. Veiled cell (1 d in culture): Both inward and outward currents are present. B. Branched cell (1 d): outward currents predominate. All records corrected for leak and capacity current. Lower panels: Hoffman modulation contrast photomicrographs of the recorded cells. Calibration bars, 20 μm.

A Veiled Neuron (24 hrs)

B Branched Neuron (24 hrs)

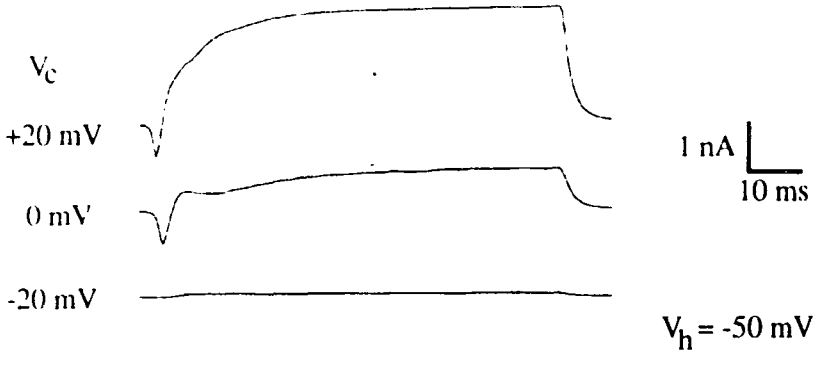

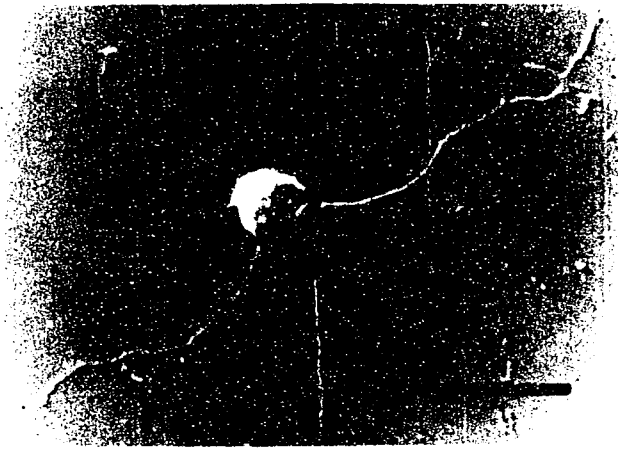

Figure 4-2. I_{Na}: Inward current (corrected for leak and capacity current) from a veiled neuron in solutions minimizing Ca and outward current ($[Na^+]_o$ = 220 mM, half normal). Superimposed traces show response to a command of 0 mV before and after addition of 0.5 μM TTX. Note complete abolition of inward current; the rise time of the current is probably a function of the limiting effect of cell capacitance on clamp speed. I(V) plot from a different cell maintained at 10°C (leak and capacity subtracted) shows peak at +20 mV; extrapolation to reversal potential gives +58 mV ($[Na^+]_o$ = 110 mM, $[Na^+]_i$ = 10 mM, T = 10°C, Calculated E_{Na} = +62 mV). All neurons in this and subsequent Figures 24 - 48 hr. in culture.

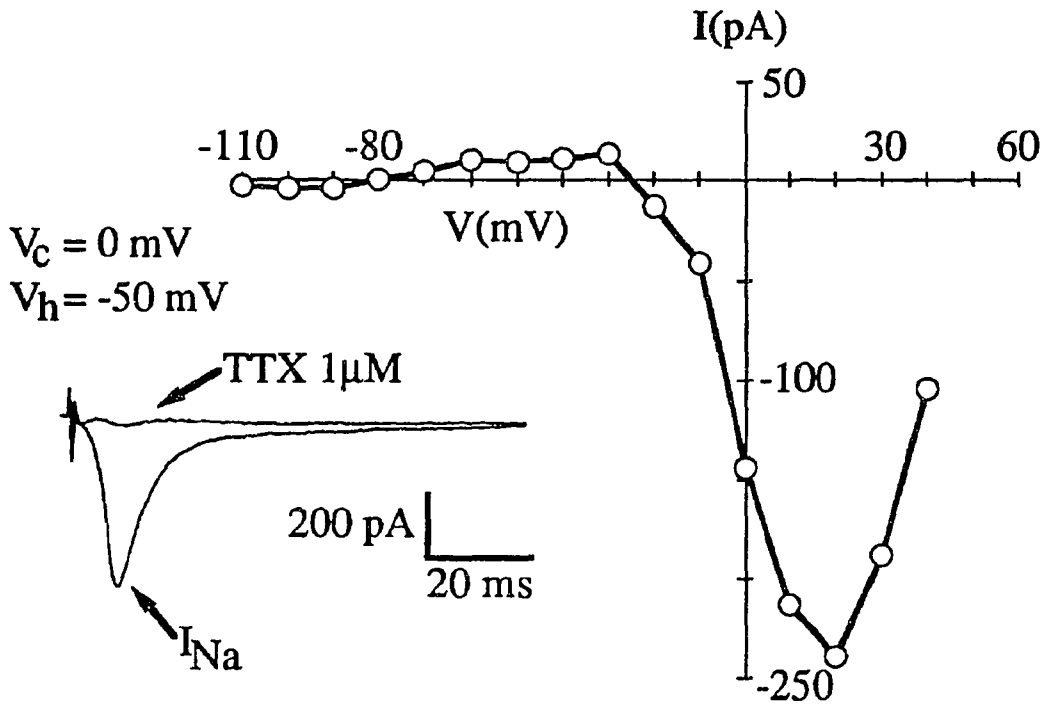
I(pA)
50
-110
-80
30
60
V(mV)
V_c = 0 mV
V_h = -50 mV
TTX 1μM
200 pA
20 ms
I_{Na}
-100
-250

Figure 4-3. Identification of I_{Ca} in veiled cells. A. I(V) curve, drawn from leak and capacity subtracted records, showing peak current (o) and the current remaining at the end of a 720 msec command (▲) recorded under conditions designed to eliminate Na and K currents, holding potential (V_h) -40 mV. These curves are typical of those obtained under optimal experimental conditions in showing activation beginning at -30 mV, peak at +10 mV, and lack of reversal even at +60 mV. B. Effect of varying $[Ca^{2+}]_o$ and Sr^{2+} substitution, plotted from the raw data. Measurements were made at the end of a 160 msec command (all from the same neuron). External solutions presented in the following order: 1.3 mM Ca^{2+} (□), 13 mM Ca^{2+} (o), 13 mM Sr^{2+} (▲). Note increase in current amplitude with increased divalent concentration, ability of Sr^{2+} to replace Ca^{2+}, and shift of I(V) curve approximately 20 mV left in Sr^{2+}. C. I(V) curves from a single neuron in 13 mM Ca^{2+} (o) and in the same solution with the addition of 0.5 mM Cd^{2+} (▲). D. Responses of neuron in C to command of +10 mV in the two salines (V_h = -40 mV). Note lack of inward current when Cd^{2+} is present (raw data).

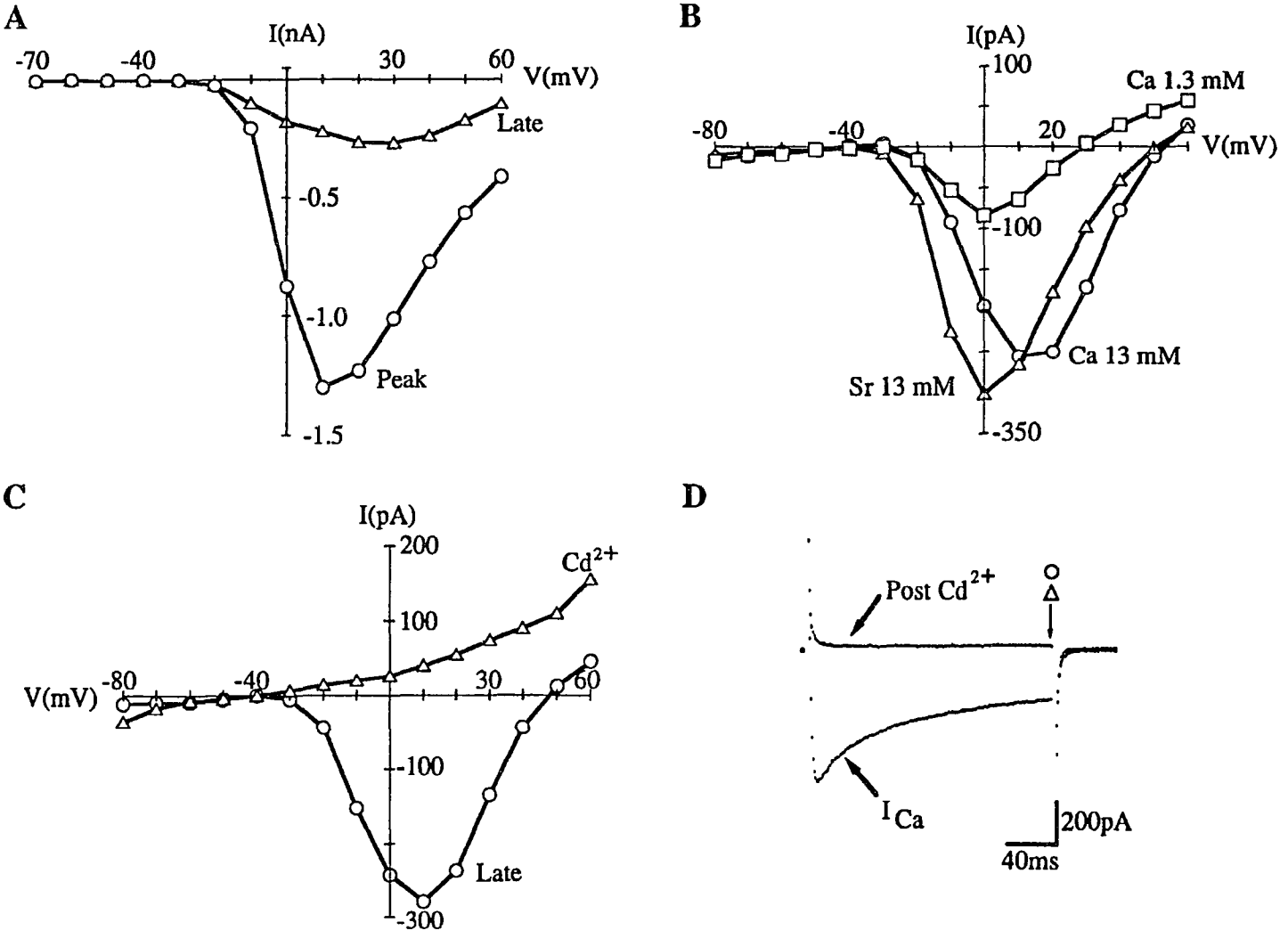
A
I(nA)
-70
-40
30
60
V(mV)
Late
-0.5
-1.0
Peak
-1.5
B
I(pA)
100
Ca 1.3 mM
-80
-40
20
V(mV)
-100
Ca 13 mM
Sr 13 mM
-350
C
I(pA)
200
Cd2+
100
V(mV)
-80
-40
30
60
-100
Late
-300
D
Post Cd2+
ICa
200pA
40ms

Figure 4-4. There is little steady state inactivation of I_{Ca} at a V_h of -40 mV. Leak and capacity subtracted I(V) curves from a V_h of -40 and -80 mV are plotted together and demonstrate that there is little change in the peak current. Inset: Superimposed leak- and capacity-subtracted records generated by a 720 msec command to +10 mV from a V_h of -40 and -80 mV, from a separate series of experiments using abbreviated protocols to minimize the effects of rundown. Note that peak current amplitudes are virtually identical and that there is only a slight difference in current amplitude at the end of the step.

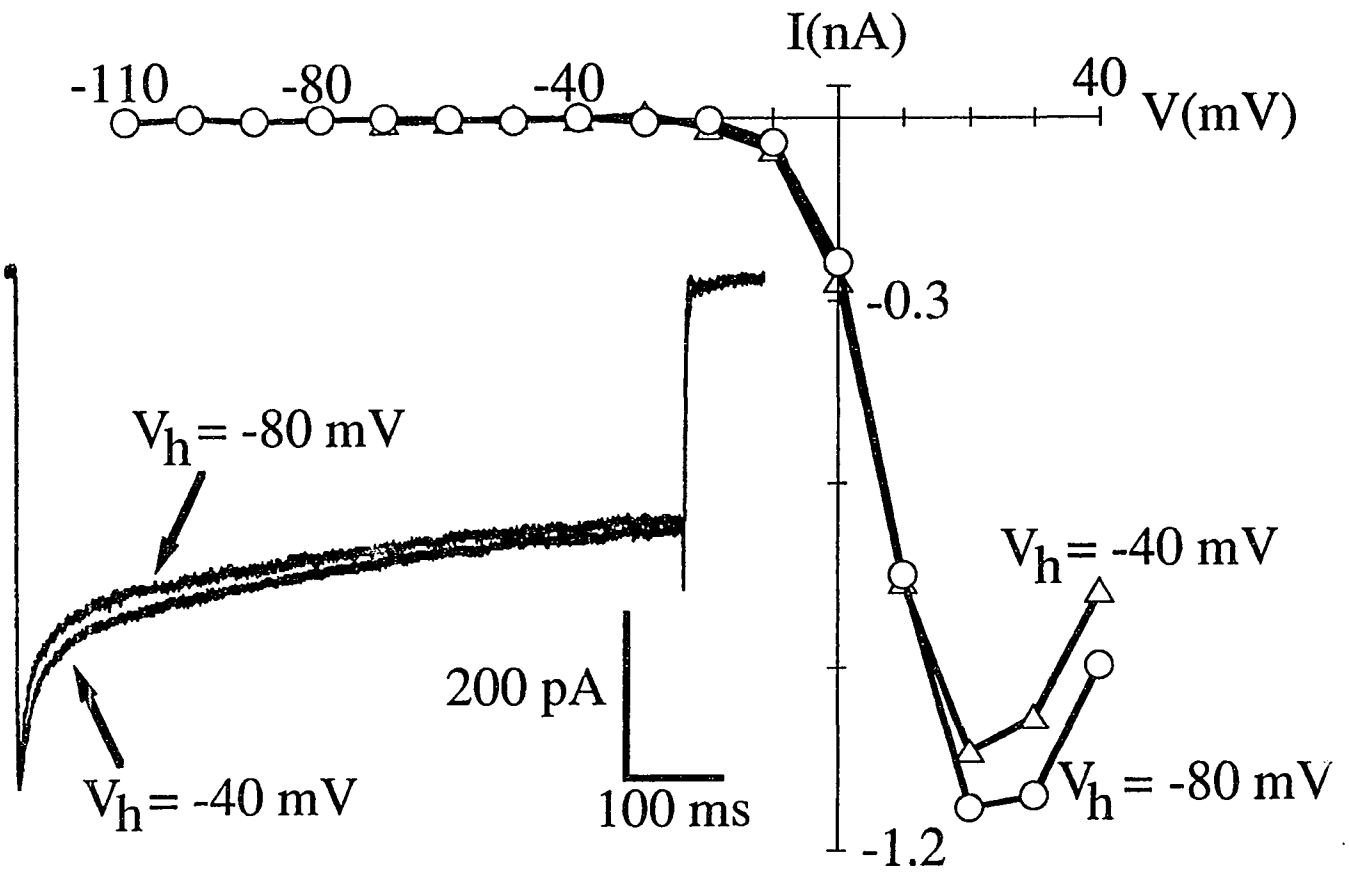
I(nA)
-110
-80
-40
40
V(mV)
-0.3
V_h= -80 mV
V_h= -40 mV
200 pA
100 ms
V_h= -40 mV
V_h= -80 mV
-1.2

Figure 4-5. Prepulse voltage (A and B) and interpulse interval (C and D) affect test-pulse current amplitude. A. Superimposed leak- and capacity-subtracted current responses to the test pulse (V_c = 0 mV) portion of the voltage protocol (prepulse duration 200 msec, prepulse voltage -30 to +60 in 10 mV increments, interval 200 msec, test pulse duration 720 msec, control = no prepulse; all records leak and capacity subtracted). Note the enhancement of the test pulse current following the prepulse to +60 mV. B. Plot comparing the test-pulse current (▵, normalized with respect to control, indicated by dashed lined) and the I(V) relation (○, normalized with respect to the maximal inward current). Note that maximal depression of the test-pulse current follows the prepulse generating maximal inward current. Note enhancement of test-pulse current over control following large prepulses. C. Superimposed leak- and capacity-subtracted current responses to the test pulse alone (control, largest peak) and for the responses to the test pulse after a variety of interpulse intervals ranging from 15 msec to 1 sec. D. Semilogarithmic plot showing recovery of the test-pulse I_{Ca} with increasing interpulse interval (data normalized with respect to control). Recovery is maximal for intervals >1 sec, but was never complete even for intervals as long as 10 sec.

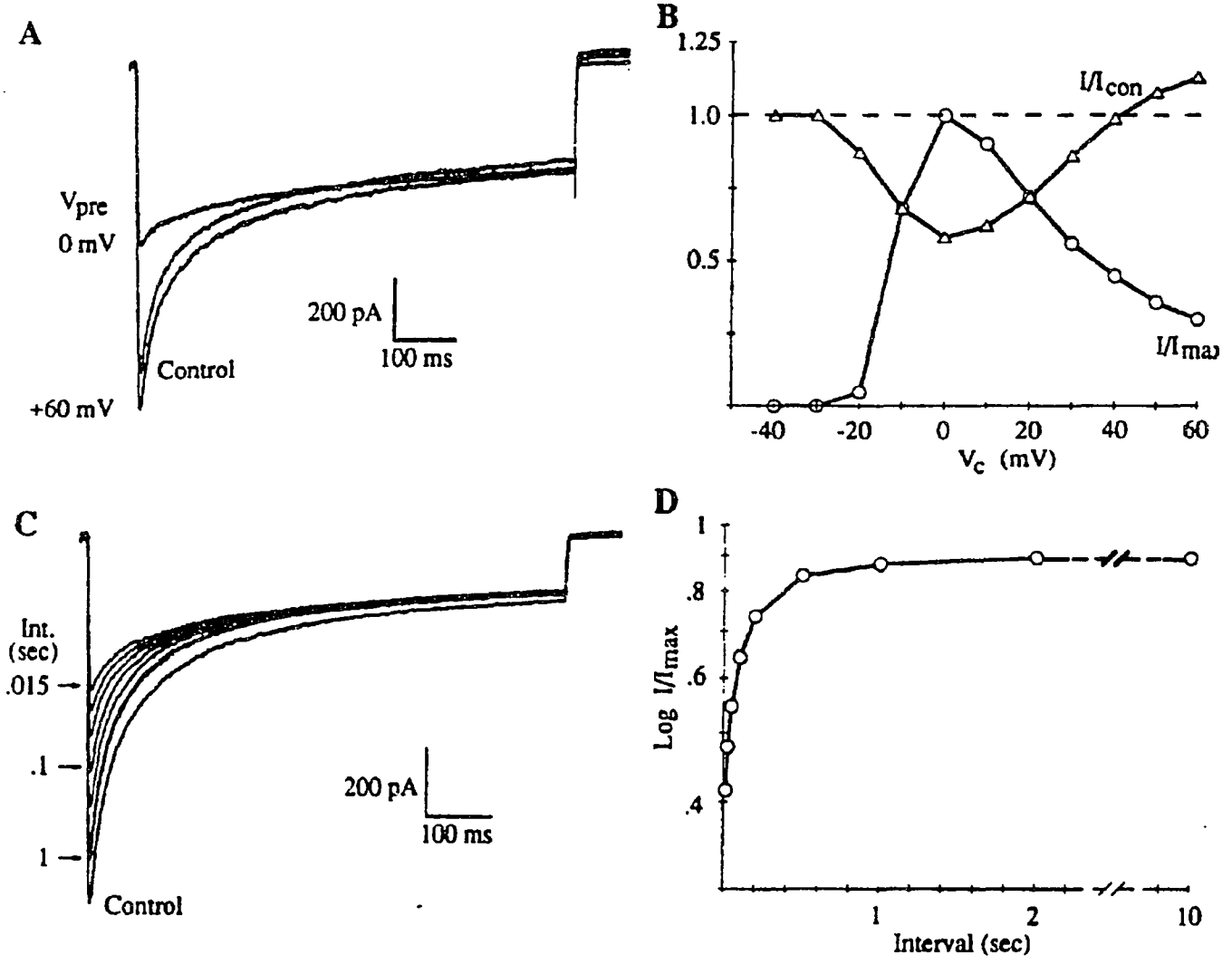
A
Vpre
0 mV
+60 mV
Control
200 pA
100 ms
B
1.25
1.0
0.5
I/Icon
I/Imax
-40
-20
0
20
40
60
Vc (mV)
C
Int.
(sec)
.015
.1
1
Control
200 pA
100 ms
D
1
.8
.6
.4
Log I/Imax
1
2
10
Interval (sec)

Figure 4-6. Substitution of Sr^{2+} for Ca^{2+} affects the decay process. A. Maximal current responses of a single veiled neuron recorded in 13 mM Ca^{2+} and then in Sr-substituted solution. The magnitude of decay of I_{Sr} is substantially smaller that of I_{Ca}. B. Superimposed responses of the same neuron to V_c = +20 mV. Note similar peak amplitude and again the smaller decay in Sr. C. Superimposed current responses to V_c = +40 mV (same neuron). Note that the difference in decay magnitude has been much reduced at this highly depolarized potential. (V_h = -40 mV).

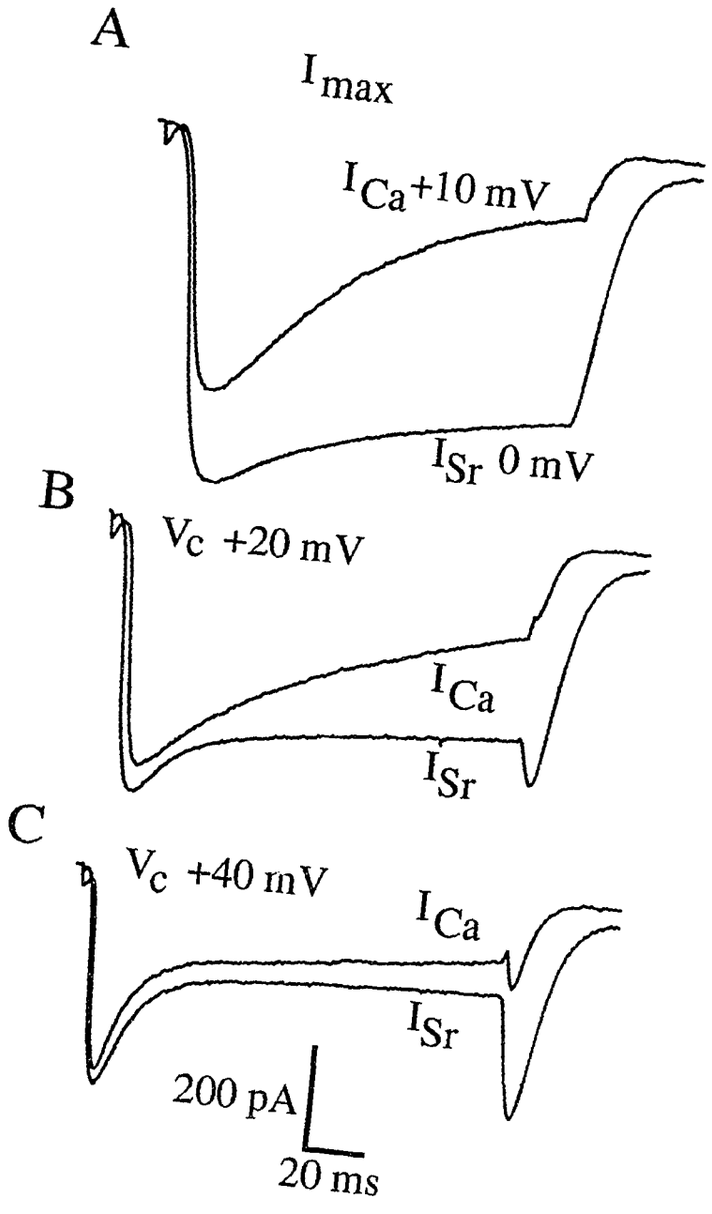
A
I_{max}
I_{Ca}+10 mV
I_{Sr} 0 mV
B
V_c +20 mV
I_{Ca}
I_{Sr}
C
V_c +40 mV
I_{Ca}
I_{Sr}
200 pA
20 ms

Figure 4- 7. A. Late outward current (I_K): I(V) curve plotted from uncorrected current measured at the end of 80 msec voltage clamp commands from V_h of -50 mV. The curve is typical of all cells for measurements made at 80 msec or later. Inset: superimposed current records for three commands to the voltages indicated. Early outward current appears to be absent (see below). Inward currents have been blocked in these and all records shown by addition of TTX (0.5 μM) and Cd^{2+} (0.5 mM) to the external solution. (Branched neuron, 20 μm diam.) B. Early outward current (I_A). Upper panel. Non-leak subtracted records showing the presence of I_A during commands from -80 mV. Lower panel. Similar records illustrating the dependence of I_A on holding potential (calibration bars apply to both sets of records). C. I(V) plot of: Δ, uncorrected peak outward currents observed during a series of commands from -80 mV showing activation; O, peak currents at +20 mV from different levels of V_h showing removal of inactivation; and ◊, late current at +20 mV from different levels of V_h to show the lack of effect on I_K. The V_h for half inactivation was -45 mV in this neuron (x = -46 mV, n=9). (Branched neuron, 20 μm diam.)

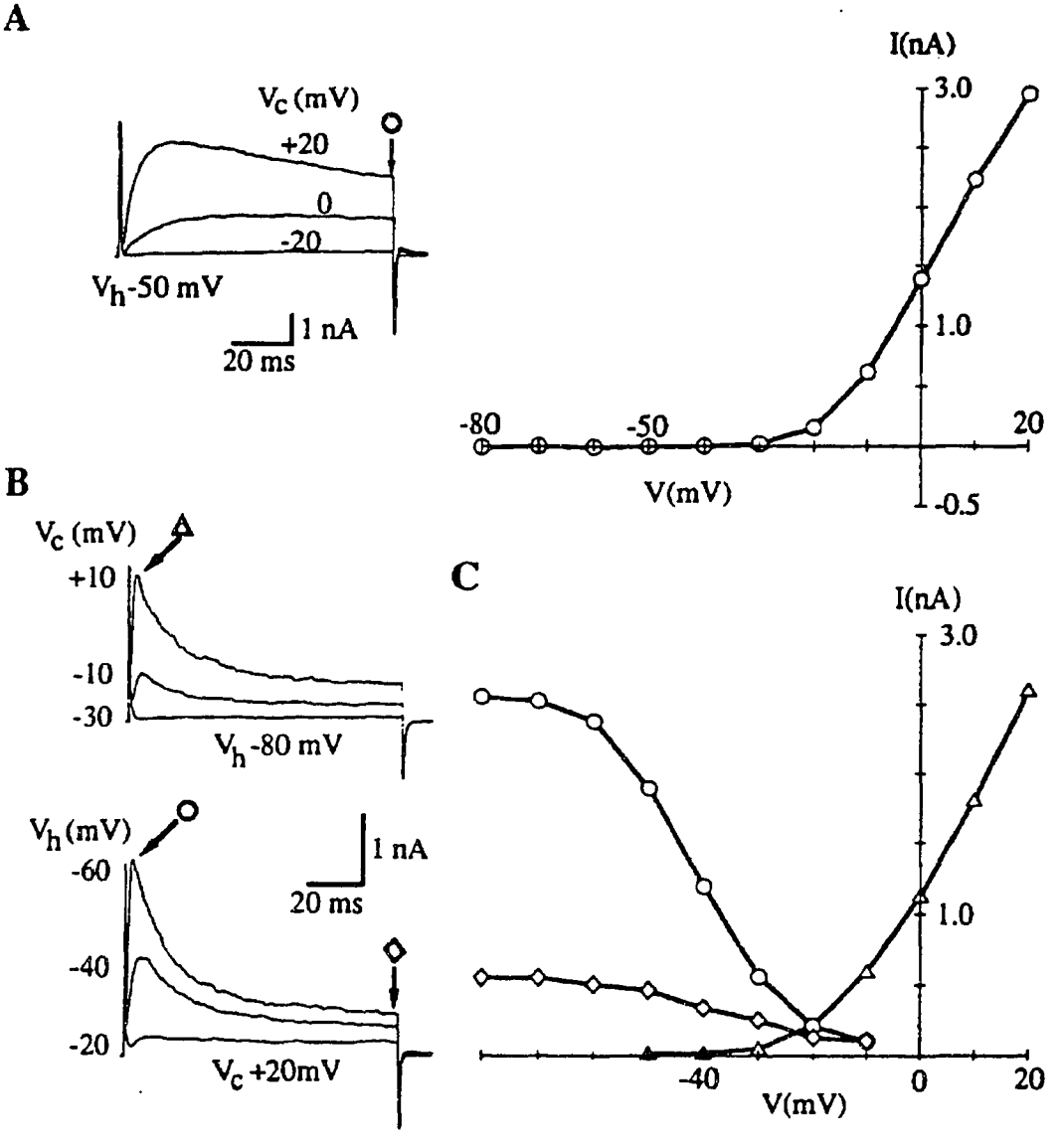
A
V_c (mV)
+20
0
-20
V_h-50 mV
1 nA
20 ms
I(nA)
3.0
1.0
-0.5
-80
-50
20
V(mV)
B
V_c (mV)
A
+10
-10
-30
V_h-80 mV
V_h (mV)
-60
-40
-20
V_c +20mV
1 nA
20 ms
C
I(nA)
3.0
1.0
-40
0
20
V(mV)

Figure 4- 8. Outward current reversal potentials. Plots of tail current amplitude vs. observation potential. Activation of outward current was achieved using a 10 msec command to +20 mV from the V_h indicated. A. Curve typical of cells in normal $[K^+]_o$. Inset shows records used to construct this plot. (Veiled neuron, 37 µm diam.) B. Curves from a neuron bathed initially in 11 mM K^+ and then in 110 mM K^+ (E_K indicated). The reversal potential in raised K^+ is within 3 mV of the calculated E_K. Note the more linear curve in elevated K^+. (Veiled neuron, 37 µm diam.)

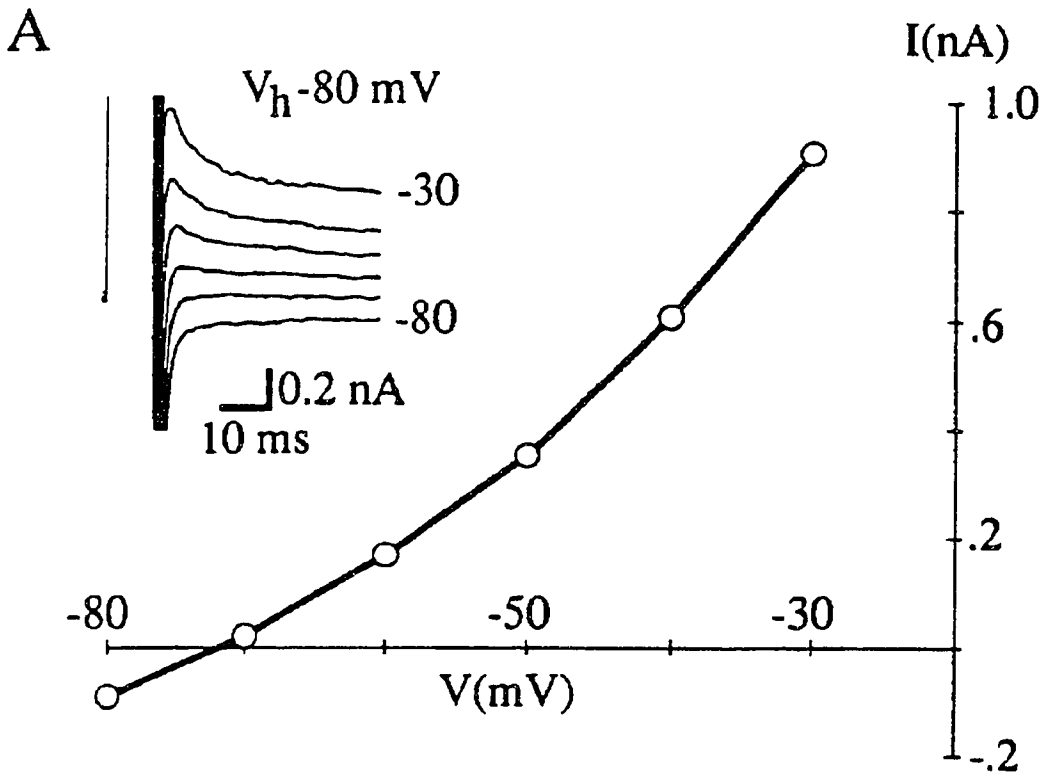
A
I(nA)
V_h-80 mV
1.0
-30
.6
-80
0.2 nA
10 ms
.2
-80
-50
-30
V(mV)
-.2

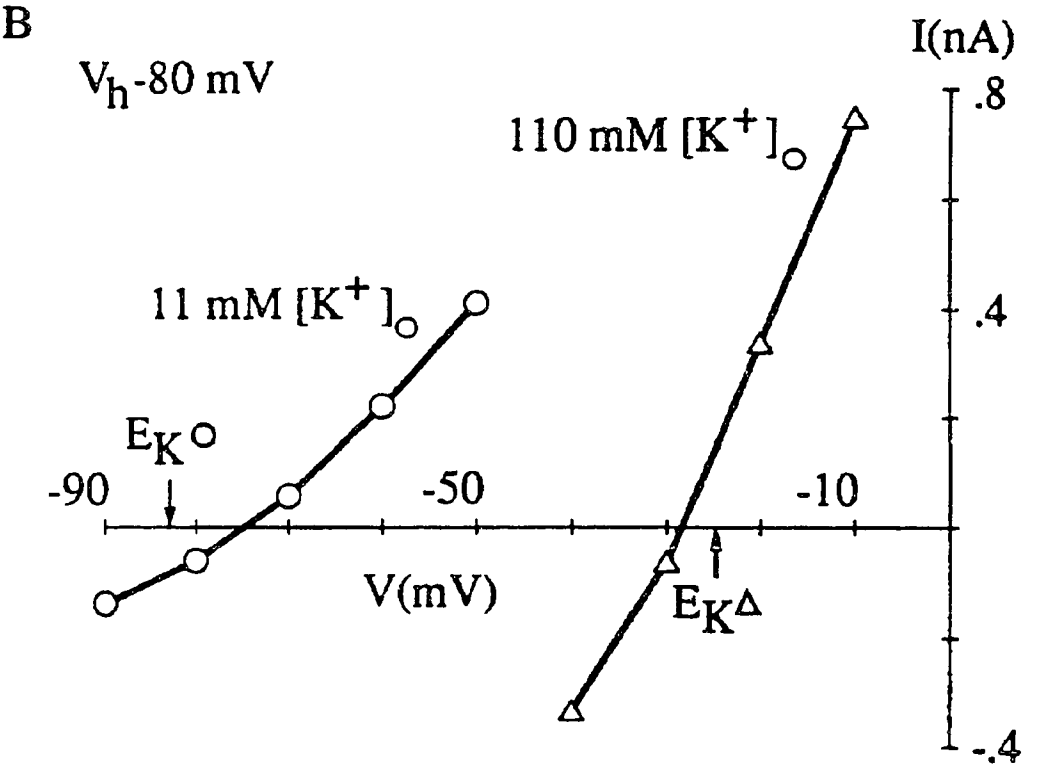
B
I(nA)
V_h-80 mV
.8
110 mM $[K^+]_o$
11 mM $[K^+]_o$
.4
E_K
-90
-50
-10
V(mV)
E_K
-.4

Figure 4-9. Increased late outward current observed in some neurons following addition of 4-AP. A. Records typical of 60% of cells examined. After addition of 4-AP (3 mM), the early peak current was absent and late current was augmented in this cell by 85%. Subsequent addition of TEA-Br (50 mM) inhibited the current. (Veiled neuron, 32 µm diam., see also Fig. 10B). B. Records typical of the other 40%. No effect of 4-AP on late current. Veiled neuron, 34 µm, diam. C. Records typical of experiments in which 4-AP was added after TEA; no effect on late current. (Veiled neuron, 38 µm diam. Calibration bars in C apply also to B.) Records in A, V_h-70 mV, V_c +10 mV; in B and C, V_h -80, V_c +10 mV.

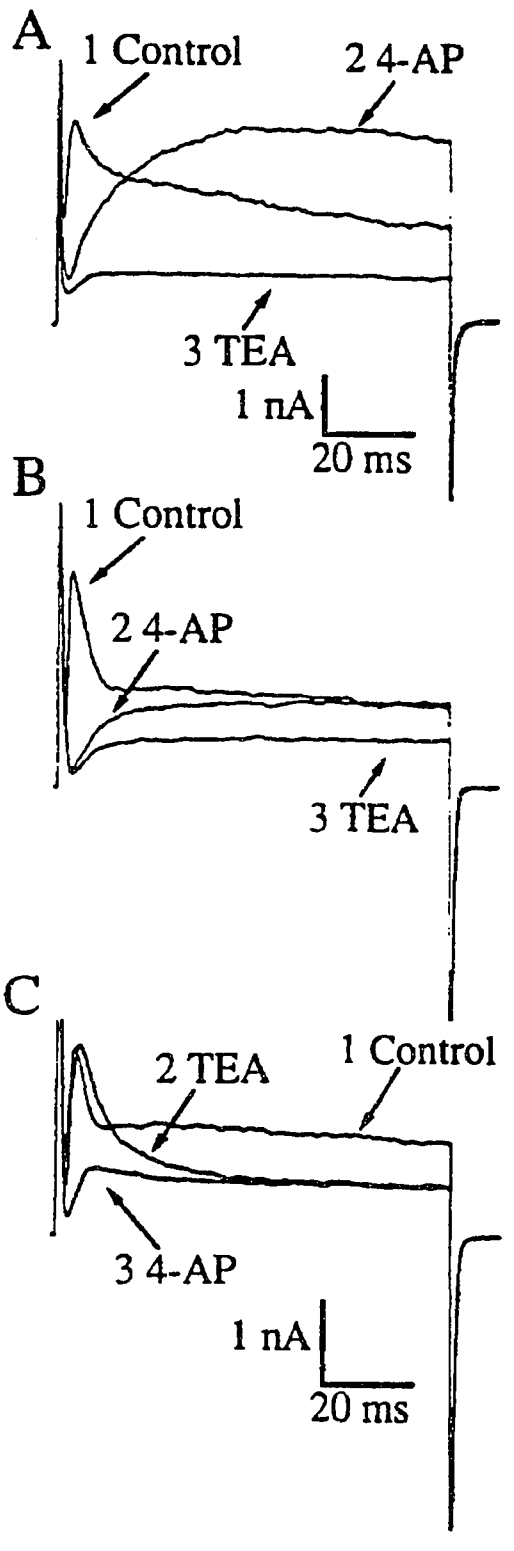
A
1 Control
2 4-AP
3 TEA
1 nA
20 ms
B
1 Control
2 4-AP
3 TEA
C
2 TEA
1 Control
3 4-AP
1 nA
20 ms

Figure 4-10. A. Effect of TEA-Br (50 mM) in a neuron in which the I_K was not enhanced by 4-AP and in which I_A was not apparent even from V_h = -80 mV (see inset). I(V) curve from current measurements (uncorrected for leak and capacity current) at the end of 90 msec commands before (O) and after (▲) addition of 30 mM TEA (approximately 50% reduction). (Veiled neuron, 32 µm diam.) B. Inhibition of I_A by 4-AP. I(V) curve obtained by plotting peak current (uncorrected for leak and capacity current) for commands to +20 mV vs. V_h before (O) and after (▲) the addition of 3 mM 4-AP (post-4-AP measurements made at the same points in time as the corresponding peaks in control records). Inset: Superimposed records for V_h of -80 mV and V_c +20 mV, before and after addition of 4-AP. Note in 4-AP the lack of an early peak of outward current, and failure of hyperpolarization to increase the current. Note in the inset the increase in late current following the addition of 4-AP. (Veiled neuron, 37 µm diam., see also Fig. 9A.)

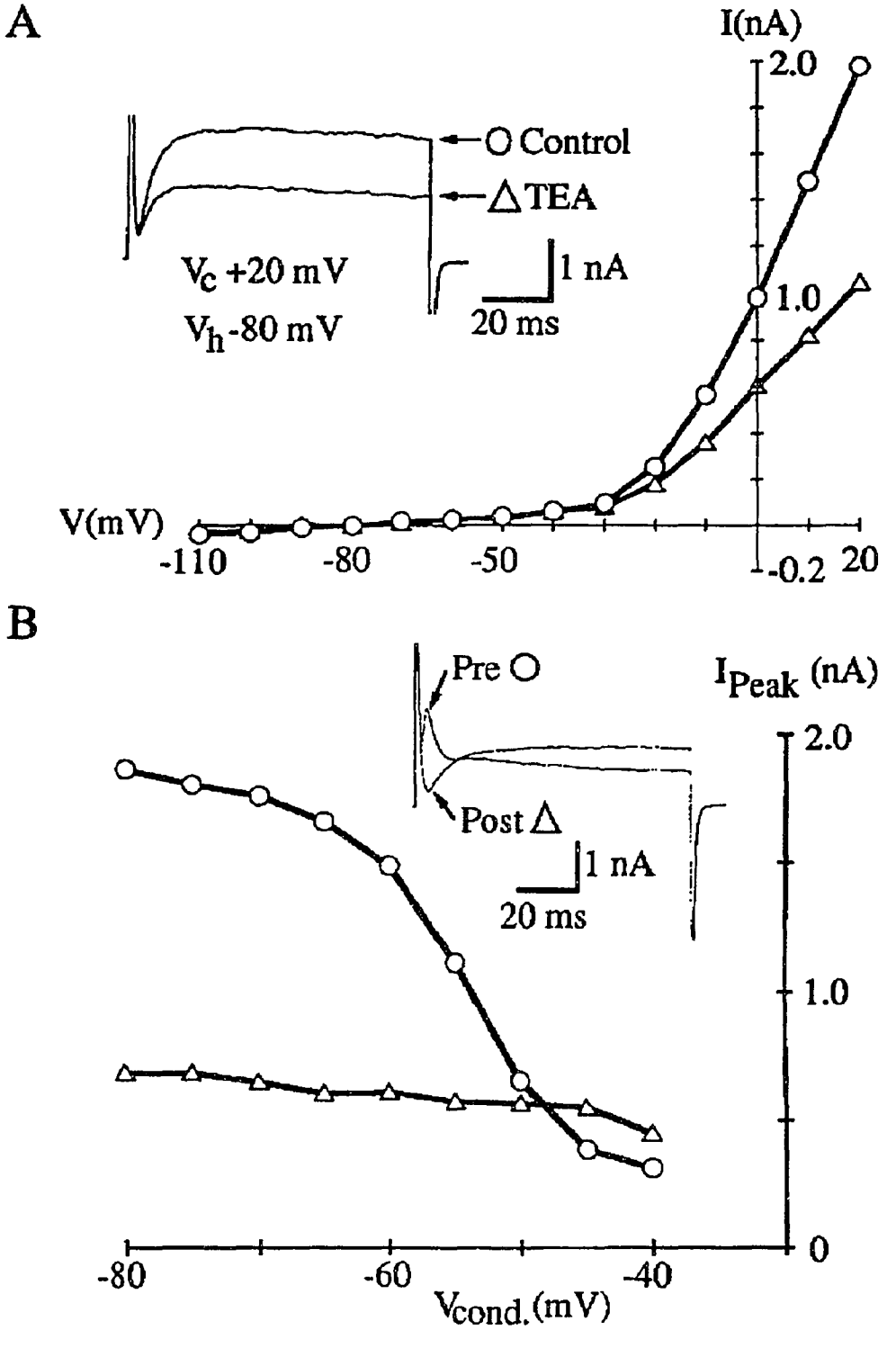
A
I(nA)
2.0
1.0
O Control
△TEA
Vc +20 mV
Vh -80 mV
1 nA
20 ms
V(mV)
-110
-80
-50
-0.2
20
B
Pre O
Post △
1 nA
20 ms
IPeak (nA)
2.0
1.0
0
-80
-60
-40
Vcond.(mV)

CHAPTER 5

CALCIUM REGULATORY RESPONSES OF ADULT NEUROSECRETORY NEURONS REGENERATING DISTINCT MORPHOLOGIES IN DEFINED CULTURE

Introduction

Intracellular free calcium concentration ($[Ca^{2+}]_i$) has been identified as a sculptor of neuronal morphology because of its influence in guiding developing (Bentley *et al.*, 1991) and regenerating (Mattson and Kater, 1987; Kater *et al.*, 1988; Kater and Mills, 1991) neurons. $[Ca^{2+}]_i$ have been shown to influence morphology and have been studied in developing sensory neurons *in situ*, and *in vitro* in a variety of embryonic and adult neuronal preparations (Kater *et al.*, 1988; Silver *et al.*, 1989; Ivins *et al.*, 1991; Garyantes *et al.*, 1992; Al-Mohanna *et al.*, 1992). What range of basal $[Ca^{2+}]_i$ exists and whether inhibition of mechanisms that regulate $[Ca^{2+}]_i$ can influence outgrowth morphology has not previously been addressed in crustacean neurons; however, $[Ca^{2+}]_i$ changes have been reported from crab stomatogastric ganglion neurons *in situ* (Ross and Graubard, 1989). In addition to this report, a preliminary report has appeared addressing $[Ca^{2+}]_i$ in regenerating peptidergic neurosecretory bag cells of the mollusc *Aplysia* (Miller *et al.*, 1991).

Adult neurons from the X-organ - sinus gland system, the major peptide neurosecretory system of Crustacea, have recently been cultured (Cooke *et al.*, 1989). These neurons consistently display robust, characteristic outgrowth morphologies that, at least for one morphological type, corresponds to its hormonal contents (Cooke *et al.*, 1989). These neuronal morphologies occur from individually isolated cells in completely defined conditions that can be as simple as saline supplemented with glucose and L-glutamine (Cooke *et al.*, 1989; Grau and Cooke, 1992). In most preparations used to study outgrowth mechanisms, it is necessary to supplement the medium with factors in order to initiate outgrowth, or use embryonic neurons. The cultures of X-organ neurons, therefore, provide controlled conditions under which to study intrinsic mechanisms of outgrowth under well-defined conditions and without cell-cell interactions.

One neuronal type extends a large veil from the distal end of a residual neurite; these cells are immunoreactive for crustacean hyperglycemic hormone (CHH). A number of cells with long filamentous directed branching outgrowth patterns show immunoreactivity indicative of red pigment concentrating hormone (RPCH) or molt inhibiting hormone (MIH) (see Cooke *et al.*, 1989).

Electrical activity and calcium regulation are important physiological regulators of secretory function in neurons (Katz and Miledi, 1967; Cooke *et al.*, 1977; Cooke and Haylett, 1984; Cooke, 1985; Stuenkel, 1985; Lemos and Nordmann, 1986; Zucker and Llando, 1986; Nagano and Cooke, 1987; Zucker and Haydon, 1988; Augustine *et*

al., 1991; Mulkey and Zucker, 1991), and these mechanisms may also influence regenerative outgrowth (Cooke *et al.*, 1989).

Here, I report ratiometric observations of fura-2 loaded neurosecretory cells to characterize the basal $[Ca^{2+}]_i$ and changes of $[Ca^{2+}]_i$ in response to depolarizing stimuli. The experiments sought to detect differences between calcium regulatory mechanisms of the cells displaying distinct outgrowth morphologies. When challenged with a high potassium (K) stimulus, differences were apparent in the ability of the cultured neurons to restore $[Ca^{2+}]_i$ which appeared related to the morphological type, the extent of outgrowth, and the age of the neurons. Portions of this work appeared previously in abstract form (Graf, 1992).

Methods

Animals, Dissection, and Primary Cell Culture

Adult male land crabs (*Cardisoma carnifex*) of approximately 200 g were used for this study and were obtained from Christmas Island, Republic of Kiribati. The medulla terminalis X-organ cell group was dissected from the eyestalk, enzymatically treated with trypsin, and neurons were isolated and cultured at low density under completely defined conditions as described previously (Cooke *et al.*, 1989). Cells were plated onto German coverglass (35 X 50 mm; Carolina Biological) coated with 0.001% poly-L-lysine-(MW > 300,000; Sigma Chem. Co.). At the time of dye

loading, the coverglass with adhered neurons was transferred to a custom-made chamber for optical and electrophysiological experiments.

Current Clamp Electrophysiology

Conventional current clamp recordings were made from X-organ neurons before and after the addition of 5X and 10X potassium saline to determine the extent of depolarization. Filament containing electrode glass (1.2 mm diameter) was pulled to resistances higher than 30 MΩ (with 3 M KCl). Electrodes were connected to a conventional microelectrode amplifier as described in the iontophoretic loading procedure described below.

Whole-cell current-clamp recordings were made with an Axoclamp 2A amplifier (Axon Instruments) equipped with an HS-2 headstage (X=0.01). Seal formation was performed in "bridge" mode. The electrode transient was nulled during seal formation. The filtered data were digitized (10 to 400 μsec/data point) and stored on the fixed disk of an 80286-based personal computer using the data acquisition and analysis program pCLAMP (V 5.5, Axon Instruments). Recordings were made at room temperature (24 - 26°C). Cells were visualized at 400X on the stage of an inverted microscope (Nikon Diaphot) equipped with Hoffman modulation optics (Modulation Optics). Patch pipettes were pulled from 1.5 mm O.D. thin-walled capillary tubing (World Precision Instruments, TW150F-4) on a vertical pipette puller (David Kopf Instruments, model 700 C) and fire polished with a microforge

(Narishige, model MF-83). Pipettes were coated with Sylgard (Dow Corning, 184 elastomer kit) to reduce capacitance. Pipette-to-bath resistances ranged from 1 to 10 megohms (MΩ).

Solutions

Internal: K-Gluconate 300 (in mM), NaOH 10, Mg-ATP 5, EGTA 5, HEPES 50, pH adjusted with KOH; External: NaCl 440, KCl 11, $MgCl_2$ 24, $CaCl_2$ 13.3, Na_2SO_4 26, HEPES 10, D-Glucose (omitted for crab saline) 10, pH adjusted with NaOH.

Characterization of Cell Morphological Type

Determinations of morphological types as veiling or branching were based upon the following criteria as previously reported in Cooke *et al.*, 1989: Neurons were designated 'veiling' if they produced a flat, rounded extension from the stump of the surviving neurite. Neurons were designated branching that produced one or more neurites that branched successively at least twice. Adhered neurons were allowed to regenerate for up to 4 hours to aid in the identification of cells before the addition of altered medium that might influence outgrowth.

Imaging System

The imaging system consisted of an inverted microscope (Nikon Diaphot) equipped with an oil immersion objective (40X Nikon Fluor 1.3 N.A.), dry phase-contrast objectives (Nikon, 10X; 40X), and a modulation contrast video relay system (Modulation Contrast) to record outgrowth while simultaneously monitoring $[Ca^{2+}]_i$.

Fura-2 Loading

Cell Permeation Method

Dishes of neuronal cultures containing medium were drained of roughly 90% of the culture medium. Dishes were filled and exchanged with at least 3 volumes of crab saline prior to dye loading. Routinely, 50 µL of dimethyl sulfoxide (DMSO) was added to 50 µg of fura-2/AM to make a 1 mM stock working solution. To that, 10 µL of a 25% w/w pluronic solution in DMSO was added and the resulting solution was vortexed briefly.

The fura-2/AM/pluronic/DMSO solution was added to an appropriate amount of crab saline to give a final fura-2/AM concentration of 1 to 5 µM. The neuronal cultures (in saline) were exchanged with the fura-2/AM-containing saline solution and allowed to incubate at room temperature for periods of 1 to 2 hours. After incubation in fura-2/AM, the neuronal cultures were rinsed with crab saline and allowed to de-esterify in crab saline for at least 3 hours.

Iontophoresis of Free Acid

Fura-2 was dissolved in filtered H_2O (0.22 μm pore size) or in 100 mM KCl to facilitate monitoring of membrane responses. This provided final fura-2 concentrations of 10 mM. Conventional microelectrodes were fabricated with tip resistances between 30 - 50 MΩ (measured in 3 M KCl) from fiber-bearing 1.2 mm diameter pipette glass (WPI), measured with a micrometer to reduce variability. In some cases bevelling the pipette tip aided in cell penetrations and the passing of dye into cells. Equal on-off duty cycles (0.5 s each) of hyperpolarizing current were used to push the net negatively charged fura-2 into the cells. Current magnitudes were typically 2 nA (range 0.1 nA for smaller "tighter" cells to 4 nA for larger cells). Current injection was monitored using a "virtual ground" amplifier (10 mV/nA) connected to the bath electrode. In some cases, dye introduction via iontophoresis was coupled with pressure injection. Pulses of positive pressure (5-10 psi, 0.5 s duration at 0.01 Hz.) were delivered to the electrode. Cellular membrane penetration and voltage responses were monitored via the microelectrode connected to a current clamp amplifier (WPI, Model M-707) and displayed on a storage oscilloscope (Tektronics Co.). Resting membrane potentials were typically -30 to -50 mV and spiking cellular activity was only detected in neurons exhibiting veiling outgrowth, in agreement with previous current clamp data obtained using the whole-cell configuration (see Meyers *et al.*, 1992).

Cell Loading Levels

The fura-2 concentration that resulted from AM and iontophoretic/pressure injection loading was estimated by comparing the intensity of data arrays ratioed from loaded cells with known concentrations of fura-2 free acid in microslides of thicknesses comparable with soma and neurites (In Vitro Dynamics, Rockaway, NJ). Loading was generally very light with values ranging from 10 - 50 μM. Light loading levels are preferable for studies addressing cellular buffering kinetics since the buffering contribution of the $[Ca^{2+}]_i$ indicator is minimized (Neher and Augustine, 1992).

$[Ca^{2+}]_i$ Determination

Indicator fluorescence ratios were converted into approximate $[Ca^{2+}]_i$ using the equation of Grynkiewicz and colleagues (1985):

$$[Ca^{2+}]_i = K_d\,[(R - R_{min})/(R_{max} - R)]\,\beta$$

where R is the fura-2 fluorescence ratio at 340 and 380 excitation (340/380), K_d is the dissociation constant for fura-2 and Ca^{2+} (800 nM), R_{min} is the fluorescence ratio obtained from a 20 μM fura-2-containing a zero-added-$CaCl_2$-5 mM-EGTA-intracellular-like medium (in mM: KCl, 300; NaCl, 10; HEPES, 50; pH 7.4 with KOH). R_{max} is the fluorescence ratio from a fura-2 containing intracellular-like $CaCl_2$-saturated medium with fura-2 added. β is equal to the fluorescence ratio of fura containing zero-added-$CaCl_2$-5 mM-EGTA calibration medium over $CaCl_2$-saturated

calibration medium at 380 nm. A series of R_{min} and R_{max} values were used that changed with the neutral density filter configurations used, and $[Ca^{2+}]_i$ were then assigned based on the specific calibration data set for that particular neuron. All calibrations resulted from microslide calibrations with free acid. A cytoplasmic viscosity correction factor (0.85X) was multiplied by R_{min} and R_{max} to compensate for the differences between the calibration and cytosolic solutions (Poenie, 1990). Error in $[Ca^{2+}]_i$ measurements introduced by the optical configuration was determined to be ± 0.025 ratio unit (roughly 20 nM) by comparing ratio images at different focal lengths of fura-2 filled microslides of calibrated dimensions.

In situ calibrations using ionomycin (2 μM in DMSO for 1 min) and A23187 (1 μM in DMSO) were attempted but gave inconsistent values for R_{min} and R_{max}, so they were not used.

Video Calibration

The maximum and minimum intensities useful for fluorescence imaging without saturating the camera were determined by dividing an intracellular-like solution (300 mM KCl) containing 20 μM fura-2 free acid and adding 1 mM $CaCl_2$ to one part (to obtain an intensity maximum) and 5 mM EGTA to the other part (to obtain the intensity minimum). These solutions were independently viewed at 340 nM on the microscope stage, and a 25 X 25 pixel area of interest was monitored in the middle of the field of view. The camera and A/D settings in the computer software were

adjusted to optimize the intensity spread (from 0-256 grey values). For example, settings were adjusted so that minimum $[Ca^{2+}]_i$ readings were set at grey level 5 and at 250 for maximum $[Ca^{2+}]_i$ readings, both at 340 nm. The same procedure was used with the 380 nm filter and UV transmitting neutral density filters were inserted in the optical path so that emission remained within useful intensity range for excitation at both wavelengths for both minimum and maximum $[Ca^{2+}]_i$ solutions.

Camera Settings and Lag

Analog camera settings were as follows: manual gain, 90% maximum; offset, 30% from 0; and sensitivity 75% of maximum. Camera lag characteristics of the SIT camera were compensated for by comparing the difference between the detected fluorescence of a fura-2 loaded cell with and without a delay in acquiring the image following opening of the shutters. It was determined that a 500 msec exposure before acquiring images at each wavelength was necessary to avoid introduction of lag contamination.

Image Acquisition

Sixteen images were acquired (digitized from the analog-camera generated signal) at 340 ± 5 nm and digitally averaged and then at 380 ± 5 nm and averaged, and digitally subtracted from the resultant averaged images. One image acquisition cycle required 2 s. The background image was obtained by imaging an area of the

coverglass devoid of cells and debris; acquiring and averaging 16 frames. The images at 340, 380, and the digitally ratioed 340/380 images were captured by a frame grabber and stored on the harddisk of a 80386-based computer. Imaging software (Image-1 and Fluor; Universal Imaging Inc.) was used to change the grey values to pseudocolor and further process the images for presentation.

Results

Intracellular Calcium Levels in X-organ Neurons

To define basal levels of $[Ca^{2+}]_i$, a total of 84 fura-2 loaded neurons were studied from cultures whose age ranged from freshly dissociated to two weeks. Since $[Ca^{2+}]_i$ levels have not been previously measured from regenerating crustacean neurons, observations were collected to examine the variability of resting values from X-organ cells. The distribution of $[Ca^{2+}]_i$ within individual neurons was generally uniform, although some variations were seen between the soma and the veil, such as those seen in figure 5-1. The resting levels of $[Ca^{2+}]_i$ for veiling and branching neurons are summarized in table 5-1. Limiting the analysis to somata of neurons for which complete calibrations were obtained, resting levels in veiling neurons averaged 168 ± 98 nM (n = 16; mean ± standard deviation) and 187 ± 85 nM, (n = 9) in branching neurons. Veiling neurons undergoing active veil formation (age range 12 hr to 2 days in this study) had $[Ca^{2+}]_i$ of 153 ± 81 nM, (n = 10), a relatively wide range for cells

exhibiting optimal outgrowth. Veiling neurons of 3 days and older had values of 193 ± 126 nM (n = 6). Branching neurons had basal values of 171 ± 53 nM (n = 4) at 1 - 2 days and older branching neurons with extensive outgrowth averaged 199 ± 109 nM (n = 5). Two older branching neurons that had not produced extended outgrowth averaged 481 nM (see Fig. 4). Excluding these two, analysis using Student's t-test ($p > 0.05$) showed no significant differences between the resting values of veiling and branching cells; or regenerating and stable state veiling or branching neurons. A subset of cells (n = 3) were monitored for an hour-long period to control for individual variation and showed that they did not vary within error of the system.

Stimuli Producing Increases of $[Ca^{2+}]_i$

Increases in the neuronal $[Ca^{2+}]_i$ were initiated by application of crab saline altered to have 5 times (55 mM) normal potassium (high K^+). Depolarizing saline was applied either via bath exchange (n= 15) or by ejection from a pipette near the cell (n=3). In other experiments, neurons were depolarized by current pulses applied via an intracellular microelectrode. Increases in $[Ca^{2+}]_i$ in response to K^+ elevation generally occurred within 10 seconds of pipette application of K^+.

A subset of cells (not dye loaded; n = 9, 7 veiling and 2 branching neurons) were penetrated with a conventional microelectrode, then exposed to bath-applied 5X K^+ saline as shown in Figure 5-2, A. Resting values ranged from -20 to -40 mV as measured with conventional electrodes. Most veiling neurons rested toward the

depolarized end of the range. These observations are in agreement with those reported in Chapter 4 using the whole-cell configuration. When high K^+ was added to the veilers, they were observed to depolarize to approximately -15 to -5 mV. These absolute membrane potential values are close to the -30 to -20 mV threshold for activation of I_{Ca} reported in Chapter 4, and account for the observation that many neurons were spiking upon penetration with a conventional microelectrode. High K^+ treatment initiated low frequency spikes in many neurons, similar to those shown in Fig. 7A. Branching cells depolarized about 10 mV but showed no spiking. This is consistent with the observation of net inward currents in veilers but not in branchers under voltage clamp (Chapter 4; Meyers *et al.*, 1992). The bath-applied K^+ caused depolarizations that increased smoothly to the new membrane potential within less than one minute of K^+ application. Cells repolarized within 10 minutes upon removal of the high K^+ by exchange of the bath with normal saline. In two veiling cells, repolarization to near rest values occurred in the continued presence of high K^+ within 3 minutes of application (see Figure 5-2,B).

Calcium Increases

High K^+ Induced $[Ca^{2+}]_i$ Increases

Changes of $[Ca^{2+}]_i$ in response to high K^+ differed for cells of different morphology and outgrowth status, as summarized in table 5-1. Averaging all of the

veiling somata, increases of several hundred nanomolar were observed in veiled neurons (n = 15). $[Ca^{2+}]_i$ of actively veiling neurons (12 hours to 2 days) rose to an average of 3.4 times (range 1.4 to 9) their resting levels in the somata (n = 9) and 4.9 times (range 2.3 to 8.4) their resting levels in veiling regions (n = 4). The $[Ca^{2+}]_i$ increase occurred in all anatomical regions of veiling neurons: soma, neurite, and lamellipodium, whether the potassium was applied with an electrode or by bath exchange (Figure 5-1 and 5-3). In veiled neurons older than 4 days the magnitude of the responses was generally smaller, averaging two times rest, as measured from the soma (n = 3). Branched neurons, as a group, also responded to high K^+ stimulation with $[Ca^{2+}]_i$ increases but the magnitudes averaged roughly half the size of vigorously growing veiling cells, 1.9 times (range 1.3 to 2.7, n = 8) as measured at the soma. One- or two- day old branching cells showed the smallest magnitude increases. The somata of a few cells older than four days responded with increases of close to 3 times rest (n = 3). Figure 5-4 shows a high K^+-induced $[Ca^{2+}]_i$ response of ~ 3X rest in the neurites of a day 3 branched neuron.

$[Ca^{2+}]_i$ Decreases

In some actively veiling neurons (a subset of 12 hour to day 2 veiling neurons), the veil (and soma to a lesser degree) showed a unique ability to reduce high K^+-induced $[Ca^{2+}]_i$ increases (n = 7). Neurons were exposed to high K^+ saline for 1-2 minutes. Time to peak for $[Ca^{2+}]_i$ ranged from within a minute to at most 2 minutes.

In the case of some of the rapidly regulating veils, $[Ca^{2+}]_i$ restoration to within 20% of rest occurred within 5 minutes of the potassium induced peak (n = 4). Some observations were made in which high K^+ was left in the bath for a longer period. Four veilers were observed to reduce $[Ca^{2+}]_i$ in the continued presence of the high K^+. Figure 5-1 presents an example. Rapid restoration may represent neurons that were capable of repolarizing the membrane to rest in the continued presence of high K^+, as demonstrated for a non-fura-loaded cell in Fig. 5-2, B.

The veils and somata of a second category of actively veiling cells exhibited some of the largest $[Ca^{2+}]_i$ increases observed, but then showed little recovery, whether or not the K^+ was removed within 1 minute. An example is shown in Figure 5-3. In this group of neurons, the $[Ca^{2+}]_i$ was decreased to an average of only 84% of the peak level, as measured 5 minutes after the peak (n = 4).

Branching cell somata demonstrated an age-related ability to reduce $[Ca^{2+}]_i$ that appeared to correspond with extent of outgrowth (Figures 5-4 and 5-5). Neurons up to 3 days in culture were unable to effectively decrease experimentally increased $[Ca^{2+}]_i$, with the levels staying within 95% of peak, as measured 5 minutes after the peak (Fig. 5-4; n = 3). By contrast, older branching neurons, usually with extensive outgrowth, were able to quickly decrease their $[Ca^{2+}]_i$ to within 30% of resting levels within 5 minutes (Figure 5-5, n = 3). Neurons without outgrowth, the ones with higher basal $[Ca^{2+}]_i$, could not reduce the high K^+-induced increases, averaging 90% of peak (n = 3).

Current Injection

Depolarizing current pulses of between 0.5 nA and 1 nA for at least 10 ms were required to elicit an action potential by each pulse in the veiling neurons in normal medium. Fura-2-loaded cells were stimulated at between 5 and 10 Hz. Five hertz stimulation did not result in increases in the $[Ca^{2+}]_i$, and actually lead to slightly decreased levels in most cells tested (4 of 5). In one cell, stimulation that induced action potentials at 10 Hz for 5 minutes increased the $[Ca^{2+}]_i$ by 50 nM. The $[Ca^{2+}]_i$ then promptly returned to rest levels after cessation of stimulation. As a control for the fidelity of fura-2, the cell was exposed to ionomycin, a calcium ionophore, at 1 μM. $[Ca^{2+}]_i$ increased to more than 10 fold the value reached during 10 Hz stimulation (Figure 5-6). Figure 5-7 shows typical responses of intact veiling and branching neurons to current depolarization steps, such as those used to obtain figure 5-6.

Discussion

This report provides observations of $[Ca^{2+}]_i$ from unstimulated and depolarized regenerating neurons that consistently produce two distinct morphology patterns under the same culture conditions. Measurements of basal $[Ca^{2+}]_i$ from unstimulated neurons of both morphology types of various ages in culture did not show statistically significant differences. Cellular responses to depolarizing stimuli do reveal differences

in mechanisms that regulate $[Ca^{2+}]_i$ that are associated with morphological type: 1) Veiling (immunoreactive to CHH antisera) but not branching neurons have voltage-dependent Ca current (Chapter 4). That branching neurons, of the same morphology category, are immunoreactive to more than one antisera (RPCH and MIH) suggests that I_{Ca} may contribute toward the establishment of cell morphology, since at least two hormonally determined cell identities exist for cells that establish the same type of morphology pattern in defined culture, yet branchers consistently lack I_{Ca}. 2) Somata of veilers typically show larger increases of $[Ca^{2+}]_i$ to K^+ depolarizations than do those of branching neurons. $[Ca^{2+}]_i$ increases in the branches are very small (Fig 5-4). By contrast, actively growing veils show some of the largest increases reported. Since branching neurons have no detectable I_{Ca} during this period, the source of these $[Ca^{2+}]_i$ increases remains unclear and warrants further characterization. 3) Branching neurons appear to have poor ability to restore depolarization-induced increases of $[Ca^{2+}]_i$ toward basal levels during the time that they are establishing their morphology, whereas veiling neurons and older, established branchers are able to restore such perturbations. The rate at which $[Ca^{2+}]_i$ perturbations are restored is much more rapid in a subset of actively veiling neurons. It may be that secretory granules, the dominant organelle in veils (see Chapter 2), play a part in reducing high K^+-induced $[Ca^{2+}]_i$ elevations. It is noteworthy that a subset of branching cells have been found not to possess secretory granules as observed with electron microscopy (T. M. Weatherby, unpublished observation). These results suggest that mechanisms which regulate $[Ca^{2+}]_i$ differ with

morphology type. Two lines of evidence suggest differential sensitivities to $[Ca^{2+}]_i$ for outgrowth of the two morphological neuronal types (see Chapter 6): 1) Branching neurons will continue to grow out in medium having a Cd concentration (0.1 mM) that reversibly inhibits outgrowth of veiling neurons. This concentration of Cd also inhibits voltage-dependent Ca currents in veiling neurons. This could reflect that outgrowth is an exocytosis-dependent process in veilers but not in branchers. 2) Most branching neurons will continue to grow out processes in medium with substantially reduced Na^+ that blocks veiling outgrowth (Chapter 6). One possible effect of such a saline is to halt Na^+/Ca^{2+} exchange demonstrated in neurons (Levy and Tillotson, 1988) to be driven by the Na^+ concentration gradient. It may be fruitful to attempt to dissect out the mechanisms affecting outgrowth and $[Ca^{2+}]_i$ levels in Cd and in reduced external Na^+ over the same time frame as the observations on outgrowth so that the $[Ca^{2+}]_i$ and outgrowth states can be directly compared.

The results reported here can fit the hypothesis of a permissive/optimal range of $[Ca^{2+}]_i$ for outgrowth as proposed by Kater and colleagues (Kater *et al.*, 1988; Kater and Mills, 1991) if the permissive range is relatively large. The few X-organ neurons that did not grow had resting levels over 300 nM, which may indicate the upper end of the permissive range. The veiling "program" appears to extend membrane in a continuous manner, as opposed to a stop-and-start manner, over the active period. This program occurred over a 20 - 300 nM basal $[Ca^{2+}]_i$ range. It may be that peptidergic secretory cells are unusual in having a very wide permissive/optimal range

of $[Ca^{2+}]_i$. The variability of basal $[Ca^{2+}]_i$ observed over which active veiling resulted was much larger than for the basal values reported for actively growing identified *Helisoma* neurons (Cohan *et al.*, 1987). Signficant differences were reported between basal $[Ca^{2+}]_i$ in actively growing and stable state identified *Helisoma* neurons, but these differences were not observed for the different X-organ neurosecretory cells studied here. The variability of basal $[Ca^{2+}]_i$ levels reported for rat sensory neurons (Al-Mohanna *et al.*, 1992) was quite narrow (60 ± 4 nM) compared to X-organ neurons. It is noteworthy that the 35 nM optimum for outgrowth of the sensory neurons was well outside their basal range.

Responses of X-Organ Neurons to K^+ and Current Stimulation

Application of 5X K^+ saline results in increases of $[Ca^{2+}]_i$ in both morphology types in culture, even in cells that have not extended outgrowth. Variation in the magnitude of the $[Ca^{2+}]_i$ increase of veiling cells in response to high K^+ may be due to differences in their resting potentials and consequently differences in absolute membrane potential resulting from the high K^+. The smaller high K^+ induced responses may represent recordings from the more hyperpolarized neurons, so that depolarization results in recruiting far fewer Ca channels than the application of 5X K^+ to a neuron resting at -25 mV. As mentioned earlier, the threshold of the voltage-dependent Ca current in cultured veiling X-organ neurons has been shown to be at -30 to -20 mV (Meyers *et al.*, 1992; Chapter 4). Veiling cells having low resting

potentials were observed to spike repetitively during high K^+ additions, whereas those that rested more hyperpolarized depolarized smoothly to a new plateau 10 - 15 mV depolarized from rest. The much larger effects on $[Ca^{2+}]_i$ of high K^+ than of electrical stimulation may reflect that electrical stimulation only recruits the voltage-gated Ca channels of the plasma membrane, whereas the continuous depolarization by high K^+ may recruit other mechanisms that increase $[Ca^{2+}]_i$. The observed variability of resting potentials is consistent with an explanation of the variability in $[Ca^{2+}]_i$ increases to depolarizing K^+ if the $[Ca^{2+}]_i$ increases reflect predominantly Ca influx across the plasma membrane. Addition of caffeine evoked a relatively small $[Ca^{2+}]_i$ response in these neurons (not shown), so X-organ neurons may release some $[Ca^{2+}]_i$ from caffeine-sensitive internal stores. Since the magnitude of these caffeine-induced $[Ca^{2+}]_i$ responses was small compared to responses to high K^+ stimuli in the same cell, the caffeine response did not appear to represent the majority of the high K^+ response. Future studies are needed to dissect the relationships among the sources that contribute to $[Ca^{2+}]_i$ increases.

In experiments on other preparations, it was necessary to elicit action potentials in neurons for extended periods of time (hours), in one case in the presence of outward current blockers (Anglister *et al.*, 1982), to induce significant increases in $[Ca^{2+}]_i$ (Anglister *et al.*, 1982; Cohan *et al.*, 1987). The electrical stimulation reported here used stimuli at frequencies mirroring observations of activity recorded *in vivo* (Stuenkel, 1985; Nagano and Cooke, 1987). The relatively small change of $[Ca^{2+}]_i$

produced by electrical stimulation may also reflect highly localized Ca entry sites combined with an effective Ca^{2+}-buffering system (Neher and Augustine, 1992) that prevents the entering Ca^{2+} from influencing the averaged cytosolic $[Ca^{2+}]_i$ that fura-2 measures.

In summary, peptidergic neurons of the X-organ exhibit basal $[Ca^{2+}]_i$ varying over a wide range (20 - 300 nM) as measured in cells that regenerate processes. Differences in Ca-handling were observed that are associated with outgrowth status (active or stable), extent of outgrowth, and particularly with morphological type.

References

Al-Mohanna, F. A., Cave, J., and Bolsover, S. R. (1992) A narrow window of intracellular calcium concentration is optimal for neurite outgrowth in rat sensory neurons. *Dev. Br. Res.* **70**: 287-290.

Anglister, L., Farber, I. C., Shahar, A., and Grinvald, A. (1982) Localization of voltage-sensitive calcium channels along developing neurites: Their possible role in regulating neurite elongation. *Dev. Biol.* **94**: 351-365.

Augustine, G. J., Adler, E. M., and Charlton, M. P. (1991) The calcium signal for transmitter secretion from presynaptic nerve terminals. *Ann. New York Acad. Sci.* **635**: 365-381.

Bentley, D., Guthrie, P. B., and Kater, S. B. (1991) Calcium ion distribution in nascent pioneer axons and coupled preaxonogenesis neurons *in situ*. *J. Neurosci.* **11**: 1300-1308.

Cohan, C., Connor, J. A. and Kater, S. B. (1987) Electrically and chemically mediated increases in intracellular calcium in neuronal growth cones. *J. Neurosci.* **7**: 3588-3599.

Cooke, I. M., Haylett, B. A., and Weatherby, T. M. (1977) Electrically elicited neurosecretory and electrical responses of the isolated crab sinus gland in normal and reduced calcium salines. *J. exp. Biol.* **70**: 125-149.

Cooke, I. M. and Haylett, B. A. (1984) Ionic dependence of secretory and electrical activity evoked by elevated K^+ in a peptidergic neurosecretory system. *J. exp. Biol.* **113**: 289-321.

Cooke, I. M. (1985) Electrophysiological characterization of peptidergic neurosecretory terminals. *J. exp. Biol.* **118**: 1-35.

Cooke, I., Graf, R., Grau, S., Haylett, B., Meyers, D., and Ruben, P. (1989) Crustacean peptidergic neurons in culture show immediate outgrowth in simple medium. *Proc. Natl. Acad. Sci.* **86**: 402-406.

Fatt, P., and Katz, B. (1951) An analysis of the end-plate potential recorded with an intra-cellular electrode. *J. Physiol.* **115**: 320-370.

Garyantes, T. K. and Regehr, W. D. (1992) Electrical activity increases growth cone calcium but fails to inhibit neurite outgrowth from rat sympathetic neurons. *J. Neurosci.* **12**: 96-103.

Graf, R. A. (1992) Rapid regulation of $[Ca^{2+}]_i$ characterizes neurons showing outgrowth in defined culture. *Soc. Neurosci. Abstr.* **18**: 1468.

Grau, S. M. and Cooke, I. M. (1992) Peptidergic neurons of the crab, *Cardisoma carnifex*, in defined culture maintain characteristic morphologies under a variety of conditions. *Cell Tissue Res.* **270**: 303-317.

Grynkiewicz, G., Poenie, M. and Tsien, R. Y. (1985) A new generation of Ca indicators with greatly improved fluorescence properties. *J. Biol. Chem.* **260**: 3440-3450.

Ivins, J. K., Raper, J. A., Pittman, R. N. (1991) Intracellular calcium levels do not change during contact-mediated collapse of chick DRG growth cone structure. *J. Neurosci.* **11**: 1597-1608.

Kater, S. B., Mattson, M. P., Cohan, C. S. and Connor, J. A. (1988) Calcium regulation of the neuronal growth cone. *Trends Neurosci.* **11**: 315-321.

Kater, S. B. and Mills, L. R. (1991) Regulation of growth cone behavior by calcium. *J. Neurosci.* **11**: 891-899.

Katz, B. and Miledi, R. (1967) The release of acetylcholine from nerve endings by graded electric pulses. *Proc. Royal Soc. B* **167**: 23-38.

Lemos, J. R. and Nordmann, J. J. (1986) Ionic channels and hormone release from peptidergic nerve terminals. *J. exp. Biol.* **124**: 53-72.

Levy, S., and Tillotson, D. (1988) Effects of Na^+ and Ca^{2+} gradients on intracellular free Ca2+ in voltage clamped Aplysia neurons. *Brain Res.* **474**: 333-347.

Mattson, M. P. and Kater, S. B. (1987) Calcium regulation of neurite elongation and growth cone motility. *J. Neurosci.* **7**: 4034-4043.

Meyers, D. E. R., Graf, R. A., and Cooke, I. M. (1992) Ionic currents of morphologically distinct peptidergic neurons in defined culture. *J. Neurophysiol.* **67**: 1301-1315.

Miller, A. L., Smith, P. J. S., Rainville, C. A., Shimomura, O, Strumwasser, F., and Jaffe, L. F. (1991) Imaging free calcium in cultured *Aplysia* bag cell neurons. *Biol. Bull.* **181**: 325.

Mills, L. R. and Kater, S. B. (1990) Neuron-Specific and State-Specific Differences in Calcium Homeostasis Regulate the Generation and Degeneration of Neuronal Architecture. *Neuron* **2**: 149-163.

Mulkey, R. M. and Zucker, R. S. (1991) Action potentials must admit calcium to evoke transmitter release. *Nature* **350**: 153-155.

Nagano, M. and Cooke, I. M. (1987) Comparison of electrical responses of terminals, axons, and somata of a peptidergic neurosecretory system. *J. Neurosci.* **7**: 634-648.

Neher, E. and Augustine, G. J. (1992) Calcium gradients and buffers in bovine chromaffin cells. *J. Physiol.* **450**: 273-301.

Poenie, M. (1990) Alteration of intracellular fura-2 fluorescence by viscosity: a simple correction. *Cell Calcium* **11**: 85-91.

Rehder, V. and Kater, S. B. (1992) Regulation of neuronal growth cone filopodia by intracellular calcium. *J. Neurosci.* **12**: 3175-3186.

Ross, W. N. and Graubard, K. (1989) Spatially and temporally resolved calcium concentration changes in oscillating neurons of crab stomatogastric ganglion. *Proc. Natl. Acad. Sci.* **86**: 1679-1683.

Shibuya, I. and Douglas, W. W. (1992) Calcium channels in rat melanotrophs are permeable to manganese, cobalt, cadmium, and lanthanum, but not to nickel: evidence provided by fluorescence changes in fura-2-loaded cells. *Endocrinology* **131**: 1936-1941.

Silver, R. A., Lamb, A. G., and Bolsover, S. R. (1989) Elevated cytosolic calcium in the growth cone inhibits neurite elongation in neuroblastoma cells: correlation of behavioral states with cytosolic calcium concentrations. *J. Neurosci.* **9**: 4007-4020.

Stuenkel, E. L. (1985) Simultaneous monitoring of electrical and secretory activity in peptidergic neurosecretory terminals of the crab. *J. Physiol.* **359**: 163-187.

Zucker, R. S. and Haydon, P. G. (1988) Membrane potential has no direct role in evoking neurotransmitter release. *Nature* **335**: 360-362.

Zucker, R. S. and Lando, L. (1986) Mechanism of transmitter release: Voltage hypothesis and calcium hypothesis. *Science* **231**: 574-579.

Figure 5-1. Temporal changes in $[Ca^{2+}]_i$ of an X-organ neuron undergoing vigorous veiling outgrowth in response to a short application of 5 times potassium (high K) saline to the bath. Neuron was in culture 12 hours when $[Ca^{2+}]_i$ measurements were made from the soma (see area of interest in blue 1 in photo) and veil (see area of interest 2 in yellow in photo). Neuron was loaded with fura-2 free acid via iontophoresis, soma diameter ~ 40 μm. A. Unstimulated basal levels. B. 1 minute after introduction of high K^+. C. 2 minutes post high-K application. D. Decreasing levels of Ca 7 minutes after high-K application. Note large peak in veil and increase in soma, different resting levels in veil and soma, and rapid relaxation in $[Ca^{2+}]_i$ despite continued high K^+. Also note membrane potential relaxation in continued presence of high K^+ in figure 5-2 seen in some veiling neurons.

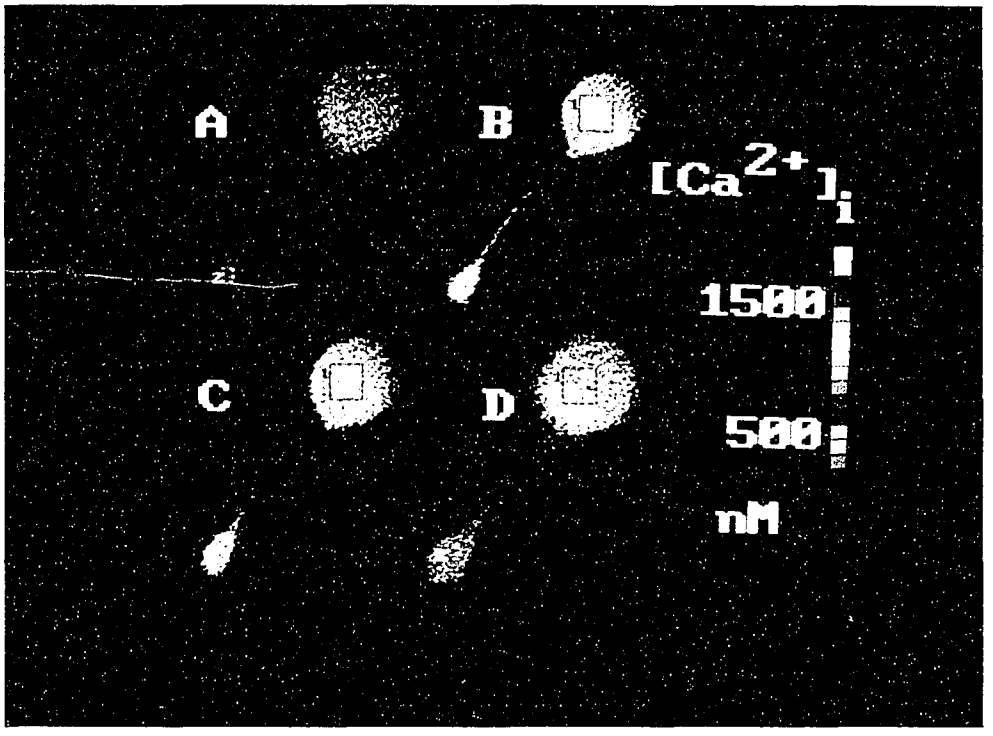
A
B
C
D
[Ca2+]i
1500
500
nM

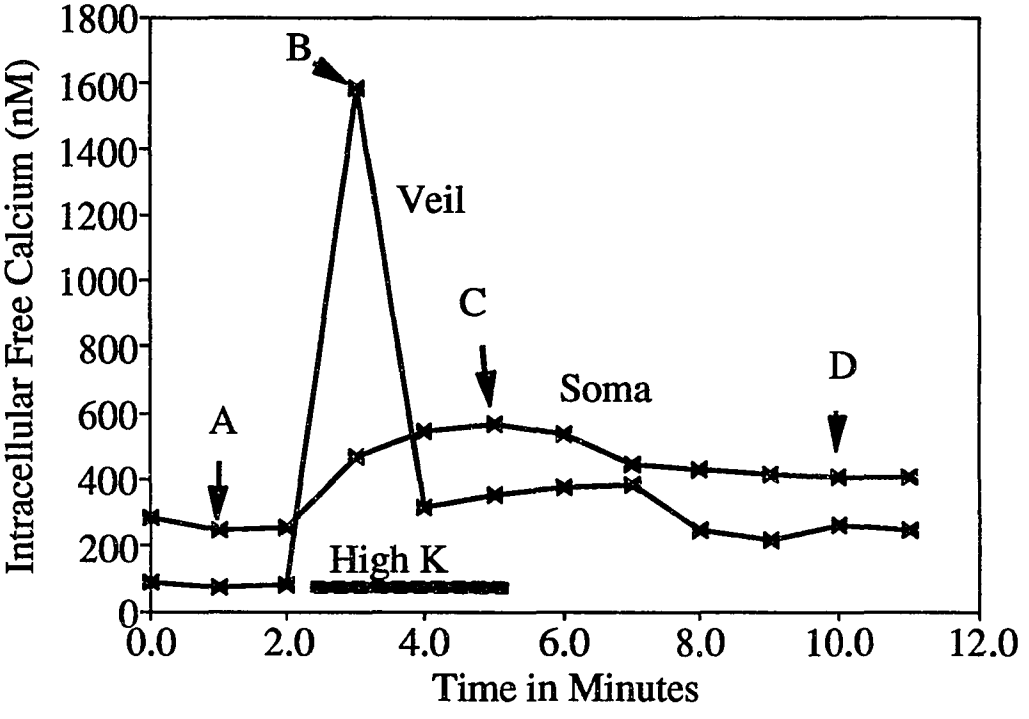
Intracellular Free Calcium (nM)
1800
1600
1400
1200
1000
800
600
400
200
0
B
Veil
C
Soma
D
A
High K
0.0
2.0
4.0
6.0
8.0
10.0
12.0
Time in Minutes

Table 5-1. Basal $[Ca^{2+}]_i$ (Resting), and $[Ca^{2+}]_i$ Responses Resulting from high K^+ Perturbations from Veiling and Branching Neurons Comparing Measurements of Actively Growing versus Non-Actively Growing Neurons. Numbers are given in nM $[Ca^{2+}]_i$, and represent means ± standard deviations, with the number of trials given in parenthesis. S= soma and V = veil, Br = branches. $t_{½}$ = approximate times for $[Ca^{2+}]_i$ to restore to one-half their peak values.

Growth Status	Veiling			Branching		
	Basal	Perturbed	Veils & Somata	Basal	Perturbed	Somata
Active (12 h - 2 d)	153±81 (10)	3.4X rest (S,9) 4.9X rest (V,4)	< 5 min (7) >20 min (3)	171±53 (4)	1.9X rest (S,8) 1.6X rest (Br,1)	>5 min (3)
Non-Active (≥ 3 d)	193±126 (6)	1.4X rest (V,1) 1.9X rest (S,4)	< 5 min (3)	199±109 (5)	~3X rest (S,3) 2.1X rest (Br, 2)	<5 min (3)

Figure 5-2. Membrane Voltage Responses from a Veiling Neuron (soma diameter 35 μm) During Exposure to 5X, 10X, and 15X K^+ saline. A and B from continuous recording from one cell, Day 1 veiled neuron. Bath was exchanged 5 times with 5X and then 10X K^+ saline. A. 5X K^+ caused approximately a 10 mV depolarization from rest, - 35 mV in this cell. Subsequent application of 10X K^+ (final) lead to a further 10 mV depolarization that plateaued. B. The addition of 15X K^+ to the previous 10X K^+ (25X K^+ final) led to a sudden large depolarization that relaxed to values slightly depolarized in the continued presence of the 25X K^+ stimulus. Removal of the electrode resulted in a return to 0 mV.

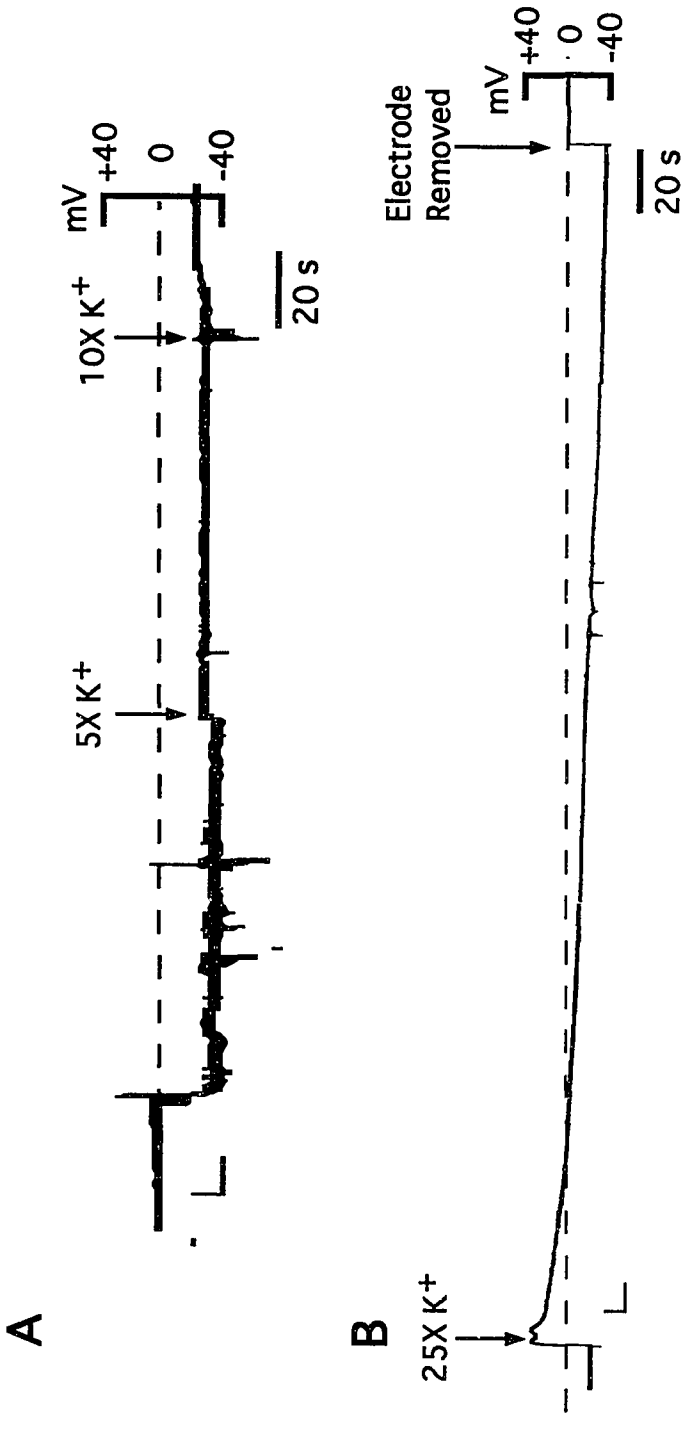
A
mV
+40
0
-40
10X K+
20 s
5X K+
B
Electrode
Removed
mV
+40
0
-40
20 s
25X K+

Figure 5-3. Temporal $[Ca^{2+}]_i$ Response of a Weakly Relaxing Neuron. Day 2 veiling X-organ primary neurite and lamellipodium in response to a 7 min application of 5X K^+ saline to the bath. Neuron was loaded with fura-2/AM. Soma is not in field. Mid-neurite width approximately 5 μm. A. Resting levels of approximately 50 nM $[Ca^{2+}]_i$. B. Peak $[Ca^{2+}]_i$ of ~ 600 nM in area of interest in veil, as shown in photo. C. Little relaxation of $[Ca^{2+}]_i$ 5 minutes after the addition of high K^+ in its continued presence.

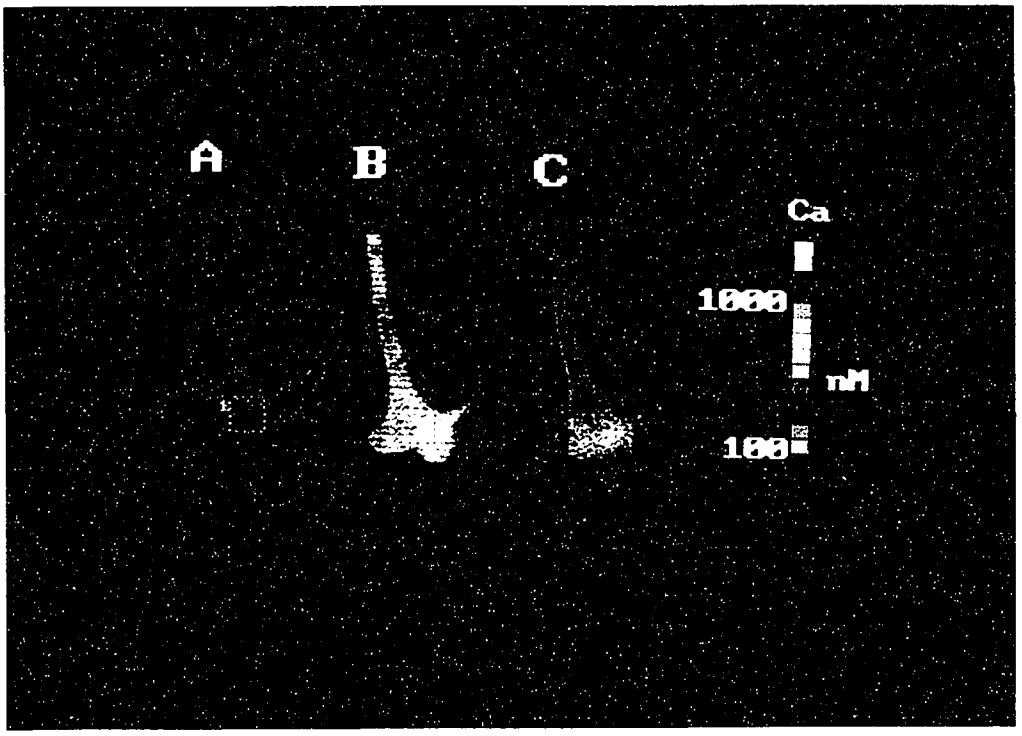
A
B
C
Ca
1000
nM
100

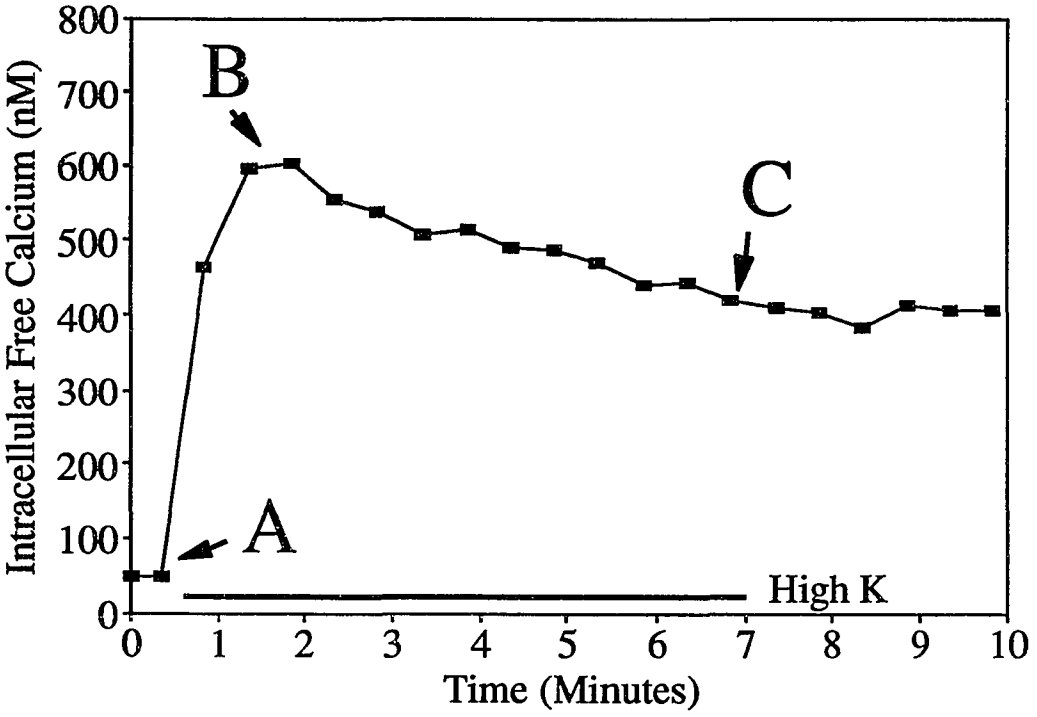
Intracellular Free Calcium (nM)
800
700
600
500
400
300
200
100
0
B
C
A
High K
0
1
2
3
4
5
6
7
8
9
10
Time (Minutes)

Figure 5-4. High K^+-induced $[Ca^{2+}]_i$ changes of a branching neuron at day 4 in culture. Soma diameter ~ 25 μm. A majority of the branching processes failed to show a fura-2 signal. A. Pre-stimulation. B. At $[Ca^{2+}]_i$ peak. C. During rinse, after removal of high K^+. Note that there is an increase in $[Ca^{2+}]_i$ from ~ 200 - 450 nM in the neurite (region of interest was distal neurite [not shown]). There is little decline in the $[Ca^{2+}]_i$ after removing the stimulus, but restoration occurs in the somata of cells at this stage (see Fig. 5-5).

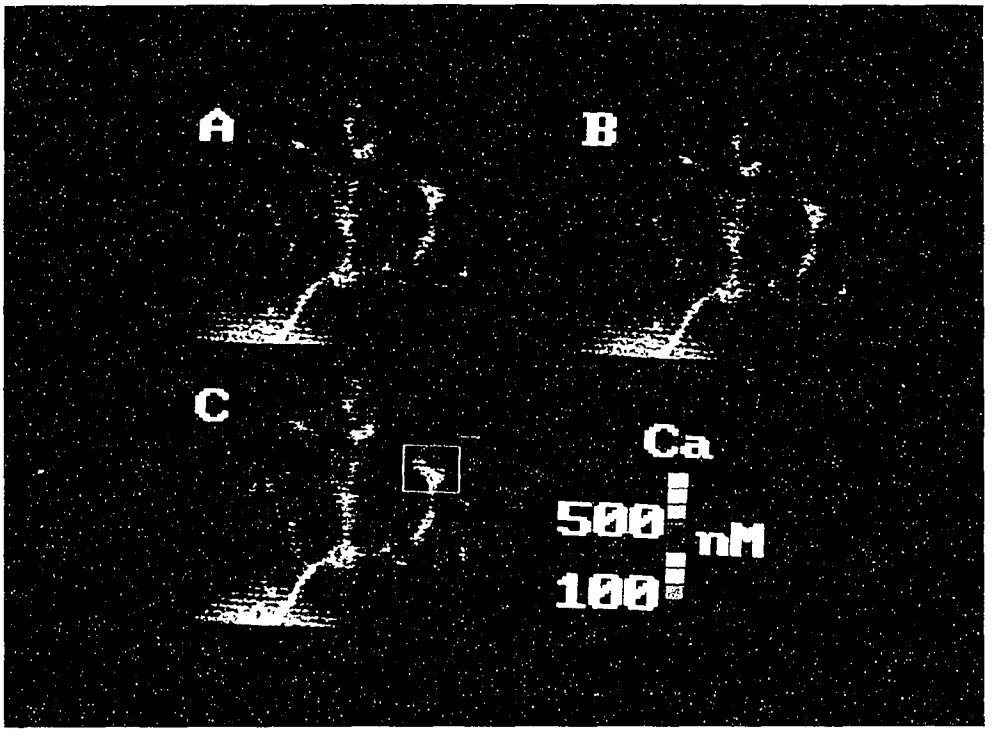
A
B
C
Ca
500
nM
100

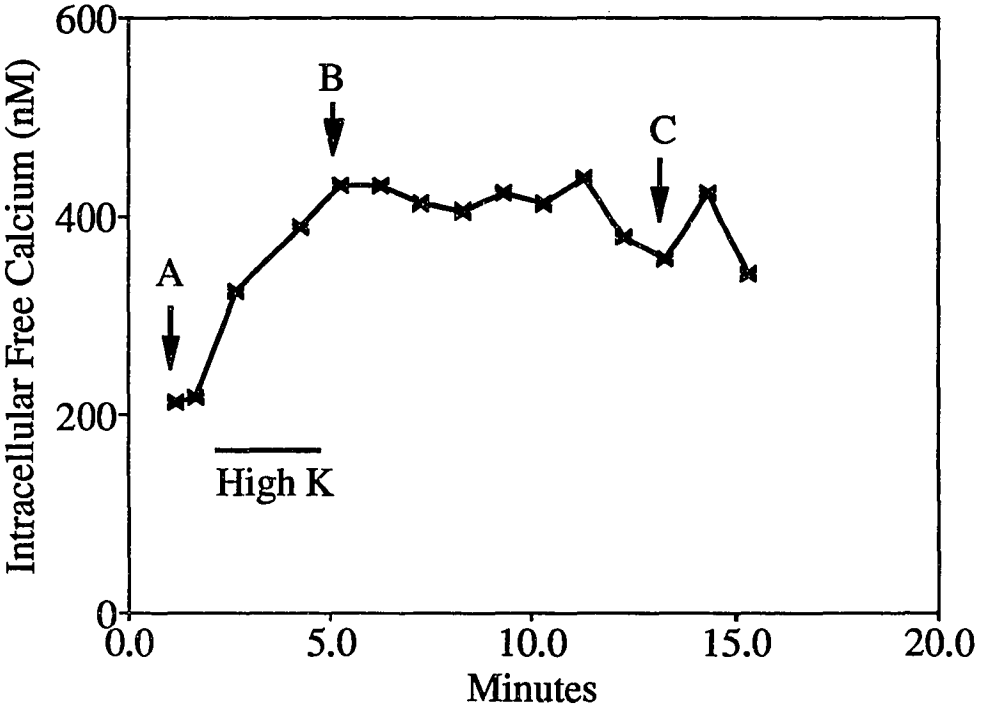
600
400
200
0
Intracellular Free Calcium (nM)
A
B
C
High K
0.0
5.0
10.0
15.0
20.0
Minutes

Figure 5-5. $[Ca^{2+}]_i$ response differences between a branching neuron and a non-growing neuron: branching neuron on the right, soma diameter ~ 20 μm. A. Prestimulation. Note cell without outgrowth rests higher than cell with outgrowth. B. 6 minutes after the initiation of the K^+ stimulus: Note that $[Ca^{2+}]_i$ is much higher in cell without outgrowth, but that increases occur in both neurons. C. ~ 10 minutes after the initiation of stimulation. Note that $[Ca^{2+}]_i$ increased and then decreased in the cell on the right, which exhibited outgrowth; whereas the unextended cell did not reduce its $[Ca^{2+}]_i$.

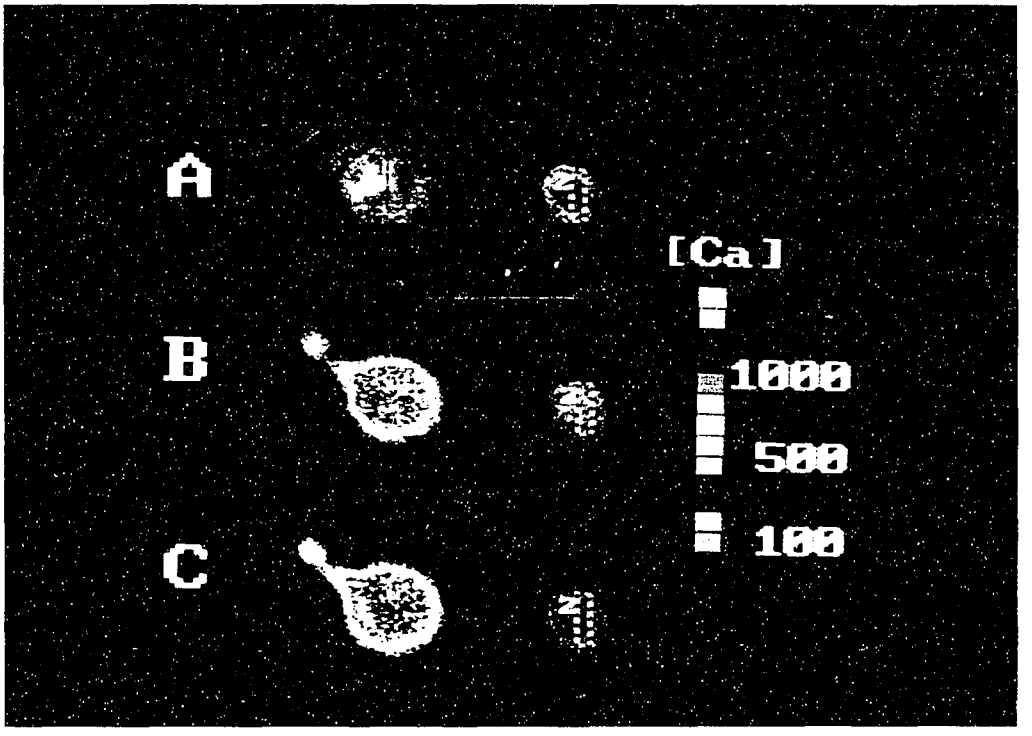
A
B
C
[Ca]
1000
500
100

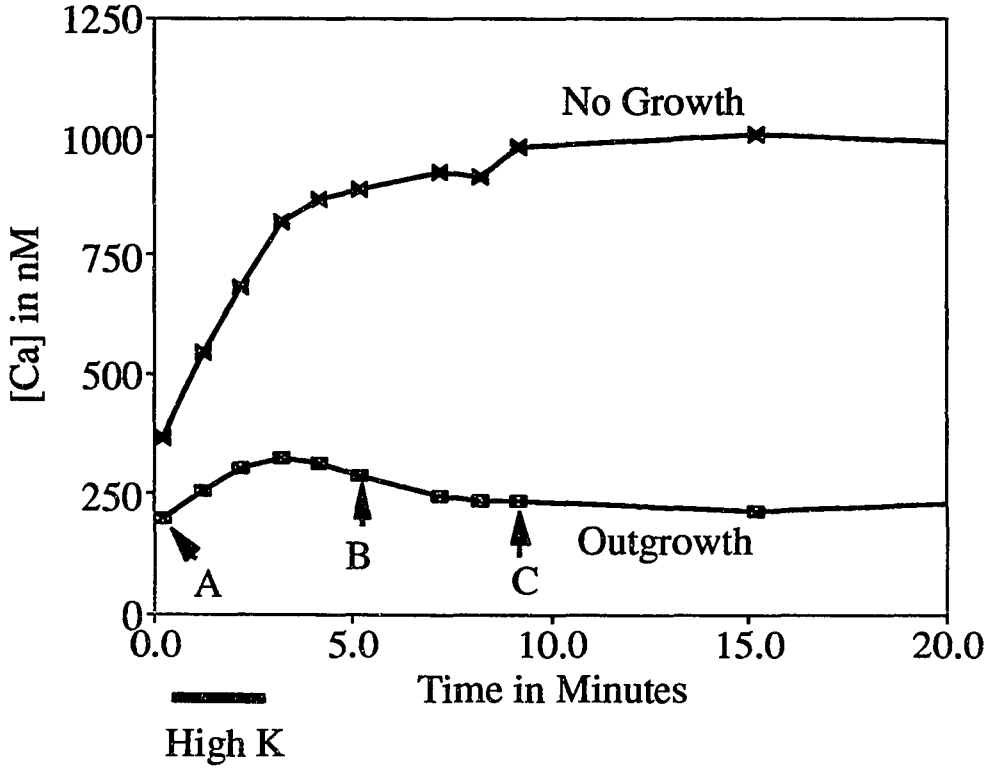
1250
1000
750
500
250
0
[Ca] in nM
No Growth
Outgrowth
A
B
C
0.0
5.0
10.0
15.0
20.0
Time in Minutes
High K

Figure 5-6. Differences in the effects of electrical and potassium stimulation on $[Ca^{2+}]_i$ homeostasis in the same veiling neuron. Fura-2 was loaded in the free acid form via iontophoresis. Addition of high K^+caused a large increase in $[Ca^{2+}]_i$ whereas subsequent depolarizing current stimulation that induced action potentials at 5 Hz (first arrow [up arrow on until down arrow (off)]), a frequency observed from *in situ* X-organ recordings, had little effect on $[Ca^{2+}]_i$. 10 Hz stimulation (second arrow set), which produced action potentials caused a slight increase in $[Ca^{2+}]_i$. Cell was finally exposed to ionomycin, a calcium ionophore, to demonstrate an active fura-2 response. Note that the high K^+ signal is of roughly equal magnitude to the ionophore response, indicating that the ionophore does not fully equilibrate $[Ca^{2+}]_o$ with $[Ca^{2+}]_i$.

CURRENT AND K STIMULATION DIFFERENCES
VEILING NEURON (16SP92V5)

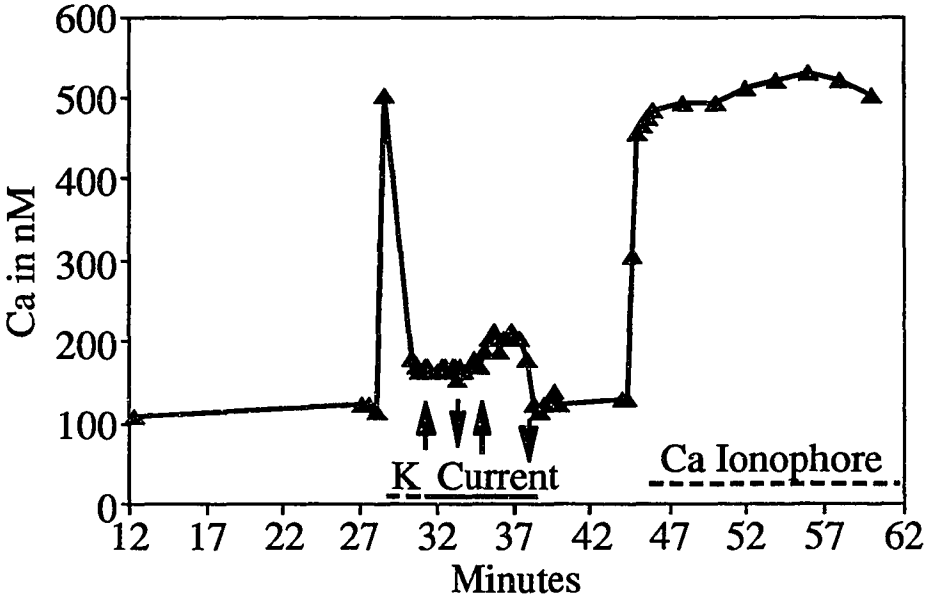

Figure 5-7. Membrane voltage responses from representative microelectrode experiments from X-organ neurons of branching and veiling morphology type in culture. Whole-cell configuration of the patch electrode technique, recorded from the soma. Dashed lines represent the 0 mV line. A. Membrane responses resulting from a depolarizing current pulse. Branching neuron was in culture 48 hours, soma diameter was 32 μm, representing the larger end of the range for branching neurons. Note resting membrane potential near -30 mV and lack of evoked action potential responses during depolarizing current stimulation as indicated by the bar. Arrow shows closest analogy to spiking observed in branching neurons. B. Spontaneous action potentials recorded from a veiling neuron 24 hours in culture (soma diameter 40 μm.). Note spontaneous increased frequency of firing (burst) in middle of trace, which occurred infrequently in veiling neurons. C. Enlarged action potential profile of veiling cell in B. Note overshooting of action potentials.

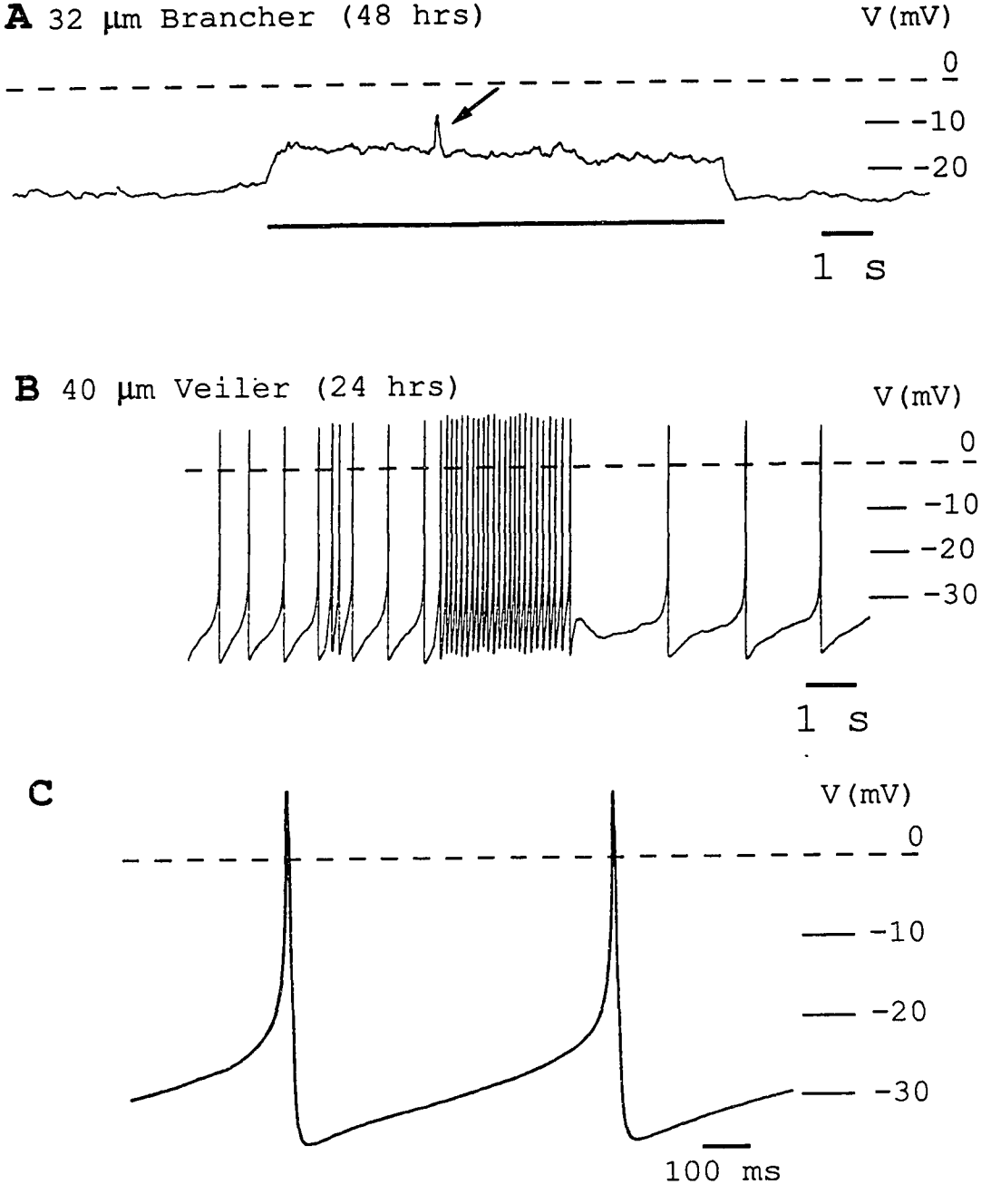
A 32 µm Brancher (48 hrs)
V(mV)
0
-10
-20
1 s
B 40 µm Veiler (24 hrs)
V(mV)
0
-10
-20
-30
1 s
C
V(mV)
0
-10
-20
-30
100 ms

CHAPTER 6

CELLULAR PROPERTIES OF REGENERATING CULTURED X-ORGAN NEURONS UNDER ALTERED MEDIUM CONDITIONS

Introduction

Numerous studies show that process outgrowth during development and regeneration can be affected by environmental stimuli (Kater and Letourneau, 1985; Letourneau, Kater, and Macagno, 1991). For example, it has been shown for a number of types of neurons from several animal groups that $[Ca^{2+}]_i$ levels over a permissive range allow outgrowth to occur, whereas levels too high or too low are not conducive to optimal outgrowth (Mattson and Kater, 1987; Kater and Mills, 1991; Al-Mohanna *et al.*, 1992). The subcellular mechanisms that contribute to calcium homeostasis appear to be different for neurons of different origin, but have been characterized for very few types. Their expression and operation are influenced by intrinsic and environmental influences, as well as age and state of outgrowth (Mills and Kater, 1990).

This chapter provides evidence that outgrowth can be inhibited by changes in culture medium that are known to influence subcellular mechanisms. These are thus implicated in cellular processes influencing outgrowth. The observations show that of the two characteristic morphology types, veiling and branching, veiling X-organ cells can rely on various Ca homeostatic subcellular mechanisms to different degrees.

Neurons destined to become veiling neurons have Ca-sensitive outgrowth regimes, since the extent of outgrowth can be inhibited reversibly with divalent cations that block voltage-dependent Ca channels. By contrast, branching neurons may not rely on these Ca channels for outgrowth since outgrowth persists in the presence of Cd, an inorganic divalent that effectively block Ca current in these cells at low concentrations. Similar studies on other systems show inhibition of outgrowth by similar blockers, but the continued outgrowth of neurons in the presence of Ca channel blockers has apparently not been reported (Mattson and Kater, 1987).

A differential effect (associated with morphology) on outgrowth occurred with reduction of the $[Na^+]_o$, expected to inhibit extrusion of intracellular Ca^{2+} for exchange with Na^+: Most branching neurons established their morphologies, yet less vigorously than controls, whereas veiling was completely inhibited.

Surprisingly, during depolarizing stimuli in the presence of altered media, the rate at which invoked $[Ca^{2+}]_i$ increases are reduced remained unchanged.

Methods

Animal, Culture, and $[Ca^{2+}]_i$ Imaging

The experiments were performed on neurons from the X-organ of the crab, *Cardisoma carnifex*, cultured in defined medium as detailed in Chapter 5.

Characterization of Cell Morphological Type

Determinations of morphological types as veiling or branching were based upon the following criteria as previously reported in Cooke *et al.*, 1989: Neurons were designated 'veiling' if they produced a flat, rounded extension from the stump of the surviving neurite. Neurons were designated branching that produced one or more neurites that branched successively at least twice. To remove any doubt, adhered neurons are allowed to regenerate for up to 4 hours to aid in the identification of cells before the addition of altered medium that might influence outgrowth.

Altered Medium Additions

Pharmacological agents were added as follows: Approximately 5 medium exchanges were made at 4 hours post-dissociation with medium containing TTX at 100 nM, Cd at 100 μM, or reduced Na^+ (440 μM) substituted with N-methyl-gluconate-Cl in otherwise normal medium. The dissociated neurons were allowed to settle and adhere in a drop of normal medium for 4 hours, during which time regenerative outgrowth began and permitted selection for further study of neurons that were clearly destined to develop veiling or branching morphologies. The dish was then flooded with normal saline for control cultures and altered medium for experimental cultures.

Results

Medium Modifications that Alter the Extent of Outgrowth

Experimental manipulation of the culture medium provides information on how calcium regulatory mechanisms influence outgrowth morphology. Figure 1 is a composite showing typical outgrowth observed under control conditions and following the medium alterations as described below.

Cadmium

The inorganic calcium channel blocker Cd was introduced to X-organ neurons at different concentrations (10 μM to 1 mM) in defined medium. Introduction of medium containing Cd at a concentration sufficient to block the inward Ca current (100 μM) blocked veiling (11 of 12; Figure 1,2C) but not branching outgrowth (8 of 9; Figure 1,1C), while control cells from the same culture exhibited both morphology types (Figure 1, 1A; 2A). It was demonstrated that outgrowth properties were not impeded by exposing cultures to Cd-containing medium for hour-long periods and monitoring subsequent outgrowth (Figure 1; 1B, 2B). Both veiling and branching outgrowth programs occur under these circumstances, although the extent of outgrowth is reduced as observed after 24-48 hours relative to control dishes from the same culture. Outgrowth of both morphological types occurred in cultures with 10 μM cadmium-supplemented medium (not shown). Outgrowth was arrested in both neuronal types after addition of 1 mM cadmium-supplemented medium (not shown).

Reduced-Sodium Medium

Veiling outgrowth is inhibited in medium having 1/10th the normal $[Na^+]_o$ (0.44 mM) (15 of 16 cells monitored; Figure 1, 2D). Distal ends of the residual neurite where veiling outgrowth generally emerges appeared bulbous and outgrowth did not project from other adhered neuronal regions either. By contrast, extensive branching outgrowth was observed, although at 24 hours it appeared less vigorous than that of controls, as evidenced by the appearance of processes that were thinner and less phase-dark than those of branching cells from the same preparation cultured in normal medium (14 of 16 monitored; Figure 6-1, 1D).

TTX

Figure 1, 1E and 2E, demonstrate the lack of effect of 1 μM TTX on outgrowth, a concentration known to block the voltage-dependent sodium current in these neurons (Chapter 4; Meyers *et al.*, 1992). Experimental cultures were indistinguishable from controls (36 of 36 monitored).

Effect on $[Ca^{2+}]_i$ of Manipulations that Inhibit Outgrowth Extent

Cadmium application at 100 μM completely blocked the increase of fura-2 fluorescence in response to a high K^+ stimulus in only 1 of 4 day 4 and older veiling cells tested. In the other three cells, large fluorecence ratio increases averaging 2.2 times rest resulted from both branching and veiling neurons, as measured from the soma (see Figures 6-2 and 6-3). These were subsequently reduced by the veiled cells,

so that at 5 min, values were within 40% of peak, just as in many control cases. The time course of the reduction is thus very similar to that of the veilers in normal medium that show rapid recovery from K^+-induced $[Ca^{2+}]_i$ increases (Chapter 5, Figure 1). The Cd was generally applied minutes before the test with Cd-containing high K^+, and small decreases in the basal fluorescence ratio often followed the initial addition of Cd. Two veiling cells were treated with Co instead of Cd. Fluorescence ratio levels increased in response to high K^+ in these cells as well, except that the increases were very small compared to those observed in Cd-treated cells. It is noteworthy that the fura-2 signal was reduced by these veiling cells in every case, with very similar kinetics to these seen in controls in which only high K^+ was added.

Effect of Reducing External Sodium on $[Ca^{2+}]_i$.

Tests of responses to a high K^+ stimulus after reducing external Na^+ resulted in large $[Ca^{2+}]_i$ increases in veiling cells (n = 3; see Figure 4). Increases observed in somata of ~ 2.5X rest are comparable to many seen in normal medium (see Chapter 5). The increased $[Ca^{2+}]_i$ was reduced to within 50% of the unstimulated basal state (n = 3) within 5 minutes in the continued presence of the stimulus.

Two branching neurons that had established extensive outgrowth by day 4 were found to be capable of reducing an evoked increase of $[Ca^{2+}]_i$ in normal medium. They were subsequently exposed to a high K^+ stimulus in reduced Na^+, after equilibrating the culture in reduced-Na^+ medium (Figure 5). The response to high K^+ in normal saline was small compared with the response of the same cell in reduced

$[Na^+]_o$ medium. Interestingly, these cells did not show any reduction of the $[Ca^{2+}]_i$ signal, even for small increases of $[Ca^{2+}]_i$ in response to brief exposures to high K^+.

Effect of Mechanically Perturbing Cells

A limited number of neurons cultured by standard procedures adhere but show very limited outgrowth. In fura-2 studies (Chapter 5) these were characterized by relatively high basal $[Ca^{2+}]_i$ (300 nM ≥ basal $[Ca^{2+}]_i$, n = 3, avg = 460 nM), and when tested with high K^+, showed small augmentations of $[Ca^{2+}]_i$ which were not reduced. In 2 cells, $[Ca^{2+}]_i$ decreased whereas in one cell the $[Ca^{2+}]_i$ increased. However, I observed that such cells produced processes within a day after mild mechanical perturbation (touches) with a fire polished electrode, but the $[Ca^{2+}]_i$ was not monitored in these cells (Figure 6).

Mild touches to distal adhered endings resulted in the induction of a veil (not shown), which continued to grow for two days, roughly the same period required for other veiling neurons to reach their stable state. Other neurons, loaded with fura-2, were similarly touched and showed changes in $[Ca^{2+}]_i$ (Figure 7) that in some cases resulted in a new resting $[Ca^{2+}]_i$ (n = 3).

Discussion

In the present study I report that experimental manipulations expected to inhibit Ca^{2+} entry or extrusion influence the extent of outgrowth in cultured crustacean neurosecretory cells to different degrees in relation to their morphology type. This suggests that the different cell types have differing reliances on $[Ca^{2+}]_i$ mechanisms for outgrowth. Outgrowth of veiling neurons is inhibited by Ca channel blockers or reduced external $[Na^+]$, but the characteristic outgrowth program appears to be unmodified, at least in the Cd case, since brief exposures to Cd-containing saline from cells destined to become veilers still resulted in the establishment of a veil. It was noteworthy that change to a medium that inhibited outgrowth was effective in stopping outgrowth that had already begun. This suggests that these media affect ongoing growth processes rather than the initiation of the process or the determination of morphology. Veiling outgrowth appears to be particularly sensitive to manipulations that are expected to alter $[Ca^{2+}]_i$ of the cell. In particular, its sensitivity to blockage of voltage-dependent Ca^{2+} entry led to a previous suggestion that exocytosis of secretory granules may supply membrane for outgrowth of these cells (Cooke *et al.*, 1989). Branching neurons, by contrast, appear not to require voltage-dependent Ca influx during the time in culture necessary to establish their morphology; they lack a detectable Ca current during the first 48 hours in culture (Meyers *et al.*, 1992), and outgrowth persists in Cd at a concentration that blocks veiling outgrowth. Therefore, they are unlikely to depend on exocytosis for outgrowth.

That brief exposure to Cd inhibits ongoing regeneration but does not alter the subsequent pattern of outgrowth after it is removed provides evidence that the extent of outgrowth is $[Ca^{2+}]_i$ sensitive but that the development of the different morphological patterns is not influenced by $[Ca^{2+}]_i$ perturbations. In *Helisoma* neurons, the same concentration of Cd that selectively blocked veiling outgrowth of the crab neurons (100 μM) statistically suppressed neurite elongation from identified motorneurons B5 and B19 at 20 - 24 hours after plating (Mattson and Kater, 1987). Lower concentrations of Cd (10 μM) resulted in uninhibited outgrowth just as reported here for the X-organ neurons.

The observation that veiling and branching neurons grew in the presence of TTX rules out an outgrowth-regulating component involving sodium channels. It has also been reported in other neuronal preparations that TTX does not inhibit outgrowth (Connor, 1986). Veiling and to a far lesser degree branching outgrowth were influenced by reduction of external sodium. Since sodium gradients play an important role in cell metabolism, it was necessary to examine the ability of the neurons to reduce perturbed $[Ca^{2+}]_i$ in reduced $[Na^+]_o$. It was unexpected that veiling neurons, the ones inhibited the most by sodium alterations, proved able to reduce the $[Ca^{2+}]_i$ at seemingly unaltered rates, even in the absence of the Na^+ gradient, which was expected to inhibit Ca^{2+} removed by Na^+/Ca^{2+} exchange. The continuation of branched outgrowth in older cells was not inhibited by reduced $[Na^+]_o$, although the vigor and extent of the outgrowth was. These neurons showed little capability to restore perturbed $[Ca^{2+}]_i$. Neurons that grow out processes in the presence of inorganic

calcium channel blockers represent somewhat of a rarity, and neurons that continue to grow in conditions that increase their $[Ca^{2+}]_i$ significantly constitute part of a small subset of studied neurons that are beginning to be recognized for their ability to produce calcium-independent outgrowth. To date, these are rat superior cervical neurons (Garyantes and Regher, 1992) and perhaps chick retinal ganglion neurons (Ivins *et al.*, 1991), although the systematic barrage of experiments conducted in this and the previous chapter relating $[Ca^{2+}]_i$ perturbations to cell morphology has yet to be reproduced in any other system.

Fluorescence Responses of Fura-2 Loaded Cells Exposed to Cadmium

When the effect of Cd^{2+} at the same concentration that blocked veiling outgrowth was examined with K^+ stimulation, a fluorescence signal with kinetics similar to those without Cd surprisingly resulted, which at face value might indicate that Ca influx occurred (see Figures 2 and 3). Published reports show that Cd interacts with fura even better than Ca (Shibuya and Douglas, 1992) and until it can be deciphered whether these signals represent Cd or Ca that in fact enters X-organ neurons, these observations must be interpreted cautiously.

My observations suggest that $[Ca^{2+}]_i$ is regulated by different mechanisms depending on not only the cell type but whether the neuron is actively growing or in a stable state. Mills and Kater (1990) have previously shown that the status of calcium regulatory mechanisms is related to outgrowth state and cell identity in regenerating *Helisoma* motorneurons. X-organ system observations reported here address

principally the morphological state, rather than outgrowth state of neurons, since X-organ neurons appear unique in their ability to reliably establish distinct morphology patterns in culture. This consistent pattern may provide insight into at least a subset of the essential intrinsic mechanisms necessary for regeneration and the establishment of a cellular morphology because the neurons were cultured under completely defined conditions, where influence from external factors seems remote. At the same time, the outgrowth in culture may not reflect the morphologies seen *in vivo* since many external cues, indispensable to correct pathfinding in the animal, are absent.

Relationship of $[Ca^{2+}]_i$ Data to Outgrowth

There exists a wide range of observations on the relationship of $[Ca^{2+}]_i$ to outgrowth--many appear conflicting. The evolving picture seems to show that a given $[Ca^{2+}]_i$ is not a universal cue for outgrowth, yet levels do appear to influence outgrowth in most neuronal culture systems. The observations on X-organ neurons provide a unique contribution to this controversy since they show for the first time a differential response of cells with distinct morphology patterns to the same experimental perturbations (i.e. Cd addition) in the same culture. Outgrowth mechanisms appear to operate in branching neurons even in the continued presence of Cd, yet the veiling growth is inhibited, a situation unparalleled in other systems. Since brief (1 hr) application of Cd onto X-organ cells led to a reversible block, it appears likely that Cd is not disrupting the growth mechanisms of veiling cells.

Time Course Differences

High K^+ challenges were used here to induce Ca responses and to probe the Ca homeostatic capabilities of the different morphology types. These observations monitor responses over a short time period relative to the time over which effects on outgrowth were recorded. Although it would be ideal to obtain observations on $[Ca^{2+}]_i$ in altered media on outgrowth simultaneously, there are technical difficulties to be overcome, such as compartmentalization of the dye within cellular organelles that may occur over such time periods (Tsien and Tsien, 1990).

References

Al-Mohanna, F. A., Cave, J., and Bolsover, S. R. (1992) A narrow window of intracellular calcium concentration is optimal for neurite outgrowth in rat sensory neurons. *Dev. Br. Res.* **70**(2): 287-290.

Connor, J. A. (1986) Digital imaging of free calcium changes and of spatial gradients in growing processes in single, mammalian central nervous system cells. *Proc. Natl. Acad. Sci.* **83**: 6179-6183.

Cooke, I., Graf, R., Grau, S., Haylett, B., Meyers, D., and Ruben, P. (1989) Crustacean peptidergic neurons in culture show immediate outgrowth in simple media. *Proc. Natl. Acad. Sci.* **86**: 402-406.

Garyantes, T. K. and Regehr, W. D. (1992) Electrical activity increases growth cone calcium but fails to inhibit neurite outgrowth from rat sympathetic neurons. *J. Neurosci.* **12**: 96-103.

Ivins, J. K., Raper, J. A., Pittman, R. N. (1991) Intracellular calcium levels do not change during contact-mediated collapse of chick DRG growth cone structure. *J. Neurosci.* **11**: 1597-1608.

Kater, S. B., and Letourneau, P. C. (eds.) Biology of the Nerve Growth Cone. Alan Liss: New York, 1985.

Kater, S. B. and Mills, L. R. (1991) Regulation of growth cone behavior by calcium. *J. Neurosci.* **11**: 891-899.

Letourneau, P. C., Kater, S. B. and Macagno, E. R. (eds.) The Nerve Growth Cone. Raven Press: New York, 1991.

Mattson, M. P. and Kater, S. B. (1987) Calcium regulation of neurite elongation and growth cone motility. *J. Neurosci.* **7**: 4034-4043.

Meyers, D. E. R., Graf, R. A., and Cooke, I. M. (1992) Ionic currents of morphologically distinct peptidergic neurons in defined culture. *J. Neurophysiol.* **67**: 1301-1315.

Mills, L. R. and Kater, S. B. (1990) Neuron-Specific and State-Specific Differences in Calcium Homeostasis Regulate the Generation and Degeneration of Neuronal Architecture. *Neuron* **2**: 149-163.

Tsien, R. W., and Tsien, R. Y. (1990) Calcium Channels, Stores, and Oscillations. *Annu. Rev. Cell Biol.* **6**: 715-760.

Figure 6-1. Typical Effects of Alterations of Culture Medium On Outgrowth Morphology at One Day in Culture. Phase-contrast photomicrographs, except C. Cells were allowed to adhere and grow processes in normal defined medium for 4 hours, to permit determination of morphological type. 1A: Two small cells in normal medium, a cell type that always branches in culture. 2A: Veiling neuron in normal medium. 1B: Branching neuron exposed to 100 μM Cd for a 1 hour period (hour 4 - 5) shows normal morphology. 2B: Veiling neuron exposed to 100 μM Cd for 1 hour period (hour 4 -5). Note that veiling outgrowth resulted at 1 day, thus brief exposure to Cd did not block the outgrowth process. C: Hoffman modulation contrast photomicrographs of branching and veiling outgrowth in medium containing 100 μM Cd introduced at 4 hours. Note that branching outgrowth occurs (1C) in the same cultures where veiling is inhibited (2C). D: A 1/10th reduction of sodium concentration from the medium does not inhibit branching outgrowth, although it appears thinner and less vigorous than controls. Note the lighter appearance of the processes under phase-contrast. Most branching neurons grow (1D) but veiling neurons do not (2D) in reduced Na saline. E: Branching (1E) and veiling (2E) neurons show normal outgrowth in TTX-containing medium.

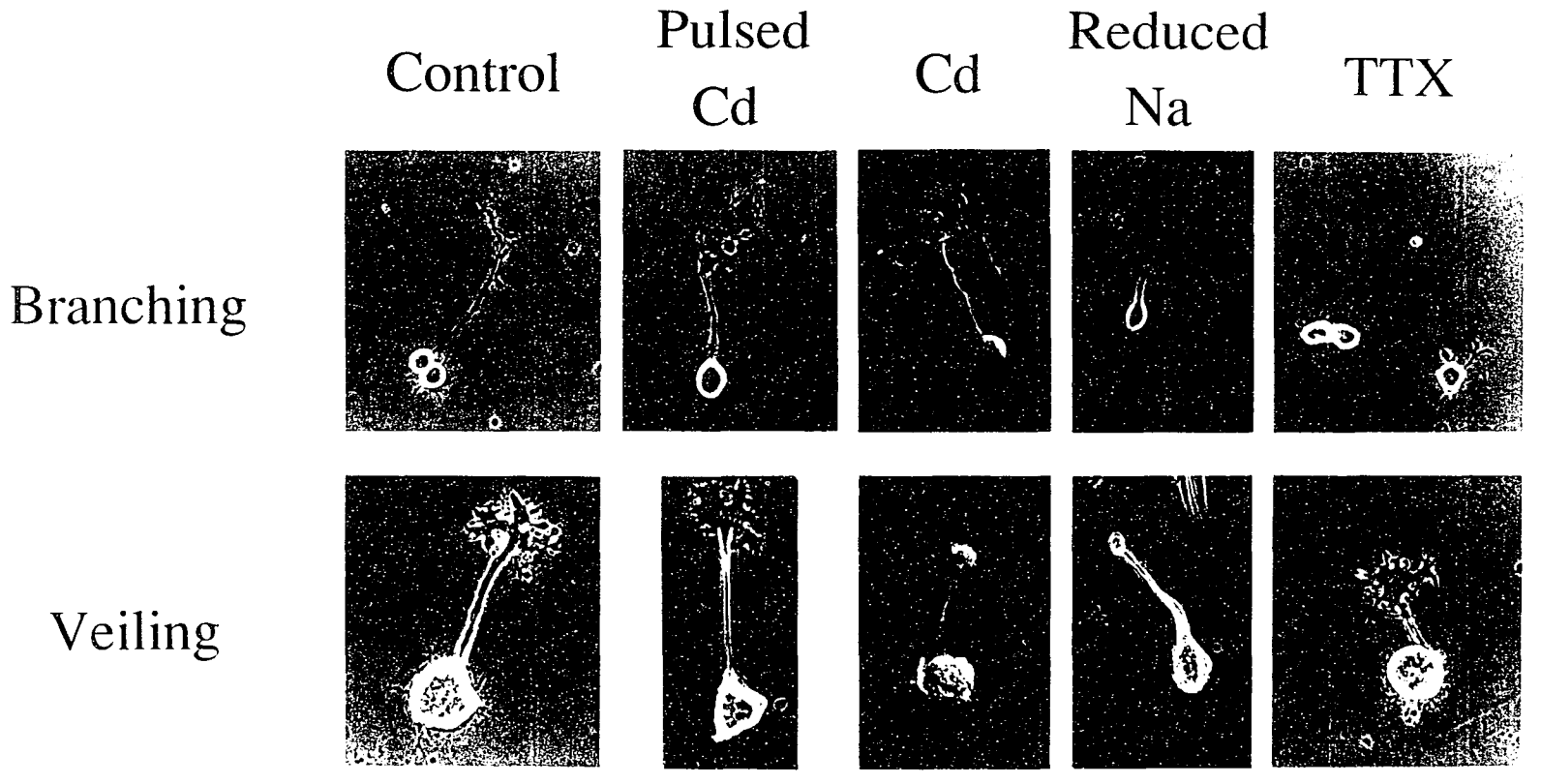
Control
Pulsed Cd
Cd
Reduced Na
TTX
Branching
Veiling

Figure 6-2 Fluorescence Changes Resulting from Addition of Cd to a Veiling Cell at the Same Concentration Used to Block Veiling Outgrowth. A non-actively-veiling cell (day 8) loaded with fura-2/AM. Note the unexpected ratio increase that results after the cell has been exposed to cadmium containing saline (100 μM) for ~ 3 minutes. Bath-applied 5X normal-K^+ saline (containing Cd) was introduced after the cells were allowed to equilibrate with Cd-containing medium. Note that the time course of both the increase and subsequent decrease of the fluorescence ratio mirrors many high K^+ responses under control conditions (See e.g. figure 5-1).

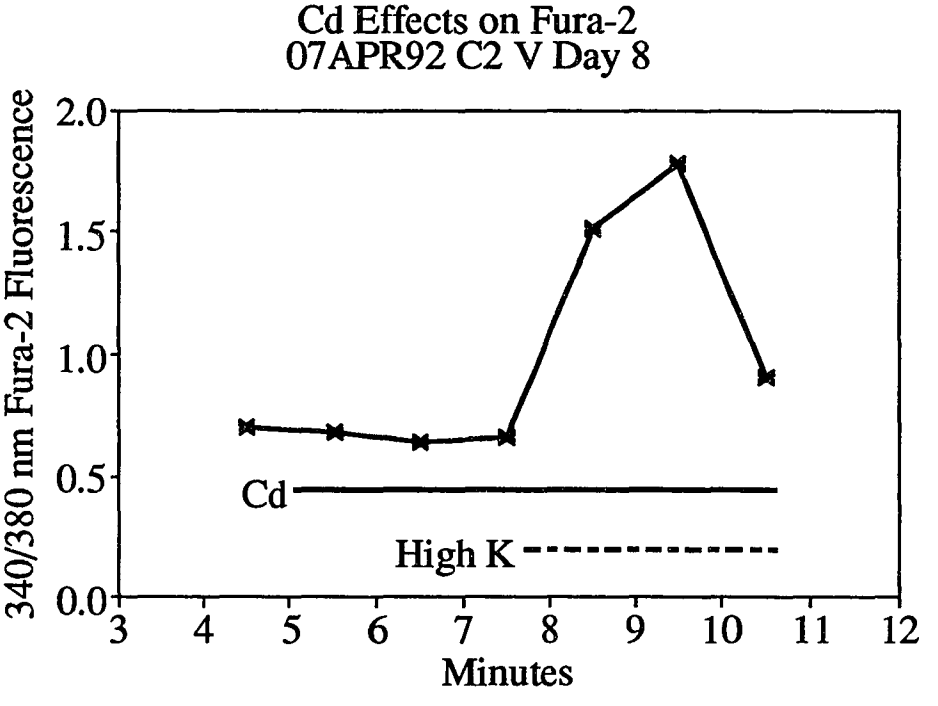
Cd Effects on Fura-2
07APR92 C2 V Day 8
340/380 nm Fura-2 Fluorescence
2.0
1.5
1.0
0.5
0.0
3
4
5
6
7
8
9
10
11
12
Minutes
Cd
High K

Figure 6-3. Fluorescence Changes Resulting from Addition of Cd to a Branching Cell at the Same Concentration Used to Block Veiling Outgrowth. Day 4 cell, fura-2/AM loaded, showing soma and processes responding with a fluorescence signal in the presence of Cd at 100 μM. Note the decline in the signal in the continued presence of Cd, similar to many responses from older branching neurons under normal conditions (see figure 5-5, cell with outgrowth).

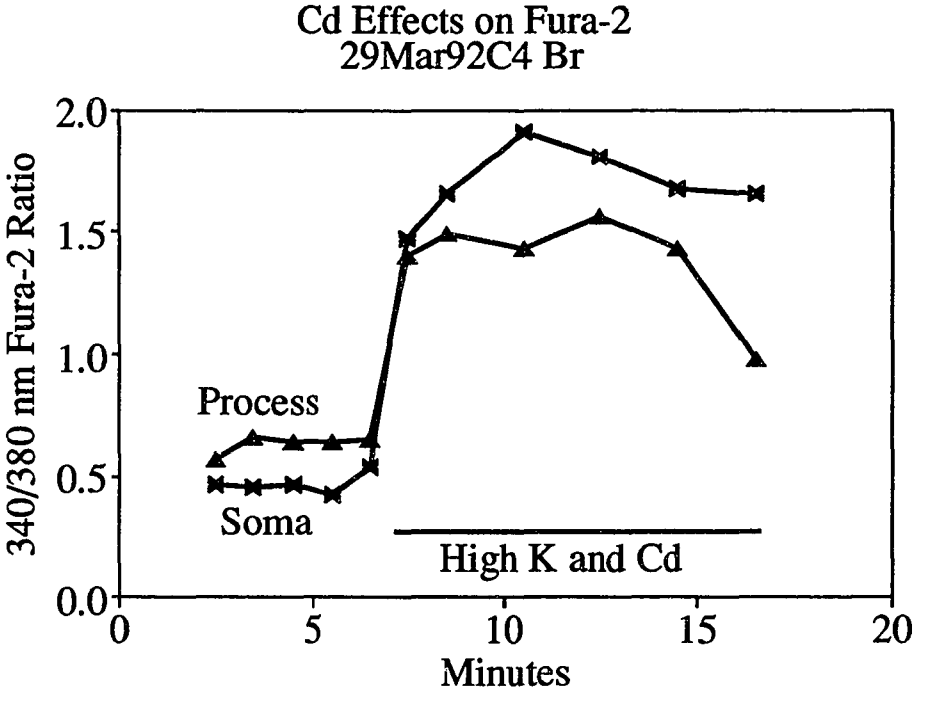
Cd Effects on Fura-2
29Mar92C4 Br
340/380 nm Fura-2 Ratio
2.0
1.5
1.0
0.5
0.0
0
5
10
15
20
Minutes
Process
Soma
High K and Cd

Figure 6-4. Calcium Responses to High K^+ From A Veiling Neuron in Reduced Sodium Saline. Day 2 in culture, fura-2/AM loaded. The neuron was first stimulated with 5X high-K^+ in normal saline, then exposed to 1/10th normal sodium saline, then 5X high-K^+ containing reduced-sodium saline. Note that the neuron decreased $[Ca^{2+}]_i$ when the external Na^+ gradient had been reduced 10 fold. Also, note that the response in reduced Na saline is larger than response to high K^+ in normal saline.

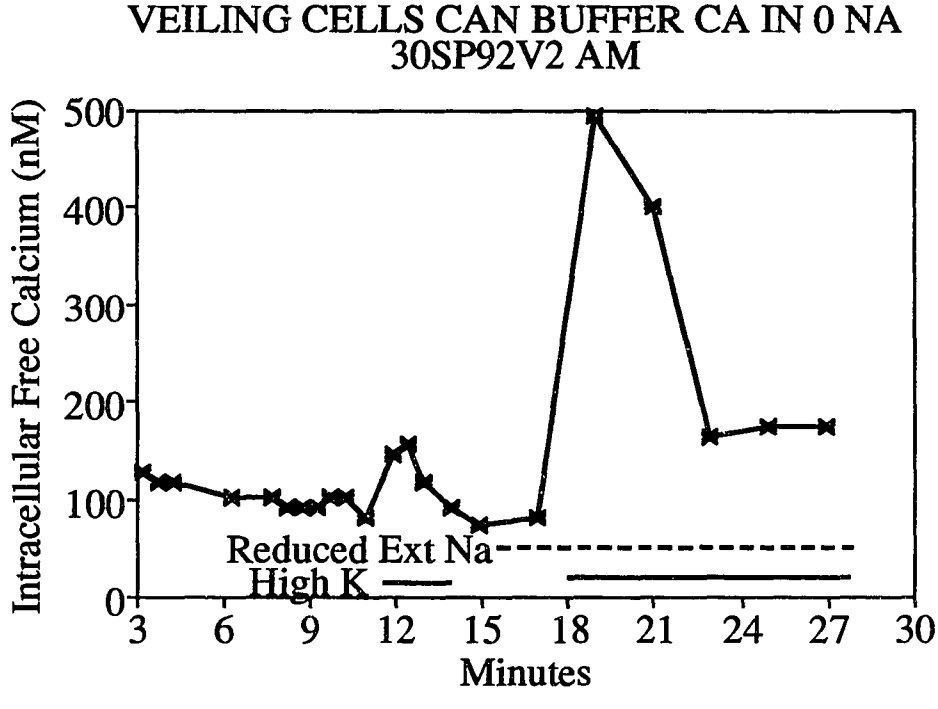
VEILING CELLS CAN BUFFER CA IN 0 NA
30SP92V2 AM
Intracellular Free Calcium (nM)
500
400
300
200
100
0
3
6
9
12
15
18
21
24
27
30
Minutes
Reduced Ext Na
High K

Figure 6-5. Calcium Responses to High K^+ From A Branching Neuron in Reduced Sodium Saline. Day 2 neuron, fura-2/AM loaded. This neuron, when stimulated with 10X K^+ produced a small increase in $[Ca^{2+}]_i$. The neuron was then rinsed in reduced sodium saline, as shown, and then exposed to 10X K^+-containing reduced-sodium saline. Note the increased response magnitude relative to that in normal saline.

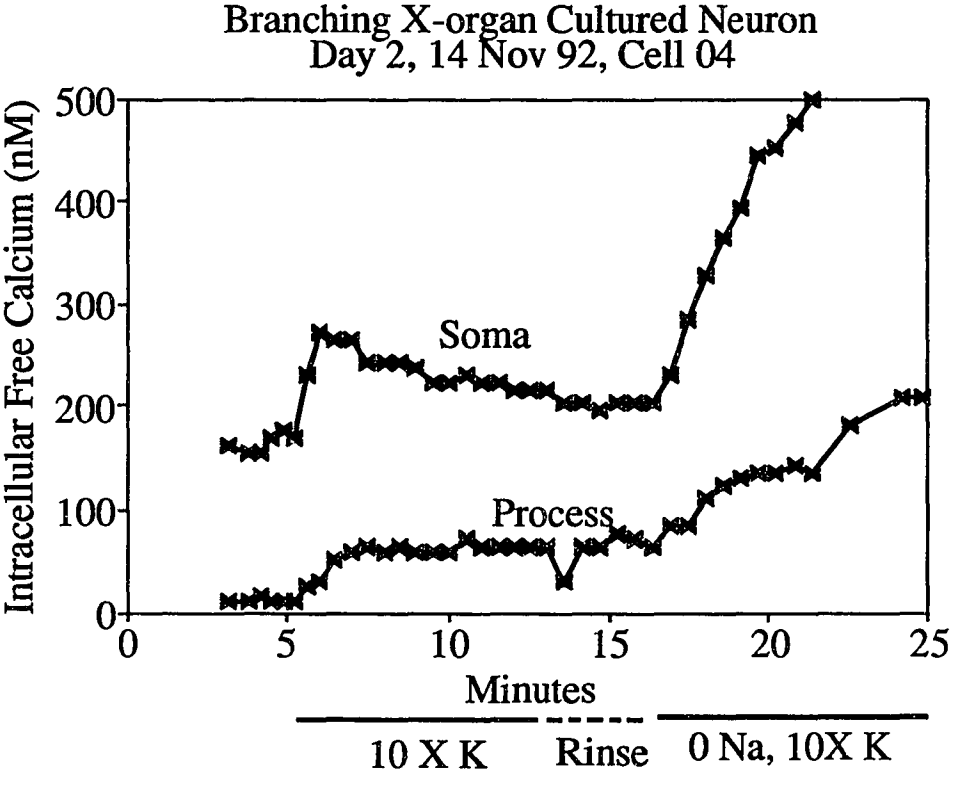
Branching X-organ Cultured Neuron
Day 2, 14 Nov 92, Cell 04
Intracellular Free Calcium (nM)
500
400
300
200
100
0
Soma
Process
0
5
10
15
20
25
Minutes
10 X K
Rinse
0 Na, 10X K

Figure 6-6. Initiation of Outgrowth Resulting from Mechanical Stimulation with a Fire-Polished Glass Probe. A neuron at day 4 with many veiling characteristics (30 - 40 μm soma width diameter, thick monopolar residual neurite, soma texture) that after being touched, sprouted outgrowth that grew for 2 days and established a veil.

Figure 6-7. Mechanical Stimulation of a Veiling Neuron Changed the $[Ca^{2+}]_i$. Day 2, fura-2/AM-loaded veiling neuron was mildly touched with the probe. Note that the $[Ca^{2+}]_i$ appears to have settled to a new resting level.

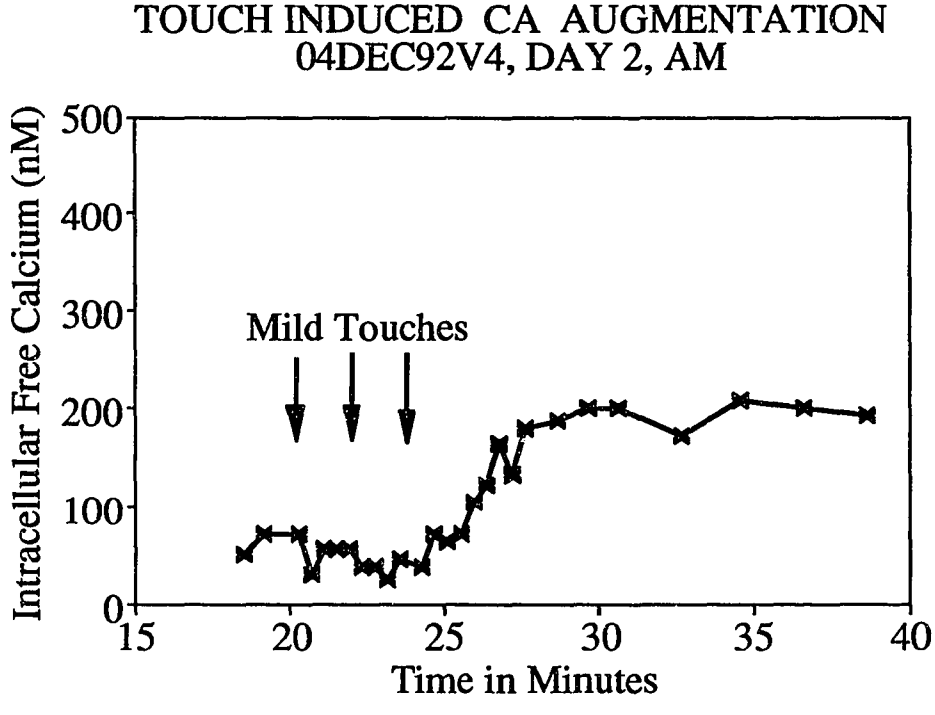
TOUCH INDUCED CA AUGMENTATION
04DEC92V4, DAY 2, AM
Intracellular Free Calcium (nM)
500
400
300
200
100
0
Mild Touches
15
20
25
30
35
40
Time in Minutes

CHAPTER 7

SUMMARY AND CONCLUSIONS

This dissertation characterizes intracellular free calcium concentration ($[Ca^{2+}]_i$) and gradients resulting from experimental perturbations in neurosecretory cells. $[Ca^{2+}]_i$ has been shown to be important for a great many cellular functions, including regeneration in neurons and exocytotic secretion in neurons and endocrine cells. Differences were found to exist in how $[Ca^{2+}]_i$ is regulated between two types of neurosecretory cells that have a very different appearance after they regenerate processes in culture.

I focussed on $[Ca^{2+}]_i$ regulatory mechanisms and their relationship to outgrowth morphology. My project stemmed from efforts to characterize Ca-handling mechanisms in relation to neurosecretion of different peptide hormones (neuropeptides). To identify and observe individual neurons, techniques not previously available were developed for the isolation and culturing of crustacean neurons.

By isolating and plating the X-organ neurons under defined conditions at low density, we have been able to observe unique process outgrowth responses that reflect intrinsic mechanisms of the neurosecretory cells. We have shown that neurons consistently produce distinct morphology patterns in culture that correspond directly, at least in the case of veiling neurons, to antisera against neurohormone crustacean hyperglycemic hormone (CHH). In the case of the other type, branching, at least two immunoreactivities, and hence different neuronal phenotypes, are implied. The highly

consistent morphologies observed are unusual relative to other neuronal systems. Also, the ability of the crustacean neurons to show vigorous outgrowth in the absence of conditioning factors appears equally striking.

Since Ca-dependent exocytosis is activated by membrane depolarizations that initiate influx through voltage-dependent Ca channels, the electrical membrane properties of the different neuronal morphological types were characterized. We found distinct differences in the voltage-dependent ionic currents present in neurons of different morphology. This observation is in agreement with studies using other neuronal culture preparations, such as motorneurons from the fresh water snail *Helisoma*. X-organ neurons differ from *Helisoma* neurons in that their ability to generate impulses can be associated with their outgrowth morphology: Cells destined to have or having veils can produce action potentials, whereas branching neurons are electrically silent and cannot be induced to spike, at least not during the 2 day period necessary to establish an extensive branching morphology. Voltage clamp findings have explained this difference: Veiling neurons exhibit two inward currents, a voltage-dependent Na^+ current blocked by TTX, and a voltage-dependent Ca current, blocked by Cd, as well as two outward currents, a transient outward current blocked by 4-aminopyridine and a delayed rectifier current blocked by tetraethylammonium ions. Inward current was not detected from branching neurons during the first two days in culture, while the two outward currents were. They may gain Ca^{2+} channels with time in culture, as suggested indirectly by the greater increase of $[Ca^{2+}]_i$ in response to depolarization seen in branching neurons of older ages in culture.

To characterize temporal and spatial changes of $[Ca^{2+}]_i$, optical techniques were used to measure the fluorescence of the Ca-sensitive vital dye fura-2. These techniques also provided the opportunity to characterize resting levels of $[Ca^{2+}]_i$. My observations tested an earlier proposal (Kater and Mills, 1991) that outgrowth occurs only when $[Ca^{2+}]_i$ is within a permissive range of values. However, X-organ neurons were found to have a wide range of basal $[Ca^{2+}]_i$, and these resting levels were not significantly different between veiling and branching neurons that were actively regenerating processes or that had established a stable morphology after a few days in culture.

In order to test whether the cells responded to depolarizing stimuli by increasing cytosolic Ca^{2+}, the cells were challenged with high potassium (high K^+) saline for relatively brief times (1 - 2 min) in otherwise normal saline or in altered media that have an effect on outgrowth. High K^+ caused increases of $[Ca^{2+}]_i$ in all cells tested (~ 4X), with large changes occurring in veiling neurons of all ages and smaller changes occurring in young branching neurons. The changes in branching neurons increased with time and the extent of outgrowth in culture.

The cultured X-organ neurons showed a differential ability to decrease $[Ca^{2+}]_i$ after stimulation that corresponded with their outgrowth morphology: some veils (and less prominently their somata) but no comparable-stage branchers were capable of decreasing K^+-elevated $[Ca^{2+}]_i$ toward resting levels quickly (to within 20% in 5 minutes). This also contrasts with recovery times of tens of minutes reported from other neuronal culture systems. Veiling neurons were capable of decreasing the $[Ca^{2+}]_i$

even in the continued presence of the depolarizing stimulus. Interestingly, when high K^+ was applied while recording the membrane potential of veiling neurons, the resting potential was seen to decrease back to resting with a time course that parallels the $[Ca^{2+}]_i$ decline in a subset of the cells. This may help to explain why the $[Ca^{2+}]_i$ declined in the continued presence of high K^+.

Decreases of $[Ca^{2+}]_i$ following a K^+-stimulated increase were not observed from young branching neurons, but in older ones, the response was similar in time course to that of a subgroup of veiling cells that showed medium rates of recovery. Thus, mechanisms or effects present and operating in veiling neurons at early and late ages may be acquired by the branchers with time in culture. Hence, there are differences in the Ca^{2+} regulatory mechanisms or their effects responsible for decreasing perturbed $[Ca^{2+}]_i$ to basal levels associated with the differences in outgrowth pattern.

$[Ca^{2+}]_i$ responses and ability to reduce $[Ca^{2+}]_i$ of veiling neurons appears to be relatively unaffected by the presence of cadmium (Cd), a blocker of voltage-dependent Ca^{2+} current, or reduction of medium Na^+ concentration, presumed to reduce the Na^+ concentration gradient by which Ca^{2+} can be removed from the cell in exchange for Na^+. Neurons were exposed to short-term high-K^+ challenges in reduced-Na^+ saline or Cd-containing saline. High K^+ challenges increased the $[Ca^{2+}]_i$ similarly to challenges in normal saline for both morphology types, and $[Ca^{2+}]_i$ decreases were still observed in neurons that had veiled. Older branching cells could not reduce the increased $[Ca^{2+}]_i$, unlike the case in normal medium.

The outgrowth of branching neurons appears to be less affected by procedures which block surface Ca^{2+} transfer mechanisms to accomplish homeostasis, than is that of veiling neurons. Outgrowth effects of Cd and lowered Na^+ additions are clear: branching outgrowth continues and veiling is inhibited. Studies on the effects of lowered $[Na^+]_o$ on resulting changes in $[Ca^{2+}]_i$ and outgrowth over a longer period of time are needed to discern whether the block of veiling outgrowth is due to block of the Na^+/Ca^{2+} exchanger, or other Na^+ dependent mechanisms such as the amino acid or glucose transporter. Cd used in combination with fura-2 to observe $[Ca^{2+}]_i$ must be interpreted with caution. The observations require confirmation with Ca^{2+}-blocking agents that do not interfere with fura-2 analyses, as Cd potentially does.

In summary, there are now a variety of conflicting observations from different experimental preparations on the relationship of $[Ca^{2+}]_i$ to outgrowth. The evolving picture seems to show that calcium is not a universal cue for outgrowth, yet it does influence outgrowth in most cases. Observations on outgrowth of X-organ neurons in culture provide a unique contribution to this controversy since they show for the first time a differential response of neurons with distinct morphology patterns to the same experimental perturbations under identical culture conditions. Outgrowth mechanisms appear to have differential sensitivities to treatments that block Ca regulatory mechanisms. However, for the X-organ neurons, unlike many other neuronal types, the ability to regenerate neuronal processes is not closely controlled by $[Ca^{2+}]_i$, and the pattern of the outgrowth appears to be independent of $[Ca^{2+}]_i$ over a wide basal range.

GLOSSARY

AKH	Adipokinetic hormone. An insect analog to crustacean RPCH. The antibody to this hormone was used to label and identify neurons in culture.
AM	Pentaacetoxymethyl ester form of a chemical. In the case of fura-2AM, the AM form facilitates the passing of the chemical across the membrane. Fura-2 is linked to 4 hydrophilic groups by ester bonds. Once inside the cell, the cellular esterases rapidly hydrolyze the hydrophilic groups (AM) and trap the chemical inside the cell.
4-AP	4-aminopyridine. Blocker of the voltage dependent transient outward current of many excitable tissues.
ATP	Adenosine triphosphate. Major source of energy for cellular metabolism and source of cAMP.

BAPTA	1,2-bis-(2-aminophenyoxy)ethane-N,N,N',N'-tetraacetic acid. A free calcium chelator with much faster binding kinetics than EGTA (see below).
Ba	Barium ion. A divalent ion that can pass through Ca channels and therefore substitute for Ca ions in current separation voltage clamp studies.
BSA	Bovine serum albumin. Used to inhibit non-specific binding in immunocytochemical staining studies.
$[Ca^{2+}]_i$	Cytosolic free Ca concentration. Very low inside cells, roughly 100 nM or 10,000 :1 (ratio of external to internal concentrations.) Using digital fluorescent ratio imaging on single cells, $[Ca^{2+}]_i$ can be calculated according to the following equation: $K_d\,[(R-R_{min})/(R_{max}-R)]F_o/F_s$.
CHH	Crustacean hyperglycemic hormone. Neuropeptide involved in regulation of glucose metabolism (78 Kd).

Current Clamp	An electrophysiological technique whereby an individual cell's membrane potential is monitored upon cell penetration with minimal current drain from the cell and allowing for membrane voltage responses to current input.
DMSO	Dimethylsulfoxide. Solvent that aids in the solubility of certain chemical agents to aqueous solutions (such as fura-2/AM to saline in this study).
E_K	The membrane potential at which there is no net flow of potassium across the plasma membrane. This is the potential at which the chemical and electrical driving forces are at equilibrium. This potential can be calculated from the Nernst equation (E_K=RT/Fln($[K]_o/[K]_i$) = 2.303 RT/Flog10($[K]_o/[K]_i$).
E_R	Reversal Potential for a response under study. This is the membrane voltage at which the electro-chemical forces of the ions involved are at equilibrium (will not flow).
EGTA	Ethylene glycol bis(β-aminoethyl ether)-N,N,N',N'-tetracetic acid. A free calcium chelator, or "binder".

ER	Endoplasmic reticulum.
F_o/F_s	The fluorescence ratio obtained at low and saturating calcium levels.
FITC	Fluorescein isothiocyanate. A fluorescent compound used in immunocytochemical studies for determining associations of specific molecules with cells (identification) and for exploring the subcellular distributions of the chosen molecule.
fura-2	1-[2-(5-carboxyoxazol-2-yl)-6-aminobenzofuran-5-oxy]-2-(2'-amino-5'-methylphenoxy)-ethane-N,N,N',N'-tetraacetic acid, pentapotassium salt. Calcium chelator and indicator useful for intra- and extracellular measurements. This indicator responds to calcium by shifting wavelengths while maintaining strong fluorescence. The ratio of fluorescences at two suitably chosen wavelengths (340/380) signals free Ca. Can be calibrated to provide values for free Ca ion.
GΩ	Gigohm. Electrical resistance unit, 10^9 ohms.

HEPES	N-2-hydroxyethylpiperazine-N'-2-ethanesulfonic acid. An acidic buffer used to buffer free H ions (pH).
I_A	Voltage-dependent and 4-AP inhibited transient outward current, present in most neurons. First described in molluscan neurons.
I_{Ca}	Voltage-dependent calcium current, which flows through voltage-dependent calcium pores, or channels, in the plasma membrane. This current is blocked by Cd. This current is present in most excitable cell types and was first described in crustacean muscle.
I_K	Voltage-dependent and TEA inhibited delayed rectifying outward current, first described in molluscan neurons.
I_{Na}	Voltage-dependent TTX blocked sodium current present in excitable tissues.
[I(V)]	Current-Voltage Relationship. Used to characterize voltage-dependent ion currents of excitable membranes during voltage clamp studies.
K_d	Dissociation constant.

MIH	Molt Inhibiting Hormone. Neuropeptide involved in regulation of molt cycle of Crustacea.
ml, mm, mg, mM, ms	Milli- liter, meter, gram, molar, second
MΩ	Megohm electrical resistance unit, 10^6 ohms
mV	Millivolt, 10^{-3} volts.
NMG-$MeSO_3$	N-methyl-D-glucamine methane sulphonate. A large macromolecule that is impermeant to voltage-dependent ion channels that is used in current separation techniques associated with electrophysiology.
Peptide D	An antibody produced by S. Grau of the Cooke Laboratory against the D peptide of the separation studies of R. Newcomb.
Pluronic	A surfactant that aids in the dispersing of a chemical throughout a soluble solution (such as fura-2/AM in DMSO, as used in Chapter 5 of this thesis.)

R	Ratio of excitation light filtered at 340 nm +/- 5nm and 380 nm +/- 5 nm. (340/380)
R_{min}	340/380 ratio of a very low free Ca-fura containing solution.
R_{max}	340/380 ratio of a fura saturating Ca-containing solution.
RPCH	Red Pigment Concentrating Hormone. Found in the X-organ and in other crustacean ganglia (stomatogastric ganglion for example). pGlu-Leu-Asn-Phe-Ser-Pro-Gly-Trp-NH_2. Peptide involved in pigmentation regulation. Causes contraction of red chromatophores; other roles.
SIT	Silicon-intensified target. A type of chip used in low-light imaging detectors such as the video camera used in this study.
TEA	Tetraethyl ammonium ion. Blocker of delayed rectifier voltage-dependent potassium current of many excitable tissues.
TTX	Tetrodotoxin. Reversible blocker of sodium channels of almost all electrically excitable tissue.

V_c	Command Voltage. The voltage the experimenter steps the cell membrane to during a voltage clamp experiment.
V_h	The voltage the experimenter holds the cell membrane at during a voltage clamp experiment. (usually near the resting potential of the cell, but not always.)
Voltage Clamp	An electrophysiological technique whereby an individual cell's membrane potential is clamped, or controlled by injecting an equal but opposite amount of current into the cell to counteract the membrane current flux (by way of a feedback amplifier.) The membrane current fluctuations that result from 'holding' the cell are studied. The technique allows regulated stepping of membrane potential while monitoring membrane current responses on a ms time scale.
XOSG	X-organ - sinus gland. Major neurosecretory structure in Crustacea consisting of ~200 neurons that send axons viathe Sinus gland nerve to the sinus gland. The sinus gland is a neurohemal organ, i.e. where the axon terminals are in close

association with hemolymph sinuses. The terminals secrete neurohormones including CHH, MIH, and RPCH.

REFERENCES

Adler, E. M., Augustine, G. J., Duffy, S. N. and Charlton, M. P. (1991) Alien intracellular calcium chelators attenuate neurotransmitter release at the squid giant synapse. *J. Neurosci.* **11**: 1496-1507.

Alberts, B., Bray, D., Lewis, J., Raff, M., Roberts, K., and Watson, J. *Molecular Biology of the Cell.* Garland: New York, 1989.

Al-Mohanna, F. A., Cave, J., and Bolsover, S. R. (1992) A narrow window of intracellular calcium concentration is optimal for neurite outgrowth in rat sensory neurons. *Dev. Br. Res.* **70**(2): 287-290.

Anglister, L., Farber, I. C., Shahar, A., and Grinvald, A. (1982) Localization of voltage-sensitive calcium channels along developing neurites: Their possible role in regulating neurite elongation. *Dev. Biol.* **94**: 351-365.

Atwood, H. L., Charlton, M. P. and Thompson, C. S. (1983) Neuromuscular transmission in crustaceans is enhanced by a sodium ionophore, monensin, and by prolonged stimulation. *J. Physiol.* **335**: 179-195.

Atwood, H. L. and Wojtowicz, J. M. (1986) Short-term and long-term plasticity and physiological differentiation of crustacean motor synapses. *Int. Rev. Neurobiol.* **28**: 275-362.

Augustine, G. J., Adler, E. M. and Charlton, M. P. (1991) The calcium signal for transmitter secretion from presynaptic nerve terminals. In: *Calcium Entry and Action at the Presynaptic Nerve Terminal.* Vol. 635 of the Annals of the New York Academy of Sciences.

Beadle, D., Lees, G. and Kater, S. *Cell Culture Approaches to Invertebrate Neuroscience.* Academic Press: London, 1988.

Benson, J. A., and Cooke, I. M. (1984) Driver potentials and the organizatin of rhythmic bursting in crustacea ganglia. Trends Neurosci. 7: 85-91.

Bentley, D. and Keshishian, H. (1982) Pioneer neurons and pathways in insect appendages. *Trends Neurosci.* **5**: 354-358.

Bentley, D. and Caudy, M. (1983) Pioneer axons lose directed growth after selective killing of guidepost cells. *Nature* **304**: 62-65.

Bliss, D. E., Durand, J. P. and Welsh, J. H. (1954) Neurosecretory systems in decapod Crustacea. *Z. Zellforsch. Mikrosk. Anat* **39**: 520-536.

Chalfie, M. and Wolinsky, E. (1990) The identification and suppression of inherited neurodegeneration in *Caenorhabditis elegans*. *Nature* **345**: 410-416.

Choi, D. W. (1990) Cerebral hypoxia: Some new approaches and unanswered questions. *J. Neurosci.* **10**: 2493-2501.

Cohan, C., Connor, J. A. and Kater, S. B. (1987) Electrically and chemically mediated increases in intracellular calcium in neuronal growth cones. *J. Neurosci.* **7**: 3588-3599.

Cohan, C. S. and Kater, S. B. (1986) Suppression of neurite elongation and growth cone motility by electrical activity. *Science* **232**: 1638-1640.

Cooke, I. M. (1985) Electrophysiological characterization of peptidergic neurosecretory terminals. *J. Exp. Biol.* **118**: 1-35.

Cooke, I., Graf, R., Grau, S., Haylett, B., Meyers, D., and Ruben, P. (1989) Crustacean peptidergic neurons in culture show immediate outgrowth in simple media. *Proc. Natl. Acad. Sci.* **86**: 402-406.

Cooke, I. and Sullivan, R. E. (1982) Hormones and Neurosecretion. In: *The Biology of Crustacea*, Vol. 3. (H. Atwood and D. Sandeman, eds.), Academic Press, N. Y., pp. 205-290.

Connor, J. A. (1986) Digital imaging of free calcium changes and of spatial gradients in growing processes in single, mammalian central nervous system cells. *Proc. Natl. Acad. Sci.* **83**: 6179-6183.

Dagan, D. and Levitan, I. B. (1981) Isolated identified *Aplysia* neurons in cell culture. *J. Neurosci.* **1**: 736-740.

Fawcett, J. W. (1992) Intrinsic neuronal determinants of regeneration. *Trends Neurosci.* 15: 6-8.

Ferlund, P. and Josefsson, L. (1972) Crustacean color change hormone: Amino acid sequence and chemical synthesis. *Science* **177**: 173-175.

Ferlund, P. (1974a) Structure of the red-pigment-concentrating hormone of the shrimp, *Pandalus borealis*. *Biochim. Biophys. Acta* **317**: 304-311.

Ferlund, P. (1974b) Synthesis of the red-pigment-concentrating hormone of the shrimp, *Pandalus borealis. Biochim. Biophys. Acta* **371**: 312-322.

Fields, R. D., Neale, E. A., and Nelson, P. G. (1990) Effects of patterned electrical activity on neurite outgrowth from mouse sensory neurons. *J. Neurosci.* **10**: 2950-2964.

Fields, R. D., and Russell, J. T. (1992) Kinetics of electrically evoked calcium transients in mouse DRG growth cones. *Soc. Neurosci. Abstr.*, 1287

Furshpan, E. J. and Potter, D. D. (1959) Transmission at the giant motor synapses of the crayfish. *J. Physiol.* **145**: 289-325.

Garyantes, T. K. and Regehr, W. D. (1992) Electrical activity increases growth cone calcium but fails to inhibit neurite outgrowth from rat sympathetic neurons. *J. Neurosci.* **12**: 96-103.

Graf, R. A. and Cooke, I. M. (1990) Primary culture of crustacean stomatogastric ganglion neurones in defined medium. *J. Exp. Biol.* **149**: 521-525.

Graubard, K. and W. N. Ross (1985) Regional distribution of calcium influx into bursting neurons detected with arsenazo III. *Proc. Natl. Acad. Sci. USA* **82**: 5565-5569.

Grisolia, S. (ed.) *Ramon y cajal's contribution to the neurosciences.* Elsevier: New York, 1983.

Grynkiewicz, G., Poenie, M. and Tsien, R. Y. (1985) A new generation of Ca indicators with greatly improved fluorescence properties. *J. Biol. Chem.* **260**: 3440-3450.

Guthrie, P. B., Lee, R. E. and Kater, S. B. (1989) A comparison of neuronal growth cone and cell body membrane: Electrophysiological and ultrastructural properties *J. Neurosci.* **9**: 3596-3605.

Harrison, R. G. (1910) The outgrowth of the nerve fiber as a mode of protoplasmic movement. *J. Exp. Zool.* **B9**: 787-848.

Haydon, P. G., Cohan, C. S., McCobb, D. P., Miller, H. R and Kater, S. B. (1985) Neuron-specific growth cones properties as seen in identified neurons of *Helisoma. J. Neurosci. Res.* **13**: 135-148.

Holliday, J., Adams, R. J., Sejnowski, T. J., and Spitzer, N. C. (1991) Calcium-Induced Release of Calcium Regulates Differentiation of Cultured Spinal Neurons. *Neuron* 7: 787-796.

Hodgkin, A. L. and Rushton, W. A. H. (1946) The electrical constants of a crustacean nerve fiber. *Proc. Royal. Soc. B* **133**: 444-479.

Ivins, J. K., Raper, J. A., Pittman, R. N. (1991) Intracellular calcium levels do not change during contact-mediated collapse of chick DRG growth cone structure. *J. Neurosci.* **11**: 1597-1608.

Kaczmarek, L. K., Finbow, M., Revel, J. P. & Strumwasser, F. (1979) *J. Neurobiol.* **10**: 535-550.

Kater, S. B., Mattson, M. P., Cohan, C. S. and Connor, J. A. (1988) Calcium regulation of the neuronal growth cone. *Trends Neurosci.* **11**: 315-321.

Kater, S. B. and Mills, L. R. (1991) Regulation of growth cone behavior by calcium. *J. Neurosci.* **11**: 891-899.

Katz, B. and Miledi, R. (1967) The release of acetylcholine from nerve endings by graded electric pulses. *Proc. Royal Soc. B* **167**: 23-38.

Kegel, G., Reichwein, B., Weese, S., Gaus, G., Peter-Katalinic, J. and Keller, R. (1989) Amino acid sequence of the crustacean hyperglycemic hormone (CHH) from the shore crab, *Carcinus maenas*. *FEBS Letters* **255**: 10-14.

Kravitz, E. A., Kuffler, S. W., and Potter, D. D. (1963) Gamma-aminobutyric acid and other blocking compounds in Crustacea III. Their relative concentrations in separated motor and inhibitory axons. *J. Neurophysiol.* **26**: 739-751.

Lankford, K. L. and Letourneau, P. C. (1989) Evidence that calcium may control neurite outgrowth by regulating the stability of actin filaments. *J. Cell Biol.* **109**: 1229-1243.

Lemos, J. R., Nordmann, J. J., Cooke, I. M. and Stuenkel, E. L. (1986) Single channels and ionic currents in peptidergic nerve terminals. *Nature* **319**: 410-412.

Letourneau, P. C., Kater, S. B. and Macagno, E. R. (eds.) The Nerve Growth Cone. Raven Press: New York, 1991.

Lipscombe, D, D. V. Madison, M. Poenie, H. Reuter, R. Y. Tsien, and R. W. Tsien (1988) Spatial distribution of calcium channels and cytosolic calcium transients in growth cones and cell bodies of sympathetic neurons. *Proc. Natl. Acad. Sci. USA* **85**: 2398-2402.

Llinas, R. R. (1988) The electrophysiological properties of mammalian neurons: Insights into central nervous system function. *Science* **242**: 1654-1664.

Malenka, R. C., Kauer, J. A., Perkel, D. J. and Nicoll, R. A. (1989) The impact of postsynaptic calcium on synaptic transmission--its role in long term potentiation. *Trends Neurosci.* **12**: 444-450.

Marty, A. (1989) The physiological role of calcium dependent channels. *Trends Neurosci.* **12**: 420-424.

Mattson, M. P. and Kater, S. B. (1987) Calcium regulation of neurite elongation and growth cone motility. *J. Neurosci.* **7**: 4034-4043.

McCarty, N. A. and O'Neil, R. G. (1992) Calcium signaling in cell volume regulation. *Physiological Reviews* **72**: 1037-1061.

McCormack, J. G., Halestrap, A. P. and Denton, R. M. (1990) Role of calcium ions in the regulation of mammalian intramitochondrial metabolism. *Physiol. Rev.* **70**: 391-425.

Meyers, D. E. R., Graf, R. A., and Cooke, I. M. (1992) Ionic currents of morphologically distinct peptidergic neurons in defined culture. *J. Neurophysiol.* **67**: 1301-1315.

Mills, L. R. and Kater, S. B. (1990) Neuron-Specific and State-Specific Differences in Calcium Homeostasis Regulate the Generation and Degeneration of Neuronal Architecture. *Neuron* **2**: 149-163.

Newcomb, R., Stuenkel, E. and Cooke, I. (1985) Characterization, biosynthesis, and release of neuropeptides from the X-organ - sinus gland system of the crab, *Cardisoma carnifex. American Zoologist* **25**: 157-171.

Newcomb, R. (1987) Amino acid sequences of neuropeptides in the sinus gland of the land crab *Cardisoma carnifex*: a novel neuropeptide proteolysis site. *J. Neurochem.* **49/2**: 574-583.

Obata, S. and Kuroda (1989) Membrane potential change in a sea urchin egg induced by calcium ionophore A23187 has the same component that is involved in the fertilization potential. *Cell Structure and Function* **14**: 697-706.

Patterson, P. H. and Chun, L. L. Y. (1974) The influence of non-neuronal cells on catecholamine and acetylcholine synthesis and accumulation in cultures of dissociated sympathetic neurons. *Proc. Natl. Acad. Sci. USA* **71**: 3607-3610.

Patterson, P. H. and Chun, L. L. Y. (1977) The induction of acetylcholine synthesis in primary cultures of dissociated rat sympathetic neurons. I. Effects of conditioned medium. *Dev. Biol.* **56**: 263-280.

Poenie, M., Alderton, J. and Tsien, R. Y. (1985) Changes of free calcium levels with stages of the cell division cycle. *Nature* **315**: 147-149.

Potter, D. D. (1956) Observations on the neurosecretory system of portunid crabs. PhD thesis, Harvard University.

Ramon y Cajal, S. *Recollections of my life.* trans. E. H. Craigie. The MIT Press: Cambridge, MA, 1937.

Ramon y Cajal, S. (1890) A quelle epoque apparaissent les expansions des cellules nerveuses de la moelle epiniere du poulet. *Anat Anz.* **5**: 609-613, 631-639.

Ratliff, F. and Hartline, H. K. *Studies on excitation and inhibition in the retina: A collection of papers from the laboratories of H. Keffer Hartline.* Rockefeller: New York, 1974.

Rayner, M. D., Starkus, J. G., and Ruben, P. C. (1993) *Hydration forces in ion channel gating. Comments on Molecular and Cellular Biophysics* (in press).

Ready, D. F. and Nicolls, J. G. (1979) Identified neurons isolated from leech CNS make selective connections in culture. *Nature* **281**: 67-69.

Reichardt, G. F. and Patterson, P. H. (1977) Neurotransmitter synthesis and uptake by isolated sympathetic neurons in microcultures. *Nature* **270**: 147-151.

Selverston, A. I. and Moulins, M. (eds.) *The Crustacean Stomatogastric System.* Springer-Verlag: New York, 1987.

Seshan, K. R. and Levi-Montalcini, R. (1973) Neuronal properties of nymphal and adult insect neurosecretory cells *in vitro*. *Science* **182**: 291-293.

Silver, R. A., A. G. Lamb, and S. R. Bolsover (1990) Calcium hotspots caused by L-channel clustering promote morphological changes in neuronal growth cones. *Nature* **343**: 751-754.

Spitzer, N. C. (1991) A developmental handshake: Neuronal control of ionic currents and their control of neuronal differentiation. *J. Neurobiol.* **22**: 659-673.

Starkus, J. G., Fellmeth, B. D. and Rayner, M. D. (1981) Gating currents in the intact crayfish giant axon. *Biophys. J.* **35**: 521-533.

Stuenkel, E. L. (1983) Biosynthesis and axonal transport of proteins and identified peptide hormones in the X-organ sinus gland neurosecretory system. *J. Comp. Physiol.* **207**: 191-205.

Stuenkel, E. L. (1985) Simultaneous monitoring of electrical and secretory activity in peptidergic neurosecretory terminals of the crab. *J. Physiol.* **359**: 163-187.

Stuenkel E. L. and I. M. Cooke (1988) Electrophysiological characteristics of peptidergic nerve terminals correlated with secretion. In: *Current topics in Neuroendocrinology.* (D. Ganten and D. Pfaff, eds.) Springer-Verlag, Berlin, pp. 123-150.

Stuenkel, E. L., Ruben, P., Cooke, I. M. and Lemos, J. R. (1990) Sodium-activated cation channels in peptidergic nerve terminals. *Br. Res.* **517**: 35-43.

Szekely, A. M., Costa, E. and Gayson, D. R. (1990) Transcriptional program coordination by N-methyl-D-aspartate sensitive glutamate receptor stimulation in primary cultures of cerebellar neurons. *Molec. Pharmac.* **38**: 624-633.

Watanabe, A., Obara, S., and Akiyama, T. (1967) Pacemaker potentials for the periodic burst discharge in the heart ganglion of a stomatopod, *Squilla oratoria. J. Gen. Physiol.* **50**: 839-862.

Webster, S. G. (1991) Amino acid sequence of putative moult-inhibiting hormone from the crab *Carcinus maenas. Proc. R. Soc. Lond. B* **244**: 247-252.

Wong, R. G., Hadley, R. D., Kater, S. B. and Hauser, G. C. (1981) Neurite outgrowth in molluscan organ and cell cultures: The role of conditioning factor(s). *J. Neurosci.* **1**: 1008-1021.

Wu, C. F., Suzuki, N. and Poo, M. M. (1983) Dissociated neurons from normal and mutant *Drosophila* larval central nervous system in cell culture. *J. Neurosci.* **3**: 1888-1899.

Zucker, R. S. (1989) Short-term synaptic plasticity. *Ann. Rev. Neurosci.* **12**: 13-31.

Zucker, R. S. and Haydon, P. (1988) Membrane potential has no direct role in evoking neurotransmitter release. *Nature* **335**: 360-362.